CHEMICAL MODULATION OF AAV TRAFFICKING

Garrett Edward Berry

A dissertation submitted to the faculty at the University of North Carolina at Chapel Hill in partial fulfillment of the requirements for the degree of Doctor of Philosophy in the Curriculum in Genetics and Molecular Biology in the School of Medicine.

Chapel Hill
2016

Approved by:

Aravind Asokan

Ronald Swanstrom

Tal Kafri

Cary Moody

Michael Emanuele

ABSTRACT

Garrett Berry: Chemical Modulation of Adeno-associated virus trafficking
(Under the direction of Aravind Asokan)

Adeno-associated virus is widely studied due to the promise it holds as a gene therapy vector. Gene therapy broadly describes strategies in which genetic material is introduced into a target cell in an effort to treat or cure disease. However, even with AAV being used as a gene delivery vector in over 100 clinical trials to date, there is still much unknown about the biology of the vector. Further understanding of the trafficking of the vector through the host cell will contribute to the safety and efficacy of the inevitable clinical trials and therapies that are to come. In this dissertation, we utilized small molecules to dissect and modulate the trafficking of AAV vectors.

Firstly, we utilized numerous small molecules to dissect the potential role of several cellular degradation mechanisms in the AAV infectious pathway. We identified the ERAD inhibitor Eeyarestatin I (EerI) as a molecule that augments AAV transduction. EerI increased transduction by approximately 10-fold in a serotype, cell type, and genome type independent manner. Additionally, EerI and the proteasome inhibitor MG132 acted in distinct ways to augment AAV transduction. Further, EerI modulated the intracellular trafficking of AAV by redirecting AAV to enlarged Rab7/LAMP1 positive vesicles. This EerI-mediated redirection of AAV protected capsids from proteasomal degradation, thereby increasing the nuclear accumulation of AAV capsids.

Next, we utilized ionomycin and BAPTA-AM to modulate the intracellular calcium environment and determined that intracellular calcium concentration influences AAV transduction. Ionomycin increases intracellular calcium concentration, and decreases transduction by approximately 10-fold. Ionomycin acts to block transduction at or before AAV nuclear entry. BAPTA-AM decreases intracellular calcium concentration, and increases transduction by approximately 10 to 100-fold *in vitro* and *in vivo*. BAPTA-AM likely acts at multiple steps in the AAV pathway to increase transduction. However, we identified that BAPTA-AM increased RNA transcription from the AAV vector genome, thereby increasing transgene protein levels.

Taken together, we demonstrate multiple methods to modulate AAV trafficking using small molecules. Furthermore, we demonstrate that use of two of these molecules, EerI and BAPTA-AM, can augment AAV transduction, providing additional strategies for increasing AAV transduction in the clinic.

To my parents Wayne and Paula
&
My fiancée Marissa Cann

ACKNOWLEDGEMENTS

First, I would like to thank my advisor, mentor, and friend, Aravind Asokan. His direction throughout my graduate career has played a pivotal role in not only the scientist I have become, but also the person I have grown into. I would also like to thank my committee members Ron Swanstrom, Tal Kafri, Cary Moody, and Mike Emanuele, for their direction and their time throughout the pursuit of my degree at UNC. Their thoughtful insight into every detail of my graduate work has made this all possible. Further, I'd like to thank both the Biological and Biomedical Sciences program and staff for accepting me into their outstanding program, as well as the Curriculum in Genetics and Molecular Biology program and staff, for their support throughout my graduate studies.

Next, I would like to thank the past and present members of the Asokan Lab, who have meant more to my experience in the Asokan Lab than they can possibly realize. Firstly, Erin Borchardt and Giridhar Murlidharan, who joined the lab at the same time and took this sometime tumultuous graduate school journey with me while providing friendship and camaraderie throughout. Secondly, I'd like to thank the postdoctoral fellows, Eric Horowitz and Nagesh Purlicherla, who demonstrated patience as they taught me much about the intricacies of being a high quality scientist. Thirdly, I'd like to thank the graduate students, past and present, including Shen Shen, Blake Albright, and Victoria Madigan, who were there along the way to support me each in their own unique way. Next, I'd like to thank the current postdoctoral fellows, Ruth Castellanos-Rivera, Victor Long Ping Tse, and Sven Moller-Tank, for being an endless source of amusement and helping to provide all of the laughs that gave, and continues to give, the Asokan

Lab its vibrant on enjoyable atmosphere. Finally, I'd like to thank the myriad of undergraduate students that have populated the lab throughout my graduate career. Sarah Jones and Andrew Troupes were instrumental in providing both laughs and the training necessary for me to perform animal experiments. Lavanya Rao, Travis Corriher, and Robert Edmiston each brought a unique flavor and humor to the lab environment, especially Lavanya, who always laughed at my terrible jokes. Leonidas Vandoros, Ryan Fogg, Becca Reardon, Kelly Klinc, Kelsey Ford, Danny Oh and Lindsay Wells were also wonderful to be around while providing helpful experimental support when it was needed the most. Last, but certainly not least, I'd like to thank Dasean Nardone-White, who was a hard-working and enjoyable person to be around, and whose dedication saved me from countless late nights in the lab.

In addition, I'd like to thank all of the individuals at Michigan State University who helped me begin my career as a scientist. I'd like to especially thank Gabriel Hamer, Edward Walker, and Steven van Nocker for each taking me under their wing and teaching me what it means to be a researcher.

I'd also like to thank my family, who have been nothing but supportive throughout my educational career, but especially during the pursuit of my Ph.D. My parents, Wayne and Paula, have never stopped believing in me, and they continue to provide moral support when it is needed the most. My sister Kira and my brother Colton have also been a big part of my pursuit of knowledge, providing encouragement along the way.

Most importantly, I'd like to thank my girlfriend of many years and my fiancée, Marissa Cann. She has been my rock throughout my graduate career. She has always been willing to listen to my tribulations with an attentive ear. Her love and support has been the biggest driving force in my success throughout my time at UNC-Chapel Hill.

TABLE OF CONTENTS

LIST OF TABLES

LIST OF FIGURES

LIST OF ABBREVIATIONS

AAP	assembly activating protein
AAV	Adeno-associated virus
AAVR	Adeno-associated virus receptor
AAVS1	Adeno-associated virus integration site 1
AIDS	acquired immune deficiency syndrome
Arf1	ADP-ribosylation factor 1
BBB	blood-brain barrier
BR	basic region
CBA	chicken-beta actin
CBh	chicken-beta actin hybrid
CLIC/GEEC	clathrin-independent carriers/GPI-enriched endocytic compartments
CMV	cytomegalovirus
CNS	central nervous system
co-IP	co-immunoprecipitation
CPV	canine parvovirus
CRISPR	clustered regularly interspaced short palindromic repeats
CTB	cholera toxin B
DMEM	Dulbecco's modified eagle medium
DMSO	dimethyl sulfoxide
DUB	deubiquitinase
EBOV	ebloa virus
EerI	eeyarestatin I

EIPA	ethylisopropyl amiloride
ER	endoplasmic reticulum
ERAD	endoplasmic reticulum associated degradation
fLuc	firefly luciferase
FGFR1	fibroblast growth factor receptor 1
FPV	feline panleukopenia virus
GABA	gamma-aminobutyric acid
GFAP	glial fibrillary acidic protein
GFP	green fluorescent protein
GPI	glycosylphosphatidylinositol
GRAF1	GTPase regulator associated with focal adhesion kinase 1
HBoV	human bocavirus
HCC	hepatocellular carcinoma
HGFR	hepatocyte growth factor receptor
HPV	human papilloma virus
Hsp90	heat shock protein 90
HSPG	heparan sulfate proteoglycan
HSV	herpes simplex virus
I_{CRAC}	calcium release-activated channel
ICV	intracerebroventricular
ITR	inverted terminal repeat
Kif	kifunensine
LPL	lipoprotein lipase

MMTV-LTR	mouse mammary tumor virus long terminal repeat
MRN	Mre11, Rad50, Nbs1 complex
MTOC	microtubule organizing center
MVM	minute virus of mice
Nab	neutralizing antibody
NLS	nuclear localization signal
NMDA	N-methyl-D-aspartate
NPC	nuclear pore complex
NS	non-structural
ORF	open reading frame
PDGFR	platelet-derived growth factor receptor
PI3K	phosphoinositide 3-kinase
PKC	protein kinase C
PLA2	phospholipase A2
PLC	phospholipase C
qPCR	quantitative polymerase chain reaction
rAAV	recombinant Adeno-associated virus
RT-qPCR	reverse transcription quantitative polymerase chain reaction
scAAV	self-complementary Adeno-associated virus
SEM	standard error of the mean
ssDNA	single stranded DNA
STB	Shiga toxin B
STX5	syntaxin-5

TBG	thyroxine binding globulin
TGN	*trans*-Golgi network
UTR	untranslated region
UV	ultraviolet
VA	viral associated
VACV	vaccinia virus
VCP	valosin-containing protein
vg	vector genomes
VP	viral protein
VP1u	VP1 unique region
VP1/2	VP1 VP2 shared region
WPRE	woodchuck hepatitis virus posttranscriptional regulatory element

CHAPTER 1: Introduction[1]

1.1 Parvoviruses

Parvoviruses are a family of non-enveloped single-stranded DNA (ssDNA) viruses. These viruses are very small, usually ~25 nm in diameter, and package similarly small genomes, generally between 4 and 6 kb in length, that are capped by terminal repeats that form hairpin structures that can be either symmetrical or asymmetrical (1). The capsids of these viruses are made of 60 viral protein subunits, termed VPs, as icosahedral capsid structures that exhibit T=1 symmetry. Parvoviruses typically have at least two VP subunits, although some parvoviruses have been shown to have up to 5 VP subunits, which are named in numerical order of decreasing molecular size (i.e. VP1, VP2 etc.) (2). These VP subunits are generally the result of alternate splicing, alternate start codons, or both. In addition, the VP1 subunit of parvoviruses have been demonstrated to have a domain that acts as a broad spectrum phospholipase A2 (PLA2) enzyme, a domain that is required for productive infection. The genome of most *Parvoviridae* has only two open reading frames (ORFs), termed *rep* and *cap*. The *rep* ORF generally contains one or more nonstructural (NS) genes that are required for DNA replication, virion assembly, and DNA packaging. The *cap* ORF contains the structural genes, VPs described above, which assemble to make up the viral capsid.

[1] This chapter includes the original publication: Berry, G.E., Asokan, A. *Cellular transduction mechanisms of adeno-associated viral vectors.* Current Opinion in Virology. *In press.*

Parvoviridae are divided into two subfamilies: *Densoviridae*, which infect invertebrates, specifically insects, and *Parvovirinae*, which infect vertebrates (3). Members of the *Parvovirinae* subfamily infect a broad range of mammalian hosts, ranging from rodents up to humans. These viruses utilize various host cell surface glycan receptors for cell attachment, with sialic acid and heparin sulfate being among the more commonly used glycans. However, the secondary glycoprotein receptors used by *Parvovirinae* vary more widely, ranging from transferrin receptor to several different growth hormone receptors. Some of the better studied *Parvovirinae* include minute virus of mice (MVM), human parvovirus B19, canine parvovirus (CPV), feline panleukopenia virus (FPV), Adeno-associated virus (AAV) and more recently, human bocavirus (HBoV). Several mammalian parvoviruses have been demonstrated to be associated with various diseases, generally affecting the young and immunocompromised of a particular species. For instance, FPV and CPV are known to cause more serious disease in kittens and puppies, respectively. Similarly, erythema infectiosum is a disease caused by human parvovirus B19 in children (4), where B19 is also known to cause complications in individuals with acquired immune deficiency syndrome (AIDS), as well as pregnant women, sometimes resulting in miscarriage.

1.2 Adeno-associated Virus and Gene Therapy

One particular parvovirus, AAV, has been well studied due to its attractiveness for use as a gene therapy vector. AAV has a range of properties that make it a promising vector for use in the clinic for gene therapy applications, leading to the use of AAV as a gene delivery vector in over 100 clinical trials to date (http://www.abedia.com/wiley/vectors). AAV has the ability to infect both dividing and non-dividing cells (5), providing the ability to deliver genes to cells that

turnover, such as hepatocytes, as well as terminally differentiated cells generally refractive to gene delivery by other methods, such as neurons. Furthermore, AAV generally does not illicit a strong immune response, reducing the risk of adverse immune reactions such as cytokine storms (6). In addition, in the recombinant form, AAV rarely integrates into the host genome, though DNA delivered by AAV can persist for long periods in an episomal state, allowing long-term expression of the therapeutic transgene (7). Moreover, AAV lacks any known pathogenicity, suggesting a superior safety profile for the use of AAV as a gene delivery vector. It is worth noting that recent studies have demonstrated the existence of partial AAV genomes that have integrated into the cellular genome of hepatocellular carcinoma (HCC) cells (8). However, the role of these integration events in the development of the tumors remains to be determined. Furthermore, such integrations of rAAV genomes have not been demonstrated in patients from AAV clinical trials. Finally, the only requirements governing packaging of DNA into AAV capsids are the existence of the flanking ITRs, and the genome size must not exceed ~5 kb (9). Therefore, any genetic material fit to these requirements can be delivered using rAAV vectors. These properties, combined with the range of known AAV serotypes, allows the targeted delivery of specific genetic cargo to desired target tissues while maintaining a good safety profile and reducing off target delivery of the transgene. It is for these reasons that AAV has been explored so widely for use as a gene therapy vector.

Taken together, the results of the AAV vectored clinical trials that have been conducted or are currently underway continue to demonstrate the superior safety profile of rAAV vectors. Furthermore, numerous successful clinical trials utilizing AAV have been performed that target gene delivery to various organs. For instance, several AAV gene therapy trails are underway that aim to treat various diseases of the central nervous system (CNS) (10, 11). Furthermore, a

number trials have been performed aimed at delivery of factor VIII or factor IX to the liver in an effort to treat hemophilia A or hemophilia B, respectively, with promising results (12). Recent success has also been demonstrated with treatment of retinal diseases. Specifically, Leber's congenital amaurosis, a congenital form of blindness (13, 14). One particular trial eventually led to the first ever commercially approved AAV vectored gene therapy product in the western world (Alipogene tiparvovec, Glybera®, EU), which aims to treat lipoprotein lipase deficiency by intramuscular injections of AAV1 packaging the gene encoding for lipoprotein lipase (LPL) (15). The growing number of successful trial results demonstrate the continually shrinking gap between AAV-mediated gene therapy and the clinic.

1.3 Biology of Adeno-associated Virus

AAV was originally discovered as a contaminant of simian adenovirus preparations and was initially thought to be defective particles, as they were not replication competent on their own (16). However, these particles were antigenically distinct and were later classified as a *dependoparvovirus*. AAV replication is dependent upon the presence of a helper virus, such as Adenovirus (16), Herpes simplex virus (HSV) (17), human papilloma virus (HPV) (18), or vaccinia virus (VACV) (19). In addition, AAV has yet to be definitively linked to any human disease, even though the majority of the human population is seropositive for AAV (20). Many unique serotypes have been isolated from a range of different species, thought the most studied serotype is AAV2.

AAV has a genome of ~4.7 kb in length with 2 genes, *rep* and *cap*, much like other members of the parvovirus family. The genome of AAV is flanked by symmetrical inverted terminal repeats (ITRs) of 165 bp each that self-anneal into t-shaped hairpin structures. The rep

gene encodes for four non-structural genes, Rep78, Rep68, Rep52, and Rep40, which are named according to their molecular weight. These genes are generated as a result of expression driven by 2 distinct promoters, p5 and p19, as well as alternative splicing. Rep78 and Rep68 have DNA binding activity and have been shown to be important in regulating the activity of the p5, p19, and p40 promoters (21). Additionally, Rep78 and Rep68 have DNA endonuclease and DNA helicase activities that are important for resolution of the ITRs during DNA replication of the AAV genome (22-24). Furthermore, Rep78 and Rep68 play a pivotal role in site-specific integration and subsequent rescue of the AAV genome into and out of human chromosome 19 at a site termed AAVS1 (25). Rep 52 and Rep40 each have DNA helicase activity and have both been shown to be required for packaging of DNA into AAV capsids (26). The *cap* gene encodes for three VP subunits, VP1, VP2, and VP3, which are all driven by the p40 promoter. The individual VPs are generated by alternative splicing as well as an alternative start codon. In addition to the VPs, assembly-activating protein (AAP), is also encoded within *cap* in an alternate reading frame (27, 28). The VPs are assembled into capsids in a VP1:VP2:VP3 ratio of approximately 1:1:10, and with 60 VPs composing a full capsid, contain five copies of each VP1 and VP2, and fifty copies of VP3 (29). The VPs all share a C-terminal domain, but VP1 and VP2 have extended N-terminal domains that play important roles in viral infection. The n-terminal region unique to VP1, termed VP1u, contains a PLA2 domain, as well as three basic regions (BRs), that are essential to viral infectivity (30, 31). The N-terminal region shared by VP1 and VP2, termed Vp1/2, also contains two of the three BRs required for virus infectivity (32). The other gene encoded by *cap*, AAP, is important for assembly of capsids (33). However, while AAP is known to have nuclear and nucleolar localization signals that are important for function (34), the specific mechanisms underlying the action of AAP remain a mystery.

Interestingly, another gene has been postulated to exist in an alternate reading frame at the 3' end of the *cap* gene (35). It was later demonstrated that an active promoter, p81, was able to drive RNA transcription of the gene, which was then named the "X" gene (36). The same group later determined that the "X" gene potentially plays a role in the AAV life cycle, particularly in DNA replication (37). However, it must be noted that the existence of the "X" gene is still debated and the proposed function of the "X" gene has yet to be replicated.

Recently, high-throughput studies have been performed that have identified a number of previously unknown AAV proteins and RNA transcripts. One such study identified a number of unique novel RNA species of various sizes corresponding to the AAV genome (38). Interestingly, one particular RNA is present in high quantities that is transcribed in the reverse direction from the p5 promoter. Furthermore, the abundance of these RNA transcripts was altered upon co-infection with helper virus. Intriguingly, this study identified a novel 18 kDa protein that corresponds to a fusion of the C-terminus of *rep* and the N-terminus of *cap*, though the function of this protein remains unknown. However, it is worth noting that this study identified an RNA transcript that is capable of encoding for the previously identified "X" gene, providing more evidence for a potential function of the "X" gene in AAV biology.

There have been numerous natural AAV serotypes that have been isolated from species ranging from cows and pigs to chimpanzees and humans. These serotypes display a vast range of properties, most notably their unique tissue tropism. These differences are generally thought to be driven by the differences in primary and secondary receptor binding. Much like other parvoviruses, AAVs bind to glycans for cell attachment. AAV2 was the first AAV to have its cognate primary receptor identified, which is heparan sulfate proteoglycan (HSPG) (39). AAV3 also binds HSPG to facilitate cell binding (40). AAV4 binds O-linked sialic acid (41), where

AAV1, AAV5, and AAV6 bind N-linked sialic acid (42, 43). Interestingly, AAV6 has been shown to bind both HSPG and N-linked sialic acid (44). Interestingly, AAV9 has been shown to utilize N-linked galactose as a primary receptor (45); the only AAV known to utilize that glycan. To date, the primary receptors for both AAV7 and AAV8 are unknown. In addition to binding glycan primary receptors, AAV uses glycoprotein secondary receptors to gain entry to the cell. A number of proteins have been identified that act as secondary receptors for AAV, including several growth factor receptors, such as fibroblast growth factor receptor 1 (FGFR1) (46), human hepatocyte growth factor receptor (HGFR) (47), and platelet-derived growth factor receptor (PDGFR) (48), as well as a number of integrins, such as α5β1 and αVβ5 (49-52). However, KIAA0319L was later identified as a universal receptor for a broad number of AAV serotypes, therefore it was given the designation AAV receptor (AAVR) (53). The differential usage of primary and secondary receptors are generally thought to be a driving factor in the various tissue tropisms of these serotypes. In fact, modification of glycosylation patterns *in vivo* have been shown to alter the tropism of both AAV9 and AAV4 (54, 55).

1.4 Trafficking of Adeno-associated virus

After rAAV binds to its surface receptor, virus is internalized via endocytosis. Mammalian cells are known to internalize extracellular material by numerous endocytic pathways, several of which have been implicated in uptake of rAAV. The first studies to investigate AAV uptake suggested that internalization of rAAV occurred via clathrin-mediated endocytosis. In these studies, transduction of AAV2 was inhibited by expression of a dominant-negative mutant of dynamin, a protein necessary for successful clathrin-mediated endocytosis

(56, 57). Additionally, internalized AAV2 colocalized with transferrin, a protein known to be internalized by this mechanism.

Interestingly, a recent study was not able to clearly identify dynamin- or clathrin-dependent endocytosis as a mechanism of uptake. Instead, the study suggests that uptake of AAV2 is dependent on the incompletely characterized clathrin-independent carriers and GPI-enriched endocytic compartment (CLIC/GEEC) endocytic pathway (58). This study demonstrated that AAV2 uptake was inhibited by dominant negative versions of Arf1, Cdc42, and GRAF1, three important effectors of the of the CLIC/GEEC pathway. In addition, AAV2 colocalized with cholera toxin B (CTB) and GPI-anchored GFP, two markers of CLIC vesicles, after internalization. In addition, this study identified EIPA as an inhibitor of CLIC/GEEC endocytosis. However, it is worth noting that EIPA is classically known as an inhibitor of macropinocytosis. Accordingly, other studies suggest a role for macropinocytosis in AAV uptake. One such study demonstrated that inhibition of Rac1 activation, a key effector of macropinocytosis, inhibits AAV internalization (59). Interestingly, another study used multiple small molecule inhibitors of macropinocytosis, including EIPA, to demonstrate that inhibition of macropinocytosis decreased transduction in some cells lines, where other cell lines, specifically hepatocellular carcinoma cells, demonstrated enhanced transduction (60).

It is worth noting that transcytosis of rAAVs has been shown to occur in polarized cells in a serotype-dependent manner, and it has been suggested that this phenomenon is dependent upon caveolin (61). In fact, an important area of inquiry regarding intrinsic qualities of individual rAAV strains in vivo is the ability of the capsid to cross the blood-brain barrier (BBB) to transduce the central nervous system. One such serotype is AAV9, which has been shown to effectively cross the BBB and infect the CNS when administered intravenously. However, one

study utilized mice that do not express caveolin-1, a key effector of caveolin-mediated transcytosis (62), and demonstrated that rAAV9 continues to traverse the BBB in these knockout mice (63), suggesting that transvascular transport of AAV9 may occur by a different mechanism.

There currently exists much contradicting data regarding the endocytosis mechanisms involved in cellular internalization of rAAV. At this juncture, there is not a clear explanation for these discrepancies. However, there are several possibilities. For instance, some studies utilize adenoviral vectors to overexpress protein effectors, dominant-negative or otherwise, therefore introducing the possibility of modifying the cellular environment prior to infection with AAV. Another possibility is that some small molecule inhibitors can affect multiple pathways, therefore clouding the results. For instance, dynasore, a dynamin inhibitor, inhibits both caveolae- and clathrin-mediated endocytosis, but also been shown to have numerous dynamin independent effects, such as disruption of lipid raft organization and reduction of labile cholesterol in the plasma membrane (64). Additionally, EIPA appears to inhibit both macropinocytosis and CLIC/GEEC endocytosis (58, 65), and there is additional evidence that EIPA partially inhibits endosome acidification (66), an essential step in AAV transduction that will be discussed later in this review. In addition, it has been hypothesized that some uptake pathways lead to successful transduction while other pathways in those same cells lead to a "dead end" for AAV (58, 59), and this is likely altered in a cell-type dependent manner. Moreover, it is likely that AAV utilizes a combination or permutation of the aforementioned endocytosis pathways in a cell-type specific manner. In fact, one study supports this idea, demonstrating that small molecule inhibitors of dynamin and CLIC/GEEC endocytosis, dynasore and EIPA, respectively, act in a synergistic manner to inhibit AAV uptake and subsequent transduction (58).

After rAAV enters the cell, it must traffic towards the nucleus in order to successfully deliver its genetic cargo. Immediately after uptake, AAV is presumably trafficked to Rab5+ early endosomal compartment, which is a feature conserved amongst many parvoviruses (67). From here, rAAV has been shown to be trafficked through a number of different compartments. Studies have demonstrated that rAAV2 traffics through both Rab7+ late endosomes and Rab11+ recycling endosomes (68). From here, AAV has been shown by numerous studies to traffic to the Golgi apparatus (32, 69, 70). One recent study showed that siRNA-mediated knockdown of syntaxin 5 (STX5), as well as disruption of STX5 by the small molecule Retro2.1, reduced rAAV transduction, suggesting that retrograde transport of rAAV to the trans-Golgi network (TGN) mediated by syntaxin 5 is important for transduction (71). Interestingly, this study was unable to confirm that Rab7+, Rab9+, or Rab11+ vesicles play a role in trafficking of rAAV to the Golgi apparatus. Recently, we demonstrated that inhibition of endoplasmic reticulum-associated degradation (ERAD) by eeyarestatin I (EerI) in HeLa cells reroutes rAAV to enlarged Lamp1+ lysosomes, thereby increasing transduction, indicating that trafficking of rAAV through the lysosome may be an important step in infection (Discussed in Chapter 2) (72). It is important to note that, as of now, no studies have observed rAAV in the endoplasmic reticulum (ER). Therefore, it is unlikely that rAAV traffics to the ER prior to nuclear entry.

Trafficking of AAV through the cellular endomembrane system is a requirement for transduction. One of the steps known to be required is endosome acidification, as the vacuolar H+-ATPase inhibitor bafilomycin A1 effectively blocks transduction (57, 73). Additionally, studies utilizing the small molecules brefeldin A and golgicide A, known to disrupt the Golgi apparatus, have shown that trafficking of rAAV through the Golgi apparatus is also required (71, 73). One important outcome of these trafficking steps is the triggering of conformational changes

in the capsid (74), namely, the exposure of the N-terminal domains of VP1 and VP2, which are located inside the capsid prior to infection (75). Exposure of these domains for successful transduction is required, as it has been demonstrated that microinjection of both complete virions, as well as VP3-only virions, directly into the cytosol do not properly transduce the cell (76). It was suggested that the AAV capsid itself has protease activity that is pH-dependent, which could possibly be triggered by the acidification of the endosome (77). However, it has yet to be determined if the self-cleavage events mediated by this activity also play a role in the exposure of the VP1/VP2 N-termini, or in other events related to transduction.

After trafficking of rAAV through the endomembrane system, rAAV escapes the endosome into the cytosol. Endosomal escape is dependent on a phospholipase A2 (PLA2) domain located in the VP1 unique region of AAV (30, 78). Studies have shown that mutation or deletion of the PLA2 domain prevents endosomal escape and subsequent transduction (79).

As is the case with AAV cell entry, differential, and sometimes conflicting, data exists regarding the intracellular trafficking of rAAV. It is likely that the trafficking pathway differs in a cell line-dependent and serotype-dependent fashion. This possibility is evident in the serotype-dependent axonal trafficking of rAAV in neurons. Furthermore, rAAV9 was identified in Rab5+, Rab7+, and Rab11+ vesicles in neurons in cell culture, but was shown to only traffic effectively along axons in Rab7+ endosomes, further supporting the notion that intracellular trafficking of rAAV is likely dependent on cell type (80).

After escaping the endosome into the cytosol, rAAV then must enter the nucleus, where it will undergo uncoating and deliver its genetic cargo. Nuclear entry of AAV has been proposed as a major rate-limiting step in the infectious pathway, acting as a literal bottleneck (57). Four basic regions (BR1-4) were identified on AAV2 that were conserved among serotypes 1-11, that were

investigated for their potential function as nuclear localization signals (NLS). BR4 is located within VP3 and was shown to have no impact on nuclear import of rAAV virions, but mutation of BR4 did result in virion assembly defects (31). However, BR3, located within both VP1 and VP2, is essential for AAV transduction (76). In addition, BR1 and BR2, to a lesser extent, are also important for AAV transduction. However, confocal microscopy studies of BR-negative mutants demonstrated that BR2 and BR3 are important for nuclear translocation (32). A recent study demonstrated that rAAV2 enters the nucleus through the nuclear pore complex (NPC) by blocking nuclear entry of rAAV2 with wheat germ agglutinin, a lectin that binds the NPC and blocks and cargo from traversing through (81). This study also demonstrated that importin-β1 is the host protein responsible for import of rAAV2 particles through the NPC. Capsid interaction with members of the importin-α family of proteins was also shown by co-IP, but their involvement in nuclear import of rAAV2 remains unclear. This route of nuclear translocation was further supported by live cell imaging technology that witnessed labeled rAAV2 particles traverse the nuclear envelope through labeled NPCs (82).

After nuclear entry, rAAV has been shown to traffic to the nucleolus. AAV capsids have been shown to interact with nucleophosmin and nucleoin, both of which localize to the nucleolus (83, 84). Interestingly, while rAAV particles remain intact and infectious in the nucleolus, it is not here that capsids uncoat and deliver their genetic payload. The capsids must egress out of the nucleolus and move into the nucleoplasm in order to successfully transduce the cell. It is not clear why AAV traffics to the nucleolus. In fact, evidence from small molecule and siRNA knockdown studies seem to suggest that nucleolar accumulation of rAAV is unfavorable for transduction (85). More investigation into possible differences in nucleolar accumulation

between cell types and serotypes will likely be helpful in dissecting the role of the nucleolus in rAAV transduction.

After AAV reaches the nucleus, the virus undergoes uncoating to release the genome. The mechanisms underlying uncoating of AAV remain unclear, though it is known that genome composition may play an important role in uncoating and genome release (86). After uncoating, the virus must undergo the crucial step which is conversion of the single-stranded genome into a double-stranded form, a process known as second-strand synthesis. This process has been shown to be a rate limiting step in infection in the absence of a helper virus (87). Second-strand synthesis is blocked by numerous cellular factors relating to cellular DNA quality control. For instance, FKBP52 has been shown to bind the ITRs and blocks second-strand synthesis (88, 89). Additionally, the MRN complex, a cellular DNA damage-sensing complex consisting of the three cellular proteins Mre11, Rad50, and Nbs1, severely blocks AAV infection at the genome level (90-92). Furthermore, other proteins involved in the DNA damage response have been shown to interact with AAV genomes, such as Ku86 and Rad52, but the specifics underlying these interactions are currently unclear (93). The AAV genomes are then circularized and concatemerized (94). Further, in the case of AAV infection with a helper virus such as Ad, integration of the genome into AAVS1 then occurs as a result of Rep68 and Rep78 activity (95). Due to the need for AAV *rep* expression, this step generally does not occur with recombinant AAV vectors. Interestingly, it has been shown that AAV capsid proteins might play a role in both second-strand synthesis and gene transcription after uncoating (96). While, the exact mechanism by which the capsid might play a role in these steps remains unclear, it has been demonstrated that splicing factors bind the exposed genome and the capsid cooperatively and block transcription (97).

1.5 AAV Vectorology

Two of the factors driving the use of AAV vectors is the simplicity of the genome and the ease of manufacturing. As previously mentioned, the only *cis*-acting elements necessary for packaging of recombinant genomes into AAV capsids are the ITRs that flank either side of the genetic cargo (9). Therefore, replacement of the *rep* and *cap* genes with any desired genetic information can yield rAAV particles that carry any promoter and transgene of interest, provided the total vector DNA length does not exceed ~5 kb. In order to manufacture these particles, the *rep* and *cap* genes with the ITRs removed are simply provided in *trans* on a separate plasmid, named pXR (98). Further, it was soon discovered that fine-tuning the levels of *rep* expression could allow for greater production of the *cap* genes (99). Specifically, it was determined expression levels of Rep78 and Rep68 inversely correlated with the expression levels of *cap* (21). Therefore, mutation of the Rep78 and Rep68 start codon to a weak alternate start codon was performed on the pXR plasmid to reduced Rep78 and Rep68 expression levels, thereby increasing capsid protein production.

When rAAV was first manufactured, co-infection of a virus with helper activity, specifically Adenovirus or herpes simplex virus, was needed in order to promote rAAV replication. This was not ideal, as additional purification steps were needed to remove the helper virus from the final preparation. This would also prove disastrous if the contaminating helper virus was not completely removed before administration of the treatment to patients. To solve this problem, the minimal Adenovirus genes necessary for replication of rAAV particles was determined (98). These genes were then added to the cell production system by either their presence in the genome of the producer cell line, as is the case with E1a and E1b in 293 cells, or on a plasmid, as is the case with E2a, E4orf6, and viral associated (VA) RNAs. When this

plasmid, called pXX6-80, is combined with a pXR plasmid and the ITR plasmid containing the gene of interest, it allows for the triple plasmid transfection method, a method that remains one of the most commonly used rAAV production method. It is also necessary to note that concurrently with the development of the triple plasmid transfection method, another system was developed in a similar fashion, but with a different approach (100). This study generated a plasmid called pDG, which contained both the Adenovirus genes necessary for rAAV production as well as the *rep* and *cap* genes lacking ITRs. To downregulate Rep78 and Rep68 expression, instead of mutating the start codon, this plasmid replaced the endogenous p5 promoter with a much weaker mouse mammary tumor virus long terminal repeat (MMTV-LTR) promoter. Use of this plasmid instead of pXX6-80 and a pXR plasmid allows for a two plasmid transfection method for production of rAAV. This method is also widely used to generate rAAV.

After the triple plasmid transfection system was standardized, several improvements began to be made to allow for production of broad range of serotypes as well as increased vector production. To achieve the first goal, the *rep* portion of the pXR2 plasmid was engineered such that the C-terminal portion of *rep* was replaced with the rep that matched the cap serotype being produced, but leaving the N-terminal portion of *rep* from AAV2 intact. This allowed packaging of genetic cargo flanked by AAV2 ITRs into the capsid of any serotype, a practice known as cross-packaging (101). This development sparked a revolution in rAAV research, allowing the production of potentially thousands of rAAV capsids, natural and synthetic, for study.

1.6 Synthetic rAAV Strains

As previously mentioned, there are numerous natural AAV serotypes that have been isolated from numerous species that each demonstrate unique tropism. For example, AAV1 is

generally used for intramuscular injections, as it transduces muscle more efficiently than AAV2 (102). AAV8 is generally used for liver-directed gene therapy, as it transduces mouse liver more efficiently than AAV2 (103). However, it must be noted that recent studies have demonstrated that AAV8 transduces non-human primate and human hepatocytes poorly compared to AAV3 (104). AAV9 is known to transduce many tissues types as well as having the ability to cross the blood-brain barrier (BBB) (54, 63). However, even with a broad range of capsids to choose from, targeted transduction of specific tissues while limiting or eliminating off target transduction remains one of the most vital requirements as individual therapies approach the clinic. To this end, many synthetic strains of AAV have been generated with a vast array of strategies that are able to overcome some of these obstacles.

One of the first methods used to produce synthetic rAAV capsids was rational design. One of the earliest successes with this approach was the generation of AAV2i8. This capsid was generated by reengineering the heparan sulfate binding footprint on AAV2 with a region from an interloop of AAV8, yielding a new synthetic vector that transduced the liver with much lower efficiency (105). Therefore, AAV2i8 became the first liver-detargeted vector. This finding let to the development of many more vectors that had similar liver-detargeted qualities. Shortly thereafter, another synthetic AAV capsid, AAV2.5, was produced. AAV2.5 was a rationally designed AAV2 capsid containing amino acid residues from AAV1 that contribute to the ability of AAV1 to transduce muscle with high efficiency (102). Additionally, this capsid demonstrated a lower level of cross reactivity with AAV2 neutralizing antibodies (Nabs), thereby making treatment available to more patients.

Another commonly used strategy for generation of synthetic capsid mutants is directed evolution of capsid libraries. This approach typically yields thousands to potentially millions of

unique capsid DNA sequences. The individual directed evolution approaches are then designed to yield new capsids with one or several desirable properties. These libraries can be generated a number of different ways. However, there are two methods that are most often utilized. One method is capsid shuffling, which utilizes random assembly of fragmented capsid DNA based on reannealing at regions of complementarity (106, 107). The number of parental strains used to generate capsid shuffled libraries can range from only two to several. A number of different studies have utilized libraries generated using most or all serotypes AAV1-9 (108, 109). One such study utilized a unique directed evolution approach to generate a capsid that efficiently transduces oligodendrocytes in the CNS (110). The other commonly used method randomizes individual regions of interest on a parental strain to generate capsids that can have new properties or that can shed light on the biology of a particular serotype. For example, one particular library generated on an AAV9 background was able to generate several capsids of interest (111). One particular capsid, AAV9.45, was detargeted from the liver, where another capsid, AAV9.24, was later determined to be deficient in galactose binding, highlighting the eventually discovered galactose binding footprint on the AAV9 capsid (112).

One intriguing set of synthetic capsids that was generated is the so-called G series. These capsids were generated by grafting the galactose binding footprint of AAV9 onto several other capsids (113). Several of these capsids demonstrated gain-of-function phenotypes, which the capsids gaining the ability to use galactose as a primary receptor. One particular G mutant, AAV2G9, was shown to be able to utilize both heparan sulfate and galactose to bind to the cell surface, which provided multiple interesting qualities. Contrary to AAV2, AAV2G9 has been shown to mediate rapid onset of gene expression *in vivo*. Furthermore, contrary to AAV9, AAV2G9 has been demonstrated to greatly reduce the leakage of the virus into the systemic

circulation when administered intracranially. The use of this type of approach is sure to grow as more is discovered regarding the function of particular motifs on the capsid surface.

An additional strategy sometimes used to restrict transgene expression to the tissue of interest relies upon modification of the recombinant genome. For instance, while constitutive promoters such as the cytomegalovirus (CMV) promoter or the chicken beta actin (CBA) promoter are often used, there are a number of tissue specific promoters that have been explored to restrict gene expression. One such example is the thyroxine-binding globulin (TBG) promoter, which has been shown to be a liver-specific promoter (114-116). Two tissue-specific promoters that are commonly used in the CNS are the human synapsin 1 promoter (117-119) and the glial fibrillary acidic protein (GFAP) promoter (120, 121), which restrict expression to neurons or astrocytes, respectively. Interestingly, the Pleiades Promoter Project utilizes human genomic information combined with a bioinformatics approach to generate MiniPromoters, which allow for cell type specific promoters for use in the gene therapy space (122, 123). One such example is the Ple34 and Ple261 promoters, which drive expression only in endothelial cells within the CNS (124). However, some promoters have been shown to also cause issues with long-term transgene expression. For instance, the CMV promoter was shown to provide high levels of transgene expression initially that eventually diminished over time, presumably due to DNA methylation of the promoter, leading to silencing of the transgene. This problem was solved by the generation of a hybrid from of the CBA promoter, called the CBh promoter (125). This promoter was demonstrated to provide ubiquitous expression, much like the CBA or CMV promoters, but without diminishing transgene expression over time. Along with promoters, the 3' untranslated region (UTR) of the transgene can also be altered to restrict transgene expression. Several studies have added microRNA binding sites to the 3' UTR of the transgene (126, 127).

These binding sites allow for tissue specific microRNA-based degradation of the transgene. One prime example is the addition of miR-122 binding sites to the 3' UTR of a gene to inhibit transgene expression in the liver (128). Taken together, combining different capsids, promoters, and 3' UTR elements will allow for great levels of tissue specific gene expression as rAAV-mediated gene therapies approach the clinic.

1.7 Strategies to Augment rAAV Transduction

One of the strategies currently used to increase AAV transduction is modification of the viral genome. As previously mentioned, second-strand synthesis has been shown to be a major rate-limiting step in AAV transduction. Knowledge of this bottleneck led to the development of self-complementary AAV (scAAV) vectors (129). These were generated by mutating one of the ITRs to remove the terminal resolution site. This had the effect of generating vector genomes that were flanked by standard ITRs but retained the mutated ITR in the middle. This mutated ITR has the effect of causing the genome to base pair together down the molecule upon uncoating, thereby bypassing the requirement for second-strand synthesis. These scAAV vectors demonstrate a striking increase in transduction that is greater than 10-fold. While this is a strategy that is commonly used, the biggest disadvantage is that the packaging capacity of scAAV vectors is much smaller than the already restricted 4.7 kb. The limit of transgene size for scAAV is only ~2.3 kb, therefore only being useful when the genes delivered are of a small size. Another modification that is commonly made to the viral genome to augment transduction is the inclusion of the woodchuck hepatitis virus post-transcriptional response element (WPRE) (130, 131). When added to the 3' UTR of the transgene, the WPRE generates a stable tertiary structure that enhances mRNA stability, thereby increasing transgene expression (132).

Another set of strategies that are being investigated involve modification of the AAV capsid to increase transduction. One of the most successful examples of this approach are the tyrosine-to-phenylalanine mutants. It was postulated that tyrosine residues on the capsid surface act as sites for phosphorylation and subsequent ubiquitination, therefore leading to capsid degradation. The resulting Y-F mutations resulted in rAAV capsids that showed marked transduction increases (133). Further mutation of possible phosphorylation sites led to the so-called Y-T quadruple mutant, a modification of the rAAV2 capsid that dramatically increases transduction (134). Further studies leveraging the knowledge of rAAV trafficking to perform rational capsid mutagenesis are important to generate vectors that more efficiently transduce tissues.

Another set of approaches that have been explored to augment rAAV transduction is the use of small molecules to alter the cellular environment to the advantage of rAAV. One of the first examples of this approach took advantage of the observation that AAV preferentially transduced dividing cells in S phase (135). Therefore, they utilized DNA damaging agents, such as UV radiation, and observed an increase in AAV transduction (136). They proceeded to demonstrate that cisplatin, a common chemotherapeutic, augmented AAV transduction by several log orders. Subsequent studies continued to identify small molecules that alter DNA related proteins. One such class of small molecules are the topoisomerase inhibitors. Both camptothecin (topoisomerase I inhibitor) and etoposide (topoisomerase II inhibitor) were shown to increase AAV transduction, and are also both either approved or in clinical trials for use as chemotherapeutics (137). Both of these molecules are known to cause accumulation of DNA damage, and therefore function in a similar manner to cisplatin to augment rAAV transduction. Hydroxyurea is another small molecule that has been shown to augment AAV transduction, the

mechanism, or combination of mechanisms, by which this may occur is unclear. For instance, hydroxurea is a DNA-damaging drug, putting in a similar class as cisplatin or the topoisomerase inhibitors. However, hydroxyurea has also been shown to disrupt the nucleolus, a process which itself has been shown to be productive for transduction (85). Furthermore, hydroxyurea has been shown to inhibit phosphorylation and subsequent activation of FKBP52, a protein that has been shown to be detrimental to AAV transduction (138).

Another class of small molecules that has been thoroughly studied for their potential to augment AAV transduction are the proteasome inhibitors. It has been hypothesized that the proteasome plays a strong inhibitory role in rAAV transduction by ubiquitin-dependent degradation of capsids before they can traffic to the nucleus. This hypothesis is supported by several studies, the first of which demonstrated a large increase in transduction of rAAV2 when cells were treated with the proteasome inhibitor MG132 (73). Since then, several more studies have shown an increase with other proteasome inhibitors, namely LLnL, bortezomib (Velcade®), and carfilzomib (139-142). Additionally, it has been shown that rAAV2 and rAAV5 capsids are a substrate for ubiquitin conjugation (139), which is often a tag for proteasome-dependent degradation. Further, we have shown that inhibition of all cellular ubiquitination events with the UBEA1 inhibitor PYR-41 increases transduction (Discussed in Chapter 2) (72). However, it doesn't appear that inhibition of ubiquitin-dependent capsid degradation by the proteasome accounts for the entire transduction increase witnessed. This could be due to a number of different factors. For instance, it is known that bortezomib can have nonproteasomal targets, such as serine proteases (143). However, it appears as though modulation of intracellular trafficking by proteasome inhibition is at least partially responsible for the observed increase in transduction, but the specific mechanisms behind this remain unclear. Several studies, taken

together, indicate involvement of both the proteotoxic stress response and the ER stress response, cellular responses that occur during proteasome inhibition. Indeed, several other approaches that induce these stress responses also increase rAAV transduction. Cellular heat shock (144), chemical inhibition of Hsp90 (a molecular chaperone) (70), and increased oxygen free radicals (145), all induce an ER or proteotoxic stress response, and all also increase rAAV transduction to a similar extent. Additionally, as mentioned above, we have also demonstrated that modification of the intracellular trafficking of rAAV2 by the ERAD inhibitor EerI increases transduction (Discussed in Chapter 2) (72). Interestingly, EerI has been shown to induce the ER stress response (146, 147), but it is not known if the trafficking changes observed are a direct result of this cellular stress. While investigation of the mechanism of transduction increase for all of the small molecules mentioned is important, it remains that all of these molecules are viable strategies that must be investigated for use as a method to increase rAAV transduction in the clinic.

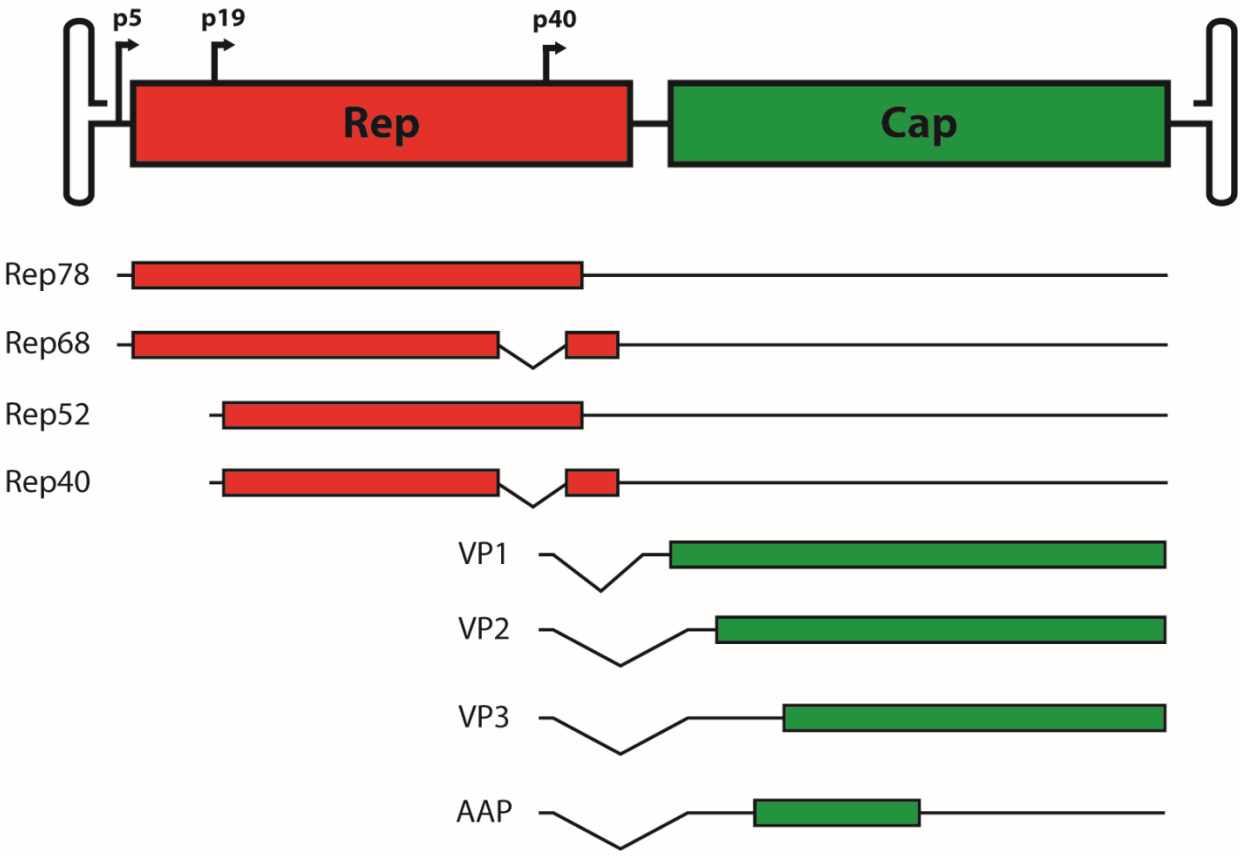

Figure 1: Schematic representation of the wildtype AAV genome. The AAV genome consists of two ORFs, *rep* and *cap*, driven by three different promoters, p5, p19, and p40. Rep78 and Rep68 are driven by the p5 promoter, with Rep68 resulting from alternative splicing. Rep52 and Rep40 are driven by the p19 promoter, with Rep40 resulting from alternative splicing. All three VPs are driven by p40, with alternate splicing resulting in VP2, VP3, or AAP. An alternate start codon results in VP2, and AAP is expressed from an alternate reading frame with an alternate start codon.

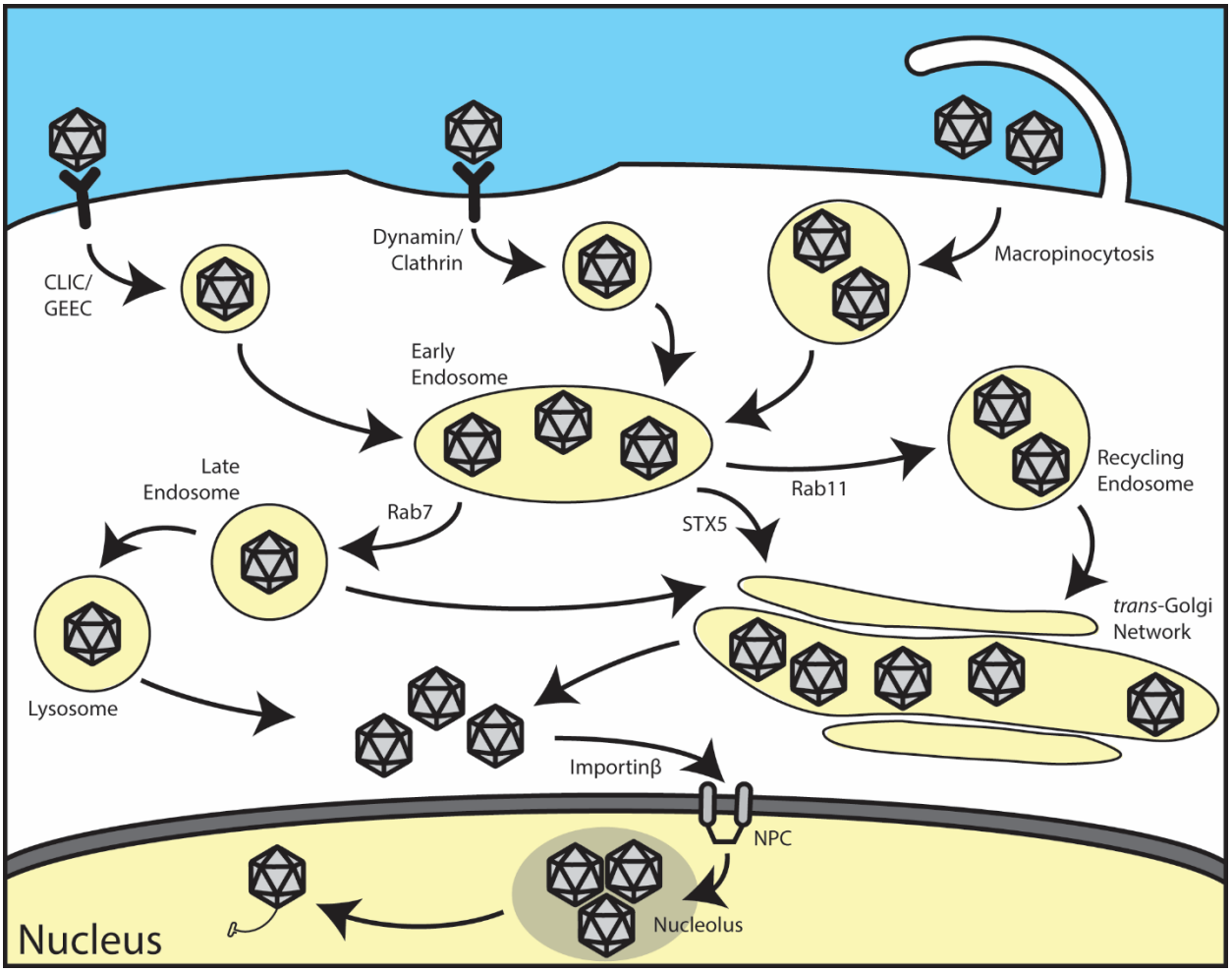

Figure 2: Model of the intracellular trafficking pathway of AAV. AAV binds to a primary/secondary receptor complex at the cell surface. Internalization occurs through a number of different cellular uptake pathways. Virus is then trafficked through the endomembrane system, triggering broad conformational changes in the virion. AAV then escapes into the cytoplasm, where is enters the nucleus through the nuclear pore complex and is trafficked to the nucleolus. AAV then traffics out of the nucleolus and proceeds to uncoat. Second-strand synthesis and RNA transcription then occurs.

CHAPTER 2: Chemical modulation of endocytic sorting augments adeno-associated viral transduction[2]

2.1 Overview

Intracellular trafficking of viruses can be influenced by a variety of inter-connected cellular sorting and degradation pathways involving endo-lysosomal vesicles, the ubiquitin-proteasome system, autophagy-based or ER-associated machinery. In case of recombinant adeno-associated viruses (AAV), proteasome inhibitors are known to prevent degradation of ubiquitinated AAV capsids, thereby leading to increased nuclear accumulation and transduction. However, the impact of other cellular degradation pathways on AAV trafficking is not well-understood. In the current report, we screened a panel of small molecules focused on modulating different cellular degradation pathways and identified Eeyarestatin I (EerI) as a novel reagent that enhances AAV transduction. EerI improved AAV transduction by an order of magnitude regardless of vector dose, genome architecture, cell type, or serotype. This effect was preceded by sequestration of AAV within enlarged vesicles that were dispersed throughout the cytoplasm. Specifically, EerI treatment redirected AAV particles towards large vesicles positive for late endosomal (Rab7) and lysosomal (LAMP1) markers. Notably, MG132 and EerI (proteasomal and ERAD inhibitors, respectively) appear to enhance AAV transduction by increasing the intracellular accumulation of viral particles in a mutually exclusive fashion. Taken together, our

[2] This chapter includes the original publication: Berry, G.E., Asokan, A. *Chemical modulation of endocytic sorting augments adeno-associated viral transduction*. Journal of Biological Chemistry. 2016 Jan 8;291(2):939-47. (PMID: 26527686)

results expand on potential strategies to redirect recombinant AAV vectors towards more productive trafficking pathways by deregulating cellular degradation mechanisms.

2.2 Introduction

Eukaryotic cells utilize tightly regulated pathways to sort and degrade internalized cargo by exploiting lysosomal proteases, the ubiquitin-proteasome system, ER-associated or autophagy-based machinery. Endoplasmic reticulum (ER) associated degradation, or ERAD, is a critical eukaryotic process that involves extraction and ubiquitination of misfolded proteins followed by their degradation by the proteasomal machinery (148). Several viral pathogens exploit this process to infect and replicate within host cells (149, 150). For instance, polyomaviruses appear to interact with ER lumen components to rearrange capsid proteins and subsequently retrotranslocate into the cytosol (151). Another constitutive degradation pathway essential for maintaining cellular homeostasis is autophagy (152). As with ERAD, several viruses have now been shown to subvert or mimic autophagy to facilitate replication and/or dissemination (153-155). The specific degradation pathway and the subsequent intracellular fate of viral proteins as well as their genomic cargo within the host cell are often dictated by a variety of preceding vesicular sorting events.

Recently, vesicular transport of non-enveloped parvoviruses such as the Minute Virus of Mice (MVM) through the ER and Golgi has been shown to accelerate progeny virus release (156). A particularly interesting member of the same parvovirus family is the helper-dependent Adeno-associated virus (AAV), which replicates upon co-infection with Adenoviruses or other viruses such as Herpes Simplex Virus or Papillomavirus. This small, non-pathogenic Dependoparvovirus contains a 4.7kb ssDNA genome packaged within an icosahedral (T = 1) capsid ~ 25nm in diameter (157). Different AAV serotypes recognize various cell surface

glycans such as heparan sulfate, sialic acid or galactose as primary receptors for attachment (158). Subsequent internalization of AAV particles into endocytic vesicles is thought to be mediated by integrins and/or specific transmembrane receptors. In addition, several diverse and cell-specific mechanisms of endocytic uptake ranging from macropinocytosis to the CLIC/GEEC pathway have been described (58, 60). Despite these differences, perinuclear accumulation within the Golgi apparatus (32, 69-71, 159) and exploitation of the nuclear import machinery for nuclear entry appear to be broadly conserved, downstream trafficking events (81).

Although these studies provide a detailed map of AAV transport within the host cell, it remains unclear whether the modulation of cellular degradation pathways such as ERAD or autophagy outlined earlier can influence AAV trafficking. Most studies to date have focused on proteasome inhibitors such as MG132 (73), LLnL (160) and bortezomib or carfilzomib (85, 142), which have been shown to increase AAV transduction through increased nuclear/nucleolar accumulation of viral particles. In the current study, we tested the effect of several small molecules that modulate the ubiquitin-proteasome system, autophagy and/or ERAD on AAV transduction. The overall goal of the study was to understand the interplay (or lack thereof) between these different cellular degradation pathways in facilitating or restricting AAV trafficking within host cells. In doing so, we identified an ERAD inhibitor (Eeyarestatin I / EerI) that deregulates endocytic sorting of AAV particles and redirects viral transport towards Rab7/Lamp1+ vesicles prior to nuclear entry. More importantly, we establish an approach to facilitate improved trafficking of AAV capsids to the nucleus through mutually exclusive, yet synergistic approaches.

2.3 Materials and Methods

Cell culture. HeLa, HepG2, and Huh7 cells were maintained in Dulbecco's Modified Eagle's Medium with 10% FBS, 100 U/ml of penicillin, 100 µg/ml of streptomycin, and 2.5 µg/ml of amphotericin B (Sigma-Aldrich, St. Louis, MO). Human fibroblasts (AG05244) were obtained from Coriell Cell Repositories (Camden, NJ) and were maintained in Dulbecco's Modified Eagle's Medium with 15% FBS, 100 U/ml of penicillin, and 100 µg/ml of streptomycin. All cells were maintained at 37°C and 5% CO2.

Antibodies, chemicals, and cell labeling reagents. Mouse anti-VCP (ab11433), rabbit anti-VCP (ab109240) and mouse anti-actin (ab3280) antibodies were obtained from Abcam (Cambridge, MA). Rabbit anti-EEA1 (C45B10) and rabbit anti-Golgin97 (D8P2K) were obtained from Cell Signaling (Danvers, MA). Rabbit anti-STX5 (110053) was obtained from Synaptic Systems (Goettingen, Germany). Goat anti-mouse-HRP antibody (32430) was obtained from Thermo-Fisher (Waltham, MA). Anti-capsid protein antibody B1 (161) was used to blot for capsid protein, where anti-capsid antibody A20 (162) was used for immunoprecipitation and immunostaining. EerI (E1286), PR-619 (SML0430), PYR-41 (N2915), 3-methyladenine (M9281), nicardipine (N7510), and spautin-1 (SML0440) were obtained from Sigma-Aldrich (St. Louis, MO). MG132 (10012628) was obtained from Cayman Chemical (Ann Arbor, MI). Bortezomib (S1013) was obtained from Selleck Chemicals (Houston, TX). BacMam 2.0 baculovirus delivering emGFP-tagged Rab7a (late endosomal marker, C10588) and LAMP1 (lysosomal marker, C10596), were obtained from Life Technologies (Carlsbad, CA).

Recombinant AAV Production. Recombinant AAV packaging chicken beta actin (CBA) promoter driven firefly luciferase (fLuc) as well as single-stranded and self-complementary vectors packaging a truncated CBA promoter driving green florescent protein (GFP) reporters were produced in HEK293 cells using the triple plasmid transfection protocol, purified and titers determined as described earlier (113, 163).

Transduction and cell viability assays. Cells were plated at a density of $5x10^4$ cells/well in 24-well plates and allowed to adhere overnight. Unless otherwise indicated, cells were treated with DMSO vehicle control or EerI for 4 hours before transduction with AAV2-CBA-fLuc at 1,000 (vector genomes) vg/cell. Cells were lysed 24 hours after using the luciferase assay system from Promega (Madison, WI) according to manufacturer instructions and read on a Wallac® 1420 Victor3 automated plate reader. Cell viability was assayed using the CellTiter Glo® Luminescent Cell Viability assay from Promega (Madison, WI) according to manufacturer instructions on the same instrument. Experiments were all performed in quadruplicate. For time course studies, EerI was provided at the designated time points by adding concentrated EerI stock solution in media to a final concentration of 10 μM.

Cell surface binding and uptake assays. HeLa cells were plated at a density of $1x10^5$ cells/well in 24-well plates and allowed to adhere overnight. Cells were prechilled at 4°C for 30 min, and then incubated with AAV2 particles at 10,000 vg/cell for 1 hour at 4°C. Cells were then washed with ice-cold PBS to remove unbound virions. Cells were then scraped off the plate and whole genomic DNA extracted using a DNeasy kit (Qiagen). In addition, cells being utilized to monitor viral uptake were transferred to 37°C for 1h, following which cells were trypsinized and washed

3 times with PBS to remove all un-internalized virions. Viral DNA was then extracted using a DNeasy kit (Qiagen).

Confocal Fluorescence Microscopy. Cells were plated on slide covers in 24-well plates at a density of $5x10^4$ cells/well and allowed to adhere overnight. Cells were plated at a density of $2.5x10^4$ cells/well and infected concurrently with the BacMam baculovirus encoding for GFP-tagged endosomal markers (20 copies/cell). Baculovirus was removed from cells 24 hours, and cells allowed to recover for an additional 24 hours prior to further studies. Cells were then treated with EerI 4 hours before incubation with AAV2 at 50,000 vg/cell. After 8 hours, cells were fixed with 2% paraformaldehyde for 15 min and then permeabilized with 0.2% Triton-X for 5 min. Cells were stained with primary antibody overnight at 4°C, and then stained with secondary antibody for 1 hour at 37°C. Cells were then mounted with Prolong Gold Antifade with DAPI (Life Technologies) and imaged using a Zeiss 710 scanning confocal microscope.

Image Analysis. Quantification of AAV particle co-localization with subcellular markers was carried out using ImageJ software using the Colocalization Analysis tools from the Wright Cell Imaging Facility website (http://www.uhnresearch.ca/facilities/wcif). In case of BacMam 2.0 incubated cells, care was taken to include only cells expressing the GFP-tagged vesicle markers in the colocalization analysis. Data is represented as Pearson's correlation coefficients. Briefly, a Pearson's correlation coefficient of 0 represents random localization where a value of 1 represents perfect colocalization. Therefore, a higher coefficient represents greater colocalization of AAV particles with the corresponding subcellular marker.

Statistical analysis. All data is expressed as mean with error bars representing standard error of the mean (SEM). A two-tailed unpaired student t-test was used for all statistical analysis. P values less than 0.05 were considered significant. Asterisks are used to indicate P values as follows: *P < 0.05; **P < 0.01; ***P < 0.005.

2.4 Results

Eeyarestatin I increases AAV transduction. Small molecule inhibitors that augment cellular degradation mechanisms have been used extensively to dissect virus-host interactions (151, 164, 165). We first treated HeLa cells with various small molecules that modulate the cellular ubiquitin proteasome system (UPS) and then incubated the cells with AAV2-CBA-fLuc. Inhibitors of the proteasome, MG132 and bortezomib, increased transduction by approximately a log order (Fig. 3), as reported previously (73, 141). Interestingly, PR-619, a pan-deubiquitinase (DUB) inhibitor, did not alter transduction, while PYR-41, an inhibitor of the ubiquitin activating enzyme UBA1, increased transduction to a degree similar as the proteasome inhibitors (Fig. 3). We then investigated a potential role for autophagy in AAV transduction, which has recently been shown to be critical in the infection pathway of numerous viruses (153-155). However, neither the autophagy inducer, nicardipine nor the autophagy inhibitor, spautin-1 altered AAV transduction (Fig. 4). We then tested endoplasmic reticulum associated degradation (ERAD) using two inhibitors, eeyarestatin I (EerI) and kifunensine (Kif). Interestingly, while Kif treatment did not significantly alter transduction, EerI treatment led to a transduction increase of approximately a log order (Fig. 5).

Since EerI has been shown to directly interact with the AAA+ ATPase VCP/p97 (166), we utilized 3 additional VCP inhibitors, ML240, NMS-873, or DBeQ to recapitulate these

results. However, as shown in Fig. 6A, none of the VCP inhibitors increased rAAV transduction with the exception of EerI. It should be noted that siRNA-mediated knockdown of VCP/p97 accompanied by significant cytotoxicity (>50%) precluding efforts to directly address the potential (indirect) role of VCP/p97 in AAV transduction (data not shown). To confirm whether the increase in transduction efficiency was due to pleiotropic effects of EerI, we transfected HeLa cells with the pTR-CBA-fLuc packaging plasmid as control, allowed 48 hours for transgene expression, and then treated the cells with EerI for 24h. We observed no change in fLuc expression as a result of EerI treatment (Fig. 6B), confirming that the effect seen exclusively affects AAV transduction and does not enhance transcription, transcript or protein stability in general.

Next, we investigated the effect of altering EerI concentration or virus dose on transduction. We observed a dose dependent increase of AAV transduction at EerI concentrations up to 15 μM, after which a decrease in transduction efficiency was observed due to cytotoxicity (Fig. 6C). Further, at an optimal EerI concentration of 10 μM, we observed a uniformly beneficial effect on transduction efficiency in HeLa cells over a broad range of viral doses ranging from 10 to 10,000 vg/cell (Fig. 7A).

EerI enhances AAV transduction independent of capsid, vector genome or cell type. We next sought to investigate whether varying AAV capsid types or cell types affected the ability of EerI to enhance transduction. We investigated this possibility by incubating HeLa cells with numerous AAV serotypes at 1,000 vg/cell. As seen in Fig. 7B, EerI uniformly increases the transduction of all serotypes tested, although at varying levels. In addition, transduction was increased in other human cell types tested, albeit at different optimal EerI concentrations based

on the toxicity profile (Fig. 8A). Further, we determined that EerI enhances transduction by AAV vectors packaging single-stranded (ss) or self-complementary (sc) GFP reporter cassettes in a similar fashion (Fig. 8B). Taken together, these data demonstrate that EerI increases transduction regardless of capsid, second strand synthesis or cell type.

EerI redistributes AAV from a perinuclear pattern to large, dispersed vesicles in the cytoplasm. Given the broad impact of EerI on AAV transduction, we assessed whether these effects were preceded by notable changes in the intracellular trafficking of AAV particles through confocal fluorescence microscopy studies. Specifically, we pre-treated HeLa cells with EerI and incubated the cells with AAV2 particles, followed by immunofluorescent labeling of AAV capsids and VCP at 2 hours, 4 hours, and 8 hours post-incubation. We observed no signification correlation between the intracellular patterns of VCP (the apparent target of EerI discussed later), and AAV capsid immunostaining at 2, 4 or 8 hours post-incubation with or without EerI treatment (Figs. 9A-C). As seen in higher magnification images (bottom panels), a steady increase in the perinuclear accumulation of AAV particles was observed over time. At 8 hours post-incubation (Fig. 9C), we observed that AAV particles redistributed from a perinuclear location to a large and dispersed punctate pattern throughout the cytoplasm upon VCP inhibition. This observation strikingly contrasts with DMSO treated cells, in which AAV virions remain concentrated in the perinuclear region (Fig. 9C, bottom panel).

EerI redirects AAV particles to late endosomes and lysosomes. In an effort to identify the nature of the punctate structures formed in the cytoplasm upon EerI treatment, we utilized the BacMam 2.0 system from Life Technologies, which allowed the delivery of GFP-tagged

versions of different endosomal markers, specifically Rab7 (late endosome) and LAMP1 (lysosome) using baculoviral expression vectors. In addition, we utilized an EEA1 antibody to stain for early endosomes. At 8 hours post-incubation, AAV particles did not appear to colocalize with EEA1+ vesicles (data not shown), indicating that AAV is not associated with early endosomes at this time interval. However, AAV particles colocalized prominently with Rab7+ (Fig. 10A) and more extensively with LAMP1+ vesicles in EerI treated cells (Fig. 10B). This increased colocalization was further confirmed by quantitation of fluorescent signal using Image J software as outlined in methods. In particular, we determined the Pearson coefficients (Table 1) for AAV particle colocalization with different subcellular markers including EEA1 (early endosomes), Rab7a (late endosomes), LAMP1 (lysosomes), Golgin-97 (Golgi) and STX5 (syntaxin 5). A statistically significant increase in Pearson's coefficients was noted for redistribution of AAV particles to Rab7 and Lamp1+ vesicles.

EerI influences an early, post-entry trafficking event during AAV transduction. To further understand the effect of EerI on AAV transduction, we systematically investigated the impact of EerI treatment on each step of the AAV intracellular trafficking pathway. First, we assessed whether EerI affects early steps during transduction, i.e., AAV capsid binding to the cell surface and endocytic uptake. As seen in Figs. 11A & 11B, EerI treatment does not alter the number of bound virions attached to the cell surface nor internalized virions at 1hr post-incubation. Further evidence supporting the notion that EerI influences a downstream step in the AAV trafficking pathway was obtained by treating cells at different time intervals before or after viral incubation. As shown in Fig. 11C, the beneficial effect of EerI on AAV transduction gradually weakened when added at later time intervals. Specifically, EerI addition as late as 4 hours after incubation

with viral particles increased AAV transduction, albeit, to a lesser degree compared to drug pre-treatment. By 8 hours post AAV incubation, addition of EerI no longer affected transduction efficiency. When considered together with confocal fluorescence data, these results suggest that EerI treatment remodels endocytic sorting of AAV particles after cellular uptake, but prior to nuclear entry.

EerI and MG132 enhance AAV transduction in a mutually exclusive manner. We next sought to characterize any similarities and/or differences of proteasome inhibitors and EerI on AAV transduction. Confocal microscopy experiments revealed a stark difference in capsid accumulation upon treatment with either EerI or MG132. As seen in Fig. 12A, where EerI treatment results in accumulation in enlarged vesicles, MG132 treatment leads to a more disseminated capsid accumulation in the perinuclear region. Further, proteasomal inhibition is thought to directly enhance AAV transduction by preventing capsid degradation in the cytosol. As a consequence, enhanced recovery of intact AAV capsids and genomes from the nuclear fraction has been reported by several groups (73, 85, 139, 142, 160). In the current study, upon EerI treatment, we observed a striking increase in the number of AAV genomes recovered after synchronized cellular uptake at later time intervals (Fig. 12B). These results were essentially identical to those obtained upon proteasomal inhibition with MG132. Specifically, no differences in recovered vg were observed at early time intervals up to 4 hours. However, as much as 80-90% of AAV genomes were recovered at 16-24 hours upon treatment with EerI in contrast to 25-35% of AAV genomes obtained from untreated cells. This data might indicate that EerI treatment appears to indirectly help protect AAV genomes from rapid degradation, in a similar manner as proteasome inhibitors.

The above described results prompted us to further consider the possibility that EerI might not only remodel endocytic sorting, but also influence AAV capsid degradation in a pleiotropic manner. To assess this possibility, cells were co-treated with EerI and MG132, alone or in combination. It is noteworthy to mention that these studies were optimized to minimize the combined cytotoxicity arising from dual drug treatment. As seen in Fig. 12C, EerI enhanced AAV transduction by 4-fold; while MG132 was twice as effective, resulting in a ~ 8-fold increase in transduction. Importantly, combined drug treatment was synergistic and enhanced AAV transduction by nearly 15-fold. These results demonstrate that cellular degradation pathways can influence AAV infection in distinct ways, which, when modulated in conjunction, can have cumulatively enhance AAV transduction.

2.5 Discussion

EerI is widely viewed as an ERAD inhibitor that is also capable of augmenting the unfolded protein response (167). In addition, EerI has been shown to block Sec61-mediated protein translocation from the cytosol into the ER (168) and was recently shown to affect productive ER exit of BK Polyomavirus (151). Intriguingly, EerI has also been reported to interfere with both retrograde as well as anterograde trafficking of endocytic cargo (169). Specifically, treatment with this drug not only delayed the trafficking of Shiga toxin to the perinuclear region and the Golgi, but also delayed escape of diphtheria toxin into the cytosol from acidified vesicles. In the current report, we observed that EerI treatment remodels the endocytic sorting of AAV particles from a conventional, Golgi-directed retrograde pathway towards late endosomes and/or lysosomes. Specifically, a large number of AAV particles were segregated in large Rab7/LAMP1+ vesicles. These observations are supported in part by earlier

studies that reported a dramatic increase in the size of endosomes upon EerI treatment (170). Further, these observations are consistent with earlier reports demonstrating that AAV transport through Rab7+ late endosomes/lysosomes is highly productive due to their high motility and faster retrograde velocities compared to early/recycling endosomes in neurons (80). Such a scenario is possible due to the low pH and high protease activity within such vesicles that could more effectively prime the AAV capsid (171) by exposing the VP1 phospholipase A2 (PLA2) domain (30) and nuclear localization signals (NLS) (31).

Another important observation is that EerI treatment completely remodeled AAV trafficking to the microtubule organizing center (MTOC) in the perinuclear region. Previous studies have indicated that AAV transduction efficiency is affected by knockdown of proteins involved in sorting retrograde cargo, such as syntaxin 5, calnexin, KDEL-R and other Golgi/ER-associated proteins (70, 71). In the current study, EerI treatment appears to decrease the colocalization of AAV particles with markers such as STX5 and Golgin-97 (Table 1), although these results were not statistically significant. Nevertheless, our results suggest that efficient vesicular trafficking can enhance AAV transduction. This overall approach towards improved AAV trafficking (depicted in Fig. 13) is further supported by (i) the increased recovery of vector genome copy numbers from within cells at time intervals as late as 16-24 hours following EerI treatment similar to that observed with the proteasomal inhibitor, MG132 and (ii) the cumulative effects of EerI and MG132 on AAV transduction.

At the mechanistic level, EerI has been shown to directly bind Valosin-containing protein (VCP) or p97, an essential component of the ERAD machinery (166, 172). However, we note that attempts to modulate AAV transduction by using other small molecule VCP inhibitors (Fig. 6A), siRNA-mediated knockdown of VCP/p97 or colocalize AAV capsids with VCP/p97

through confocal microscopy or immunoprecipitation studies were unsuccessful (data not shown). These studies are also particularly challenging due to overt toxicity displayed during RNAi-mediated knockdown of VCP as well as over-expression of wildtype or dominant negative forms of VCP. Thus, it is important to consider the pleotropic effects of chemical inhibitors such as EerI in such studies. This aspect is also consistent with earlier reports, where EerI has been shown to augment cellular processes separate from ERAD (168-170, 173). Thus, the exact molecular mechanism(s) that are implicated in the current study remain to be determined.

A key question is whether such studies have the potential for translational impact in recombinant AAV vector-mediated gene therapy. In this regard, numerous chemical inhibitors of VCP, including EerI are currently being evaluated for their potential as chemotherapeutics (174, 175). However, similar to proteasome inhibitors such as bortezomib, the effective dose and toxicity of such agents will need to be determined in preclinical animal models as well as the clinic prior to potential applications in the gene therapy setting. Nevertheless, our study constitutes an important step forward in understanding the interplay between different cellular degradation pathways that influence AAV trafficking and highlight potential strategies to modulate the same.

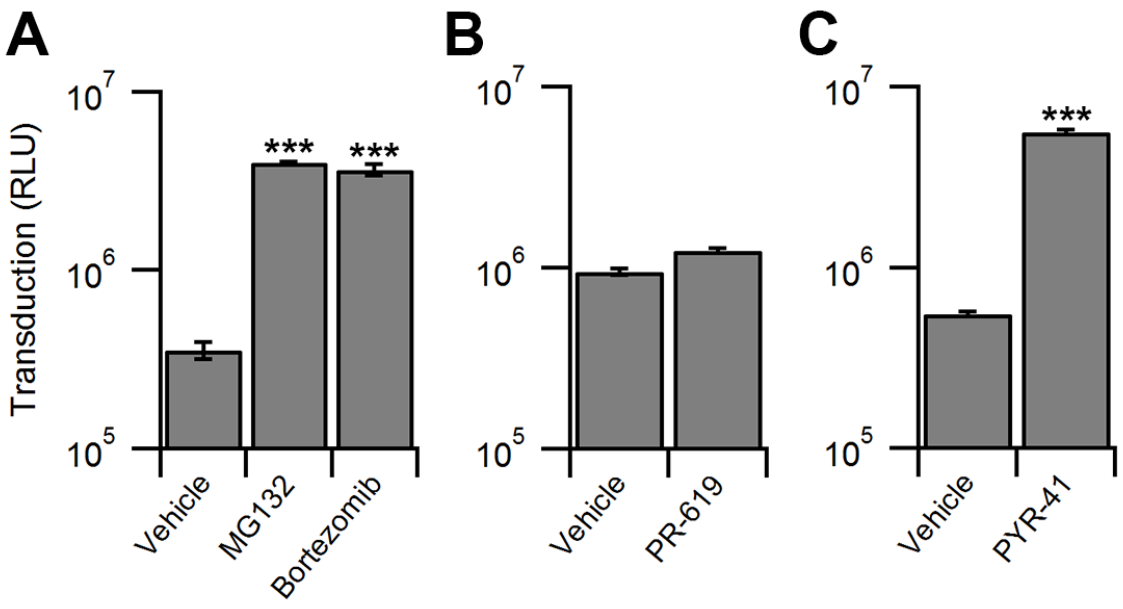

Figure 3: The ubiquitin proteasome system, but not deubiquitinases, impact AAV transduction. Luciferase reporter expression in HeLa cells pretreated with vehicle controls or inhibitors of the ubiquitin proteasome system and transduced with AAV2-Luc. Effect of proteasome inhibitors (A) MG132 (10 µM) and bortezomib (500 nM), (B) the pan-DUB inhibitor PR-619 (5 µM) or (C) the UBE1 inhibitor PYR-41 (50 µM).

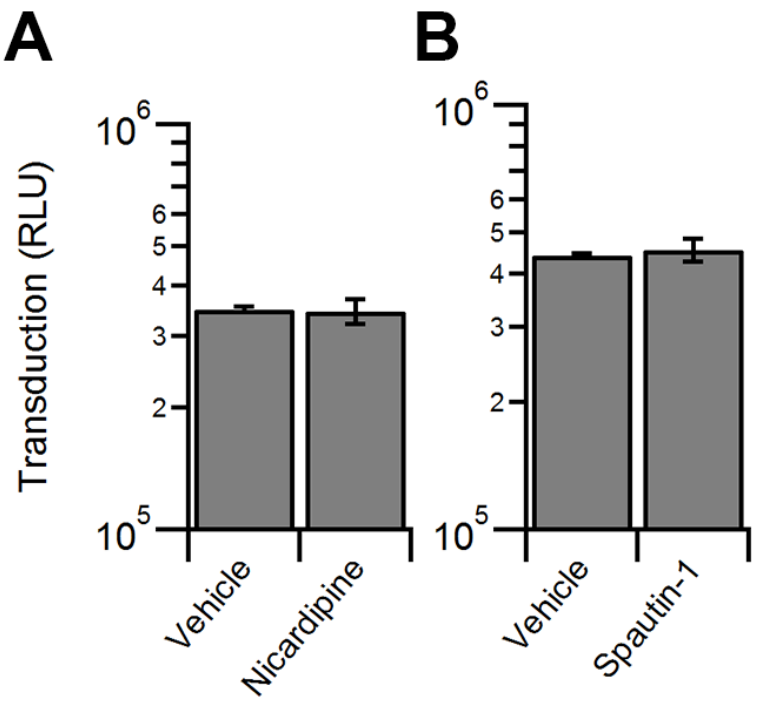

Figure 4: Modulation of autophagy does not impact AAV transduction. HeLa cells pretreated with vehicle control or autophagy modulators (A) Nicardipine (5 µM) or (B) Spautin-1 (10 µM) transduced with AAV2-Luc.

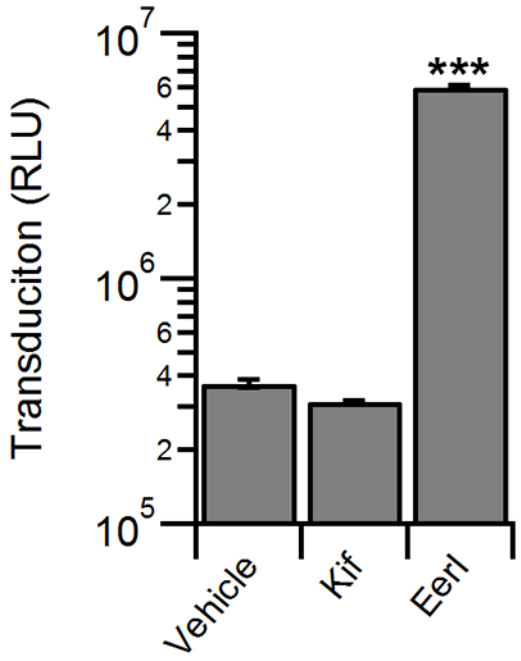

Figure 5: The ERAD inhibitor EerI, but not Kif, increases AAV transduction. HeLa cells pretreated with vehicle control or ERAD inhibitors eeyarestatin I (EerI, 10 µM) or kifunensine (Kif, 1 µM) transduced with AAV2-Luc vectors

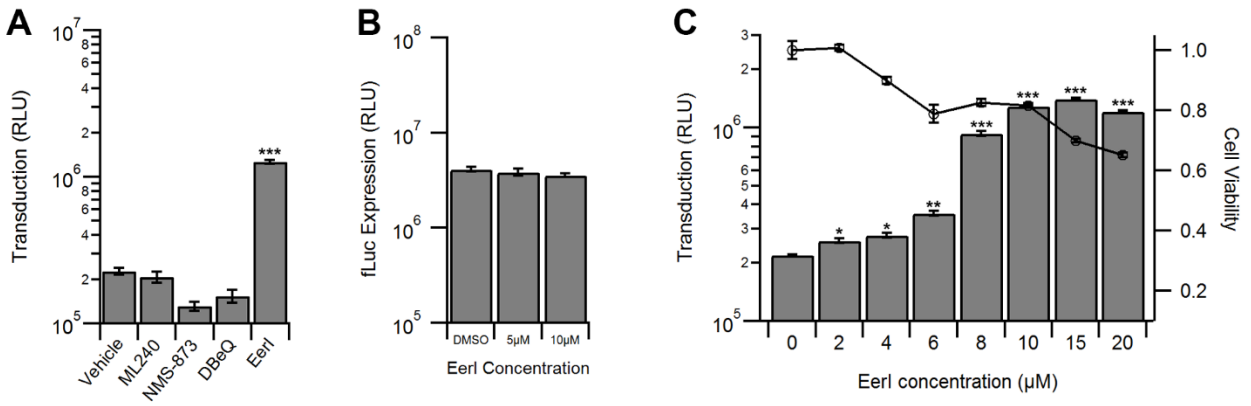

Figure 6: EerI increases vector transduction in a dose dependent manner. (A) Luciferase reporter expression in HeLa cells pretreated with vehicle control, 1 μM ML240, 1 μM NMS-873, 10 μM DBeQ, or 10 μM EerI were transduced with AAV2-Luc. (B) Luciferase expression in HeLa cells transfected with the pTR-CBA-Luc plasmid and treated with various concentrations of EerI 48h post-transfection. (C) HeLa cells pretreated with various concentrations of EerI and transduced with AAV2-Luc (grey bars) or subjected to a Cell-Titer Glo assay to determine cell viability (circles).

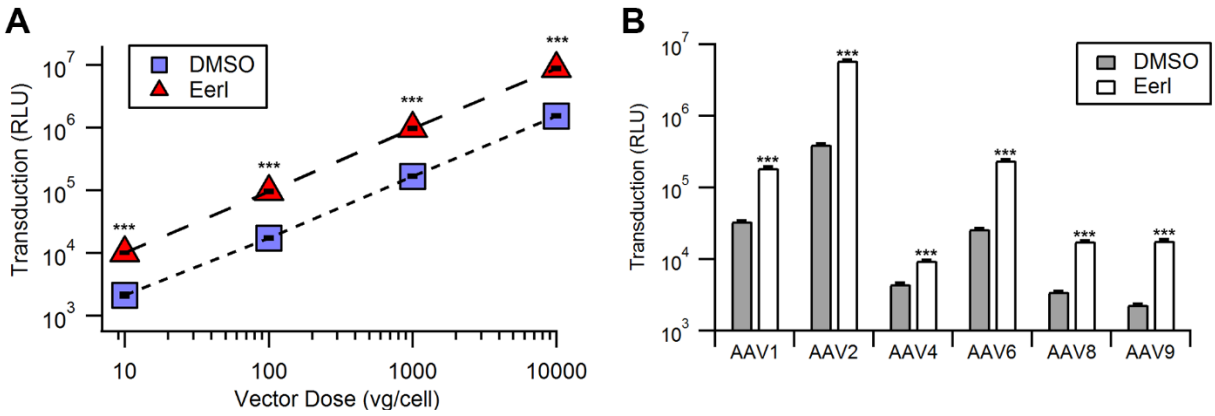

Figure 7: EerI increases vector transduction in a vector dose and serotype independent manner. (A) HeLa cells pretreated with either DMSO control (squares) or EerI (triangles) and transduced with AAV2-Luc at increasing vector genome copies (vg) per cell. (B) HeLa cells were pretreated with DMSO control (grey bars) or EerI (white bars) and transduced with various AAV serotypes packaging the Luc transgene cassette.

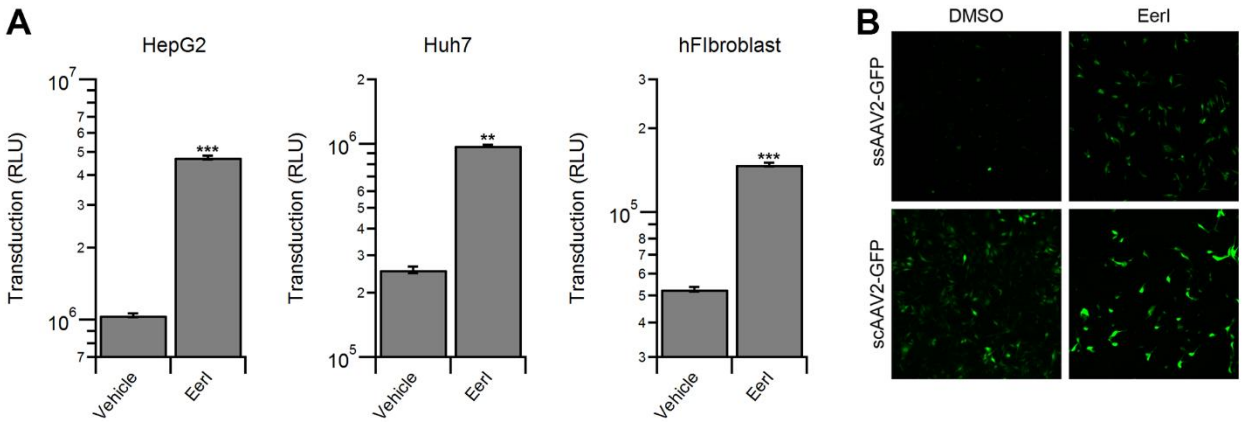

Figure 8: EerI increases vector transduction in a cell type and genome type independent manner. (A) HepG2, Huh7, and human fibroblasts (hFibro) were pretreated with EerI at concentrations individually optimized to limit cytotoxicity (HepG2, 8 µM; Huh7, 4 µM; hFibro, 4 µM) and transduced with AAV2-CBA-Luc. (B) HeLa cells were pretreated with DMSO control or EerI and then transduced with either single-stranded ssAAV2-GFP vectors or self-complementary scAAV2-GFP vectors. Cells were fixed 24h and imaged using confocal microscopy.

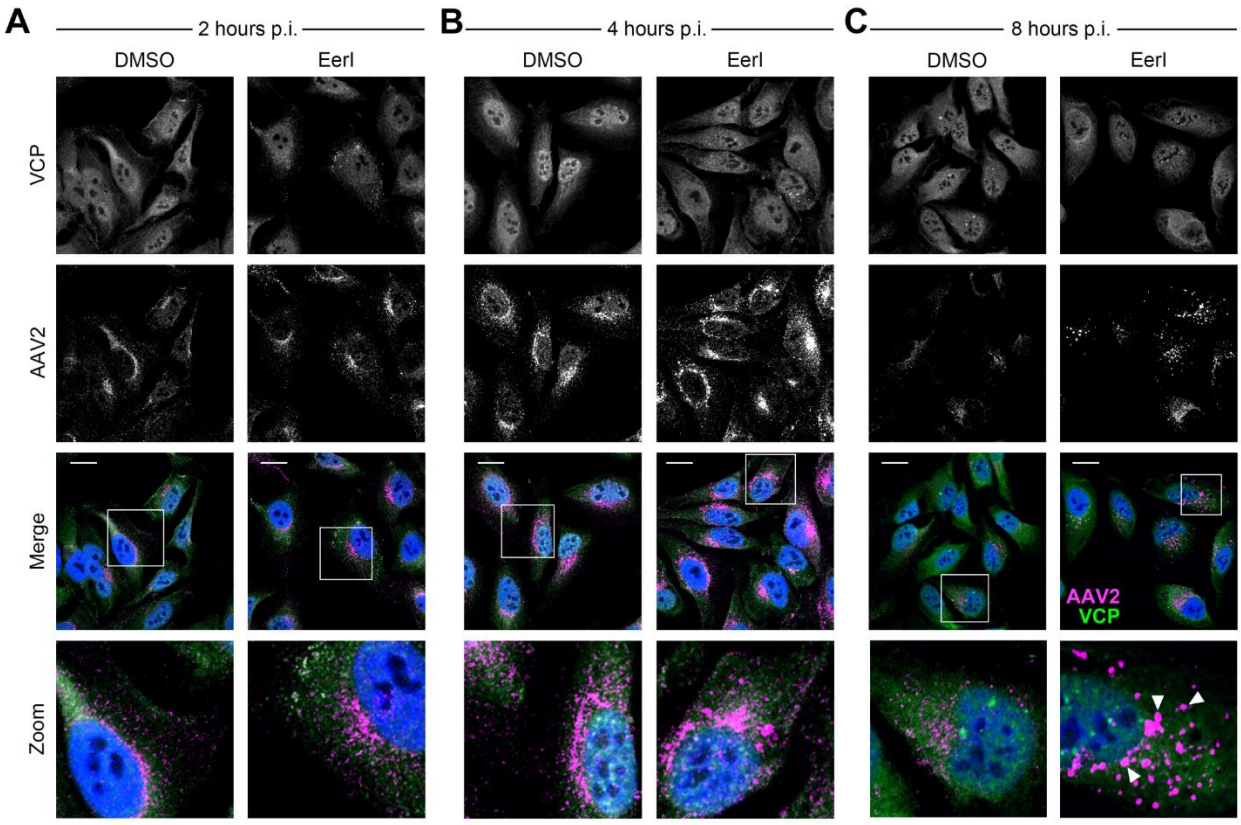

Figure 9: EerI redirects AAV particles from a perinuclear pattern to a dispersed cytosolic punctate pattern. Confocal micrographs of HeLa cells pretreated with EerI and transduced with AAV2-Luc at 50,000 vg/cell. Cells were fixed at 2h (A), 4h (B), and 8h (C), immunostained for VCP (green) and AAV2 capsid (magenta) as outlined in methods and counterstained with DAPI (blue). White inset boxes indicate areas imaged at higher magnification. Scale bar = 20 µm.

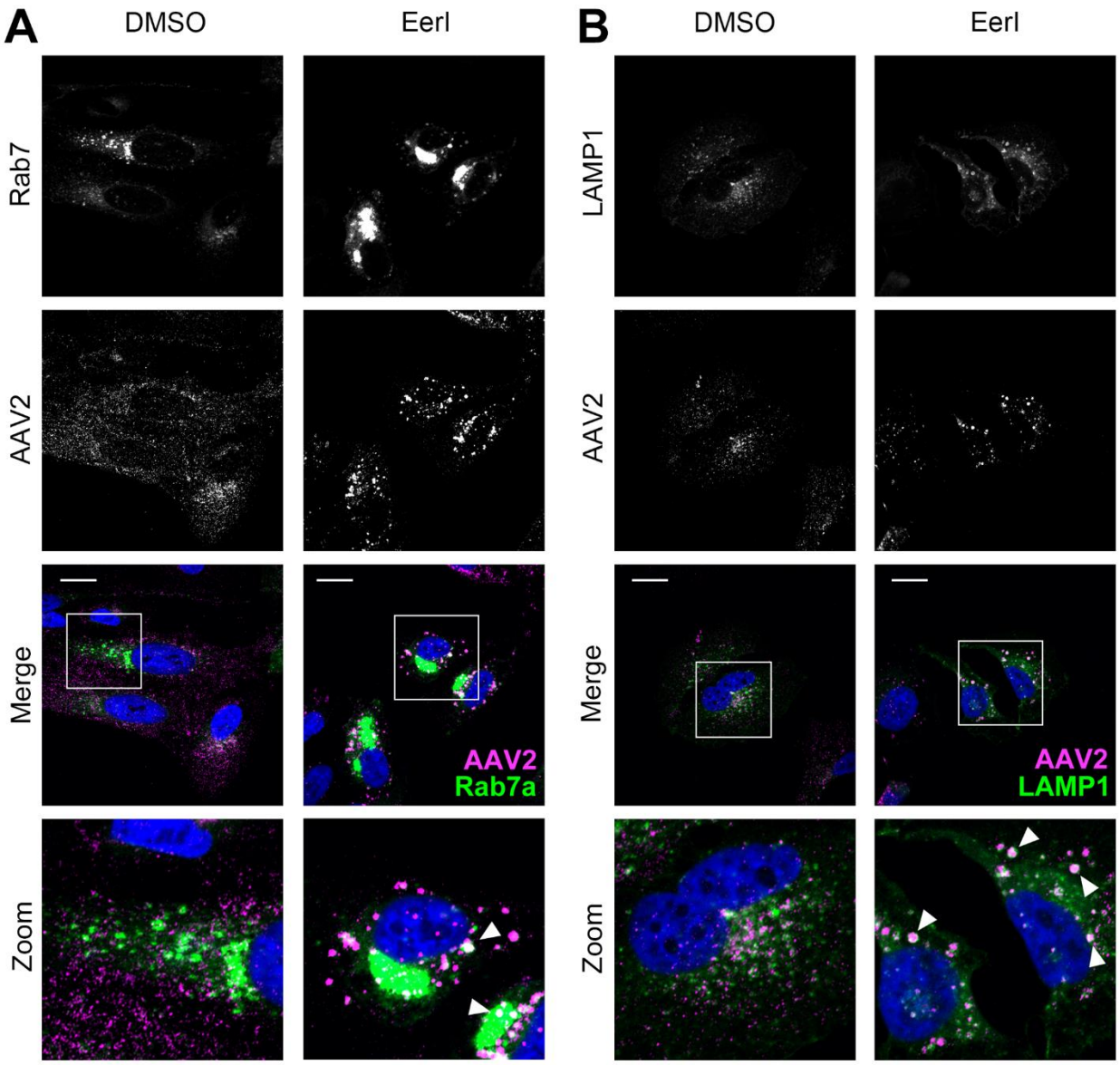

Figure 10: AAV particles accumulate within enlarged Rab7+ and Lamp1+ vesicles upon treatment with EerI. Confocal micrographs of HeLa cells infected with BacMam baculovirus encoding for GFP-Rab7a (A) or GFP-LAMP1 (B). Cells were pretreated with DSMO or EerI at 72 hours post-plating and incubated with AAV2-Luc at 50,000 vg/cell. Cells were then fixed at 8h and immunostained for AAV capsid (magenta), and counterstained with DAPI (blue). White inset boxes indicate areas imaged at higher magnification. Scale bar = 20 µm.

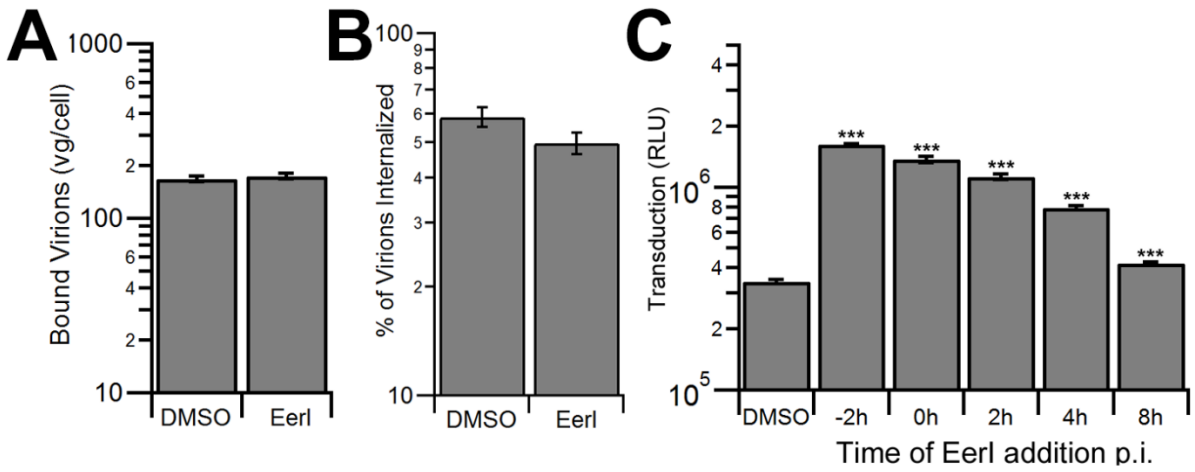

Figure 11: EerI does not alter binding or internalization of AAV. (A) Cell surface binding of AAV particles incubated on HeLa cells that were pretreated with DMSO or EerI. Viral particles were incubated on cells at 4°C for 1h, following which cells were washed to remove unbound virus and cell surface-associated vector genome DNA quantified by qPCR. (B) HeLa cells incubated with AAV particles at 4°C for 1h were washed to remove unbound virions and then shifted to 37°C for 1h to allow cellular uptake. Cells were then treated with trypsin to remove surface bound virions and internalized virions quantitated by qPCR. (C) Luciferase expression in HeLa cells treated with DMSO control or EerI at various time intervals prior to transduction with AAV2-Luc vectors.

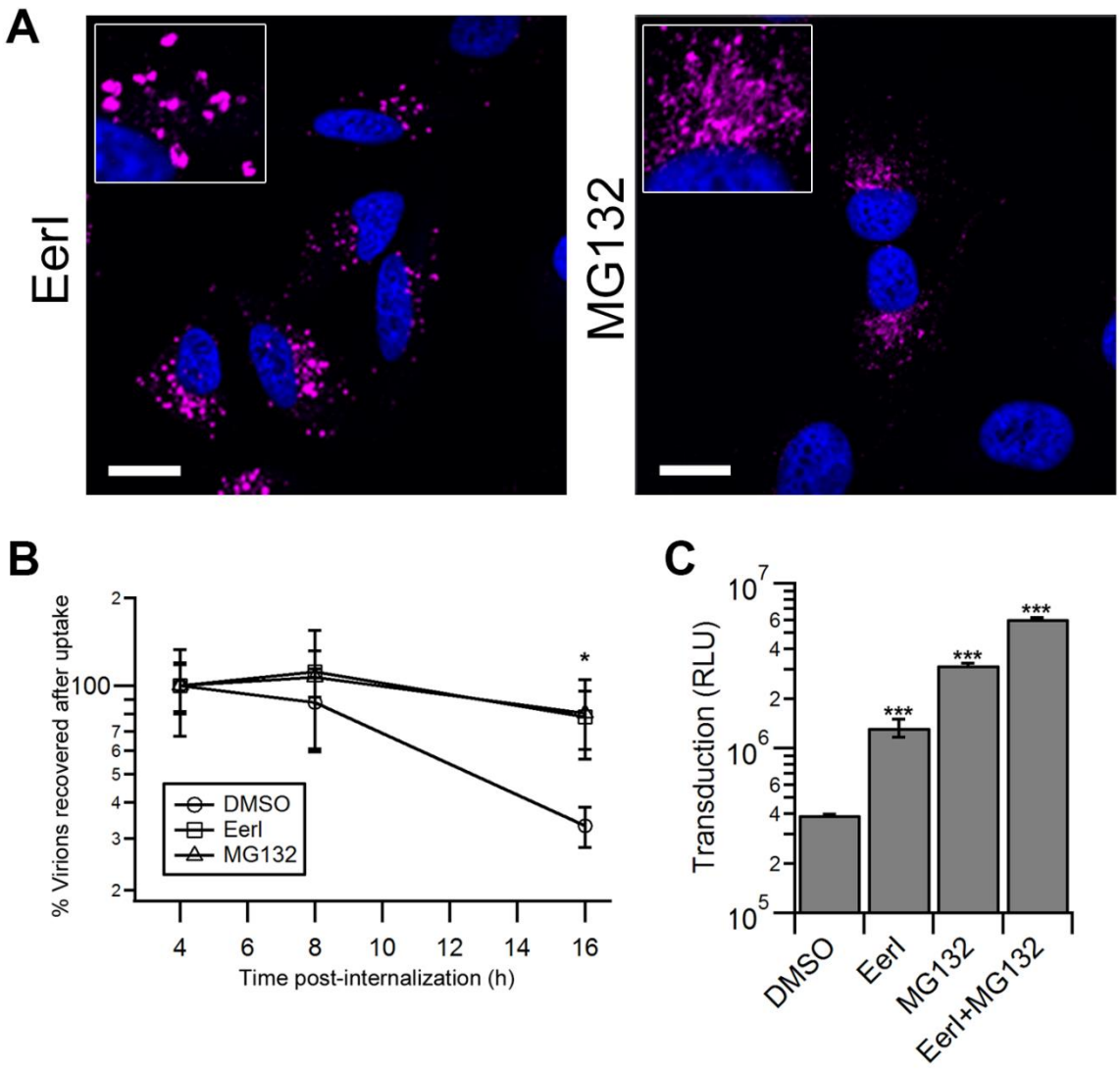

Figure 12: EerI and MG132 increase AAV transduction through distinct, yet cumulative mechanisms. (D) Confocal micrographs of HeLa cells pretreated with EerI or MG132 and incubated with AAV particles at 50,000 vg/cell. Cells were fixed at 8h, immunostained for AAV capsids (magenta) and counterstained with DAPI (blue). (E) Recovery of internalized vector genome-containing particles at different time intervals from HeLa cells pretreated with DMSO, EerI, or MG132 and transduced with AAV2-Luc as described above. (F) Luciferase expression in HeLa cells pretreated with DMSO control, EerI, MG132, or EerI and MG132 in combination and transduced with AAV2-Luc. At 4 hours post-incubation, the drugs and virus were removed and replaced with fresh pre-warmed media.

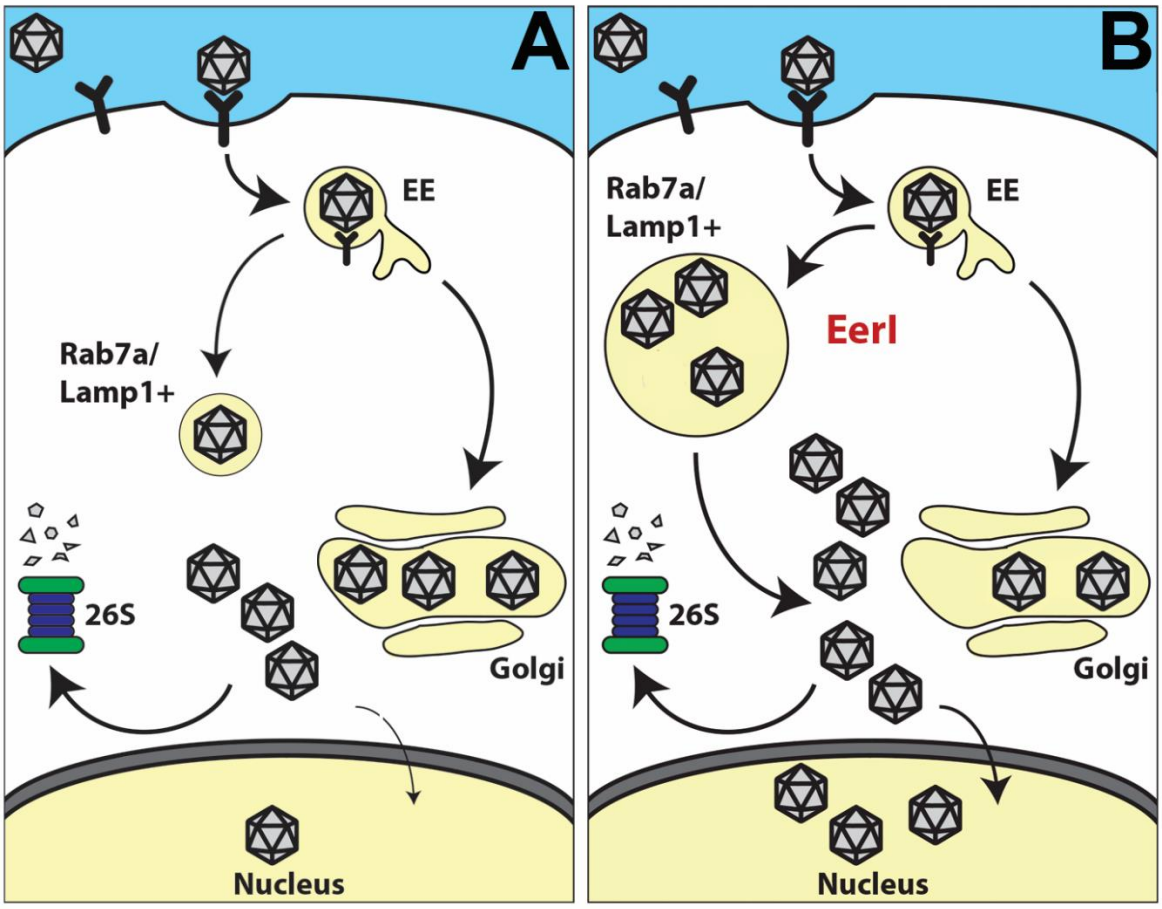

Figure 13: Schematic outlining a potential approach to enhance transduction by redirecting the vesicular trafficking of AAV particles. (A) Following cellular uptake, AAV virions are subjected to endosome-to-lysosome transport as well as retrograde transport from early endosomes to the Golgi leading to perinuclear accumulation. Cytosolic escape of AAV particles results in processing by the ubiquitin-proteasome system, which in turn limits nuclear entry and transduction efficiency. (B) In cells treated with EerI, virions appear to accumulate within Rab7a/Lamp1+ vesicles instead of a perinuclear pattern due to an unknown mechanism. Sequestration from proteasomal processing and efficient 'priming' of AAV capsids could result in increased nuclear entry and subsequent transduction.

Subcellular marker	DMSO	EerI	P-value
EEA1	0.198 ± 0.018	0.252 ± 0.040	n.s.
Rab7a	0.216 ± 0.019	0.342 ± 0.024	*P < 0.05
LAMP1	0.269 ± 0.036	0.439 ± 0.025	*P < 0.05
Golgin97	0.379 ± 0.025	0.312 ± 0.032	n.s.
STX5	0.453 ± 0.009	0.334 ± 0.042	n.s.

Table 1: Pearson coefficients for AAV colocalization with subcellular markers. Capsid immunofluorescence was determined using the A20 monoclonal antibody. Values are depicted as mean ± standard error. *P<0.05 - significant; n.s. – not significant.

CHAPTER 3: Modulation of intracellular calcium influences recombinant AAV transduction[3]

3.1 Overview

Calcium is known to play a crucial role in numerous cellular processes, generally acting as a regulator of cell signaling. Intracellular calcium is also important in the life cycles of several viruses, such as Ebola virus and rotavirus. Several small molecules and clinical compounds exist that modify the cellular calcium environment, allowing further study of intracellular calcium *in vivo*. In the current study, we sought to determine if modulation of intracellular calcium levels affects AAV transduction. Increasing intracellular calcium levels using ionomycin decreased AAV transduction by an order of magnitude while decreasing intracellular calcium levels using BAPTA-AM increased transduction by 10 to 100-fold independent of vector serotype, vector dose, or vector genome. Ionomycin and BAPTA-AM altered binding of AAV particles to the cell surface by 2-fold. In addition, RNA transcription from the vector genome was also altered by ionomycin and BAPTA-AM. Furthermore, the effect of BAPTA-AM was dependent upon the presence of extracellular calcium. In addition, *in vivo* studies performed in mice illustrate that BAPTA-AM augments transduction by AAV when administered intracranially. In summary, our results demonstrate that modulation of intracellular calcium alters AAV transduction and supports the preclinical evaluation of drugs and biologics that modulate intracellular calcium in the CNS as a strategy to increase AAV gene delivery.

[3] This chapter includes the original publication in review: Berry, G.E., Nardone-White, D.T., Murlidharan, G., Reardon, R.A., Asokan, A. *Modulation of intracellular calcium influences recombinant AAV transduction*.

3.2 Introduction

Intracellular calcium is known to play an important role in cellular homeostasis, primarily acting as an important cell signal regulator (176). Dysregulation of intracellular calcium homeostasis is a hallmark of several neurological diseases, including Alzheimer's disease and spinocerebellar ataxia, generally leading to neuronal cell death (177-182). One of the most thoroughly characterized calcium-dependent cellular processes is the fusion of synaptic vesicles with the plasma membrane in neurons (183-185). However, it is also known that protein transport within the cell can be controlled by calcium. Previously, calcium has been shown to be important in specific events during retrograde and anterograde transport of vesicles in the cell (186). While some viruses, such as influenza A, require calcium dependent cell signaling for infection (187), several viruses have demonstrated the need to modify the intracellular calcium environment to successfully infect cells. For instance, rotavirus encodes for a viroporin, a viral protein that permeabilizes the cell membrane, which specifically alters intracellular calcium to promote its own replication (188, 189). Ebolavirus (EBOV) requires calcium to successfully bud from the cell surface (190). Additionally, it was recently demonstrated that two host cell calcium pore channels are required for EBOV cellular entry, further suggesting that intracellular calcium plays a crucial role in EBOV infection (191).

Parvoviruses are single-stranded DNA viruses that contain a calcium-dependent phospholipase A2 (PLA2) domain essential for infectivity (192). Specifically, parvoviruses with mutated PLA2 domains are endocytosed efficiently, but are defective in later infectivity steps, resulting in reduced genome delivery to the nucleus (193). In the case of human parvovirus B19, activity of the PLA2 domain has also been shown to activate the store-operated Ca^{2+} channel I_{CRAC}, increasing cytosolic calcium concentrations (194). Furthermore, the enzymatic activity of

calcium-dependent PLA2 is directly correlated to calcium concentration (195). Additionally, some parvoviruses, such as minute virus of mice and canine parvovirus, have been shown to have surface loops that bind calcium, and in some cases, this activity is essential for virus infectivity (196, 197). Adeno-associated virus (AAV) is a member of the *Parvoviridae* family that has demonstrated promise as a recombinant vector for gene delivery. This small (~25 nm in diameter), nonpathogenic virus contains an ssDNA genome of ~4.7 kb. AAV capsids are made of 3 viral proteins (VPs) that are the result of alternative splicing and start codons, named VP1, VP2, and VP3, in order of decreasing molecular weight (198). VP1 is the only AAV capsid subunit that contains a PLA2 domain (30). Additionally, AAV capsids are generally assembled with a VP1:VP2:VP3 ratio of approximately 1:1:10 (29). Therefore, each AAV capsid has ~5 calcium dependent PLA2 domains. There are numerous naturally occurring AAV isolates that utilize a range of glycan receptors for cell surface attachment and glycoprotein receptors for cell entry, respectively. Several strains have been shown to utilize integrins as glycoprotein receptors, and more recently, KIAA0319L, or AAVR, has also been shown to be an important glycoprotein receptor for many strains (49, 50, 52, 53). However, despite the diverse mechanisms employed for cell surface binding and entry, many downstream trafficking steps in the AAV infectious pathway appear to be broadly conserved (199).

Several studies have characterized the infectious pathway of AAV, beginning with binding to cell surface glycans and culminating in mRNA transcribed from the AAV genome. In particular, a broad spectrum of small molecule compounds have provided significant insight into the role played by different host cell factors in AAV infection (199). In the current study, we utilized ionomycin and BAPTA-AM, intracellular calcium modulators, to study the impact of modulating intracellular calcium on AAV transduction. Overall, we attempted to identify steps in

the AAV infectious pathway that may be sensitive to intracellular calcium levels. Here, we establish two possible roles for intracellular calcium in the AAV infectious pathway. In addition, we demonstrate modulation of calcium as a strategy to increase AAV transduction *in vivo*, particularly for CNS gene transfer applications.

3.3 Materials and Methods

Cell culture. HeLa cells were maintained in Dulbecco's Modified Eagle's Medium with 10% FBS, 100 U/ml of penicillin, 100 µg/ml of streptomycin. MB114 cells were maintained in Dulbecco's Modified Eagle's Medium with 5% FBS, 100 U/ml of penicillin, and 100 µg/ml of streptomycin. All cells were maintained at 37°C and 5% CO2.

Antibodies, chemicals, and cell labeling reagents. Rabbit anti-LaminB1 (12586) was obtained from Cell Signaling (Danvers, MA). Goat anti-mouse-HRP antibody (32430) and Fluo-4-AM (F14201) was obtained from Thermo-Fisher (Waltham, MA). Rabbit anti-GFP (G10362) was obtained from Life Technologies (Carlsbad, CA). Anti-capsid protein antibody B1 was used to blot for capsid protein. Ionomycin (2092) and BAPTA-AM (2787) were obtained from Tocris Bioscience (Minneapolis, MN). Bortezomib (S1013) was obtained from Selleck Chemicals (Houston, TX).

Virus Production. Recombinant AAV packaging chicken beta actin (CBA) promoter driven firefly luciferase (fLuc) as well as single-stranded and self-complementary vectors packaging a truncated CBA promoter driving green florescent protein (GFP) reporters were produced in HEK293 cells using the triple plasmid transfection protocol and purified as described earlier.

Cell viability assays. Cell viability was assayed using the CellTiter 96® AQueous One Cell Proliferation assay from Promega (Madison, WI) according to manufacturer instructions and read on a Wallac® 1420 Victor3 automated plate reader.

Transduction assays. Cells were plated at a density of $5x10^4$ cells/well in 24-well plates and allowed to adhere overnight. Unless otherwise indicated, cells were incubated with DMSO vehicle control or drug for 4 hours before infection with AAV2-CBA-fLuc at a MOI of 1,000 vg/cell. Cells were lysed 24 hours after infection using the luciferase assay system from Promega (Madison, WI) according to manufacturer instructions and read on a Wallac® 1420 Victor3 automated plate reader. Experiments were all performed in quadruplicate. In the case of self-complimentary virus, cells were infected with scAAV2-CBh-GFP at the noted MOI and imaged were acquired using the Evos FL fluorescent microscopy system 24 hours after infection. For time course studies, either drug was provided at the designated time points by adding concentrated drug stock solution in media to the final working concentration, or virus and drug containing media was removed at the designated time point and replaced with drug-containing media without virus.

RNA isolation and quantification. Cells were plated at a density of $1x10^5$ cells/well in 12-well plates and allowed to adhere overnight. Cells were incubated with DMSO vehicle control or drug for 4 hours before infection with AAV2-CBA-fLuc at a MOI of 1,000 vg/cell. RNA was isolated from the cells 24 hours after infection using the TRIzol reagent from Invitrogen (Carlsbad, CA) according to manufacturer instructions. RNA extracts were then DNase treated using the TURBO DNA-free kit from Thermo Fisher (Waltham, MA) according to manufacturer

instructions. Reverse transcription was carried out using SMARTScribe reverse transcriptase from Clontech (Mountain View, CA) with an oligo dT primer. Quantitative PCR was then carried out using the Roche Lightcycler 96 system using primers against luciferase and GAPDH. Fold change was determined by ΔΔCt analysis.

Cell surface binding and uptake assays. HeLa cells were plated at a density of $1x10^5$ cells/well in 12-well plates and allowed to adhere overnight. Cells were prechilled at 4°C for 30 min, and then incubated with AAV2 particles at a MOI of 1,000 vg/cell for 1 hour at 4°C. Cells were then washed with ice-cold PBS to remove unbound virions. DNA was then extracted using a Blood and Tissue DNA Extraction Kit from IBI Scientific (Peosta, IA). In addition, cells being utilized to monitor viral uptake were transferred to 37°C for 1h, following which cells were trypsinized and washed 3 times with PBS to remove all un-internalized virions. DNA was then extracted as described above.

Nuclear fractionation studies. $2x10^6$ HeLa cells were plated on 10 cm plates and allowed to attach overnight. Cells were then infected with AAV2 at a MOI of $1x10^4$ vg/cell. At 16 hours post-infection, nuclear extracts were prepared using the NE-PER kit (78833) from Thermo-Pierce according to manufacturer instructions. Viral capsid accumulation in nuclear extracts was determined by western blot. Determination of nuclear vector genomes was carried out as described previously. Briefly, DNA from nuclear extract was extracted using the Qiagen PCR Purification Kit (Hilden, Germany) with modifications. Quantitative PCR was then performed as described above.

Confocal Fluorescence Microscopy. HeLa cells were plated on a 3.5mm FluoroDish (FD35-100) from World Precision Instruments (Sarasota, FL) and allowed to adhere overnight. Cells were treated with either vehicle control, ionomycin, or BAPTA-AM for 7 hours. Cells were then loaded with 5 μM Fluo4-AM in HBSS for 30 minutes at room temperature. After loading, media containing drug was replaced and the cells were incubated at 37 degrees for an additional 30 minutes prior to imaging. For dextran and transferrin uptake, HeLa cells were plated on glass coverslips and allowed to adhere overnight. Cells were then treated with DMSO, ionomycin, or BAPTA-AM for 4 hours. Cells were then allowed to internalize Alexa Fluor 488-labeled dextran (green) at a concentration of 2.5 mg/ml for 30 minutes, followed by Alexa Fluor 597-labeled transferrin (red) at a concentration of 5 μg/ml for 15 minutes. Cells were then fixed with 2% PFA, counterstained with DAPI (blue), and mounted. Cells were imaged using a Zeiss 710 scanning confocal microscope.

Animal Studies. Animal experiments were carried out with C57/B6 mice bred and maintained in accordance to NIH guidelines and as approved by the UNC Institutional Animal Care and Use Committee (IACUC). Intracerebroventricular (ICV) injections were performed as described previously. Briefly, neonatal postnatal day 0 (P0) pups were rapidly anesthetized by hypothermia for 1 min followed by stereotaxic intraventricular cerebral injections. A Hamilton 700 series syringe with a 26-gauge needle (Sigma-Aldrich) was attached to a KOPF-900 small animal stereotaxic instrument (Tujunga, CA). Mice were injected in their left lateral ventricle with $2x10^9$ vector genome-containing particles of self-complimentary AAV1-CBh-GFP with either vehicle control or BAPTA-AM in a total volume of 3 μl. Mouse brains were harvested 14 days post-injection.

Sectioning, Immunostaining, and analysis of brain tissue. After postfixation in 4% PFA, brains were sectioned into 50 micron sections using a Leica VT1200S vibrating blade microtome. Brains were then were blocked and permeabilized in 10% normal goat serum and 1% Triton X-100 in PBS for 1 hour at room temperature. Primary antibody staining was performed with mouse anti-GFP antibody overnight at 4 degrees. Brains were then DAB stained using the Vectastain ABC Peroxidase Kit (PK-4001) from Vector Laboratories (Burlingame, CA) according to manufacturer instructions. Development of the stained tissues was carried out using the DAB stain kit (D7304) form Sigma-Aldrich (St. Louis, MO). Slides were imaged by the UNC Translational Pathology Laboratory using the Aperio ScanScope XT system. Images were analyzed using the Aperio ImageScope software. Quantification analyses of tissues was performed using ImageJ software.

Flow cytometry. HeLa cells were plated in 6-well plates and allowed to adhere overnight. Cells were then treated with DMSO, ionomycin, or BAPTA-AM for 4 hours. Cells were then allowed to internalize Alexa Fluor 488-labeled dextran (green) at a concentration of 2.5 mg/ml for 30 minutes, followed by Alexa Fluor 597-labeled transferrin (red) at a concentration of 5 μg/ml for 15 minutes. Cells were then washed with PBS and stained with Zombie Violet Live/Dead stain (423113) from Biolegend (San Diego, CA). Cells were then fixed with 2% PFA and analyzed on a CyAn ADP Analyzer flow cytometer from Beckman Coulter (Brea, CA).

Proteasome function assay. HeLa cells were stably infected with lentivirus encoding for blasticidin resistance and ubiquitin-tagged GFP, which is quickly degraded by the proteasome under normal conditions. After 2 weeks of blasticidin selection, cells were treated with DMSO,

ionomycin (10 μM), BAPTA-AM (20 μM), or bortezomib (1 μM). Cells were imaged using an Evos fluorescence microscope at 10X.

Statistical analysis. All data is expressed as mean with error bars representing standard error of the mean (SEM). A two-tailed unpaired student t-test was used for all statistical analysis. P values less than 0.05 were considered significant. Asterisks are used to indicate P values as follows: *P < 0.05; **P < 0.01; ***P < 0.005.

3.4 Results

Ionomycin and BAPTA-AM alter AAV transduction in an opposing manner. In order to investigate whether intracellular calcium levels play a role in rAAV infection, we utilized ionomycin and BAPTA-AM, two small molecules that specifically alter intracellular calcium homeostasis. Ionomycin is an ionophore that allows the flow of calcium across biological membranes, therefore allowing extracellular calcium to flow into the cytosol (200). Additionally, ionomycin releases calcium from the ER into the cytosol (201). BAPTA-AM is a cell permanent version of a highly selective calcium chelator. Once BAPTA-AM enters the cell, cellular esterases cleave off the acetoxymethyl (AM) ester, activating the chelating activity and trapping the molecule inside the cell. After determining the optimal concentration at which both of these compounds do not cause overt toxicity (>80% viability) in each of the cell lines tested (Fig. 14), we determined their effect on AAV transduction. Raising intracellular calcium with ionomycin decreased transduction by 5 to 10-fold in both HeLa and MB114 cells. In contrast, decreasing intracellular calcium by BAPTA-AM increased transduction 10-fold to 100-fold (Fig. 15). This effect was independent of AAV serotype tested.

Next, we utilized fluo-4-AM, a cell permanent calcium indicator, with live cell confocal microscopy to probe the effect of ionomycin and BAPTA-AM on intracellular calcium. Fluo-4 fluorescence intensity increases drastically as a result of calcium binding (202). As expected, the fluo-4 signal increases throughout the cell as a result of ionomycin treatment. Interestingly, however, the overall intracellular signal does not markedly change as a result of BAPTA-AM treatment, although the amount of fluo-4 puncti in each cell appear to increase (Fig. 16A). However, it is worth noting that the levels of cytosolic calcium are known to be in the mid-to-low nanomolar range (203), suggesting that we might not be able to observe any reduction in cytosolic calcium concentration that results from BAPTA-AM treatment with fluo-4. We next investigated whether the levels of extracellular calcium can affect the inhibitory or augmentative effect of ionomycin or BAPTA-AM, respectively, on AAV transduction. Strikingly, while ionomycin continues to inhibit infection in the absence of extracellular calcium in MB114 cells, the transduction increase seen with BAPTA-AM treatment drops from more than 40-fold to less than 3-fold when extracellular calcium is absent (Fig. 16B). Taken together, this data demonstrates that intracellular calcium levels affect AAV transduction, and the presence of extracellular calcium is required for the augmentative effect of BAPTA-AM.

Intracellular calcium affects AAV binding but does not alter synchronized internalization or nuclear capsid accumulation. To understand how intracellular calcium modifies AAV transduction, we sought to investigate several major steps in the AAV infectious pathway. It is worth noting that, due to the mechanism of action of ionomycin and BAPTA-AM, extracellular calcium is not chelated or otherwise altered. Therefore, we did not expect any alteration in capsid binding. However, as shown in Fig. 17A, treatment with ionomycin or BAPTA-AM alters

binding of AAV2 to the cell by approximately 2-fold. Conversely, AAV internalization is not affected by either treatment in a synchronized infection (Figure 17B).

Next, we sought to determine if the levels of AAV in the nucleus are affected by intracellular calcium. As seen in Fig. 18A, quantification of AAV genomes in the nucleus by qPCR demonstrate that nuclear entry of AAV is reduced by approximately 5-fold with ionomycin treatment, indicating that either nuclear import or a previous step is altered. However, there is no observable difference in nuclear genomes upon treatment with BAPTA-AM, indicating that this step in not affected. This result is confirmed by western blot of nuclear protein extracts, demonstrating that the levels of capsid in the nucleus reflect the amount of AAV genomes in the nucleus (Fig. 18B). Densitometry of the blot was performed and confirmed a 5-fold reduction in nuclear capsid accumulation with ionomycin treatment, no difference upon BAPTA-AM treatment and an approximately 2-fold increase upon bortezomib treatment (Fig. 18C). Taken together, this data indicates that modulation of intracellular calcium alters binding by ~2-fold, but other post internalization steps in AAV transduction are also altered.

Transduction increase by BAPTA-AM is dependent upon duration of infection. Next, we sought to determine if there was a time dependent effect of intracellular calcium concentration on AAV transduction. First, we administered ionomycin and BAPTA-AM at different time points during infection and observed the effect on transduction. As seen in Fig. 19A, the inhibitory effect of ionomycin was present up to 2 hours after virus infection. However, when added at 4 hours post-infection or later, ionomycin no longer demonstrated an inhibitory effect. Conversely, BAPTA-AM increased transduction at every time point assessed up to 12 hours post-infection, albeit at steadily decreasing effectiveness (Fig. 19B). Further, we assessed the effect of duration

of viral infection on the transduction of AAV in the presence of small molecule. To achieve this, cells were pretreated with ionomycin or BAPTA-AM, and then infected with AAV2. The virus was then removed at various time points, while the cells remained in the constant presence of either ionomycin or BAPTA-AM. Interestingly, as seen in Fig. 19C, while ionomycin treatment reduced transduction by greater than 10-fold at every time point tested, BAPTA-AM treatment increased transduction by less than 2-fold upon synchronized infection (0h time point). However, the transduction increase grew at every time point to almost 5-fold at 8 hours of continuous infection. This result is unexpected, as it might indicate an effect on internalization. However, internalization is not altered by BAPTA-AM (Fig. 17), indicating that this result is likely due to another mechanism. Taken together, this data further supports the observation that ionomycin likely alters AAV transduction at or before nuclear entry, where BAPTA-AM likely alters transduction at multiple steps in the infectious pathway.

Ionomycin and BAPTA-AM alter AAV transduction independent of viral dose or viral genome via altered transcription. Next, we assessed the effects of ionomycin and BAPTA-AM in relation to viral dose and viral genome composition. As seen in Fig. 20A, the effect of both ionomycin and BAPTA-AM treatment is independent of vector dose. Furthermore, ionomycin and BAPTA-AM alter transduction of self-complementary AAV2 to a similar degree as a single stranded vector (Fig. 20B). We next aimed to rule out pleiotropic effects as a possible cause for the observed transduction changes. To this end, we transfected cells with the pTR-CBA-fLuc packaging plasmid, allowed 48 hours for transgene expression, and then treated the cells with either ionomycin or BAPTA-AM. As seen in Fig. 21A, treatment with neither drug had an effect on luciferase activity, indicating that transgene protein stability nor RNA transcription from a

plasmid vector are effected by intracellular calcium levels. Interestingly, mRNA levels from AAV delivered genomes decreased by ~20-fold upon ionomycin treatment and increased by ~2.5 fold upon BAPTA-AM treatment, concordant with the trend seen in transgene expression (Fig. 21B). Taken together, this data demonstrates that intracellular calcium levels affect AAV transduction in a viral dose and independent manner, while altering RNA transcription from the recombinant AAV genome.

BAPTA-AM increases AAV transduction in the mouse brain. Finally, we sought to determine the effect of intracellular calcium on AAV transduction *in vivo*. Calcium levels play an important role in neuronal function in the brain (184, 204). Therefore, we directly injected AAV1 packaging scGFP into the cerebrospinal fluid via intracerebroventricular (ICV) injection in neonatal C57/B6 mice. As seen in Figure 22A, co-administration of BAPTA-AM with AAV1 increases transduction in the injected hemisphere. Quantification of both transduced neurons in the motor cortex (Fig. 22B) and along the entire cortex (Fig. 22C) demonstrates 15 to 20-fold increase in transduction upon BAPTA-AM treatment. This data demonstrates that decreasing intracellular calcium with BAPTA-AM in the brain augments AAV transduction.

3.5 Discussion

Modulation of intracellular calcium has many different effects on cellular homeostasis (205). For this reason, studying the effects or intracellular calcium is quite challenging. Both ionomycin and BAPTA-AM have been shown to exert numerous related and unrelated effects on cellular homeostasis. For instance, calcium homeostasis is important for the regulation of protein kinase C (PKC) (206), phospholipase C (207), and PI3 kinase (208, 209), as well as other

important cell signaling molecules. It is important to note that cells have to maintain a >10,000-fold gradient of calcium across the plasma membrane with the cytoplasmic side at 100nM Ca++ concentration (210). Thus, it is conceivable that both ionomycin and BAPTA-AM significantly affect plasma membrane structure upon treatment and affect a diverse array of virus-cell interactions at the early binding and uptake steps (210).

For instance, PI3K activity has been shown to be important for transduction by AAV (59), specifically for integrin-directed productive AAV infection (51). Further, PKC, a protein that is important for macropinocytosis (211, 212), is strongly activated by ionomycin (213) and inactivated by BAPTA-AM (214). Macropinocytosis is an essential process for the internalization of many viruses (215) and has been implicated in internalization of AAV (59). However, we don't observe any effect of ionomycin on internalization. Intriguingly, BAPTA-AM has also been shown to selectively modifying protein transport within certain cell lines (186, 216). Specifically, BAPTA-AM was shown to inhibit retrograde transport of Shiga toxin B (STB) from endosomes to the Golgi apparatus in NRK cells (186). Interestingly, we recently demonstrated that another small molecule that inhibits trafficking of STB to the Golgi, eeyarestatin I (EerI), also augments AAV transduction (72). However, whether the mechanisms of action of EerI and BAPTA-AM are related is currently unknown.

Interestingly, ionomycin severely inhibited nuclear accumulation of AAV, indicating that either nuclear entry or an upstream step is affected. It has been demonstrated in the past that ionomycin does not alter the nuclear pore complex of nuclear import of other substrates (217, 218), and conversely, actually increases nuclear import of PLCdelta1 in MDCK and PC12 cells (219), suggesting that nuclear import might not be affected. In fact, the effect of ionomycin on AAV transduction seems to be at an upstream step, as ionomycin has no effect on transduction

when added as early as 4 hours post infection. Conversely, BAPTA-AM increases transduction by 10- to 100-fold in while not having any apparent effect on internalization, or nuclear entry, and only a minimal effect on binding. Interestingly, even with an equal amount of capsid accumulation in the nucleus, RNA transcription is increased, while transcription is not altered when the ITR plasmid is transfected alone. This finding is intriguing, as it has been shown that AAV genomes can stay associated with the capsid during and after uncoating (86). Further, this interaction of the genome with the capsid has been shown to play a role in the transcription and splicing of the transgene (97). In fact, intracellular calcium chelation by BAPTA-AM treatment has been shown to alter the splicing and expression of genes, further supporting this possibility (220). However, an increase in transcription may not be the only mechanism for the transduction increase that is witnessed.

An interesting observation is that BAPTA-AM increases transduction when added as late as 12 hours after initial infection. Furthermore, BAPTA-AM increases transduction by less than 2-fold during synchronized infection, but the transduction benefit increases with length of viral infection, with transduction increasing to approximately 5-fold when infection proceeds for 8 hours. This might indicate an increase in internalization of virus over time, but we did not observe such an effect at 1 hour. Previous studies on the effect of BAPTA-AM on endocytosis are contradictory. For instance, one study demonstrated an increase in the amount of transferrin receptor internalized upon BAPTA-AM treatment (216). Conversely, another study demonstrated a drastic reduction in uptake of both transferrin and dextran upon treatment (187). These differences may be due to cell line specific differences, though the existence of contradictory data must be taken into account. We observed a decrease in the amount of labeled transferrin and dextran in cells upon BAPTA-AM treatment (Fig. 23), however, it is possible that

the high levels of calcium seen in vesicular structures (Fig. 5b) quenched the signal from the fluorophore, clouding the results. Taken together, this suggests that while our data does not identify internalization as the primary mechanism of AAV transduction increase by BAPTA-AM in our studies, it cannot be ruled out as a factor in all cell lines.

One important observation is that the effect of BAPTA-AM on AAV transduction is dependent upon extracellular calcium, the inhibitory effect of ionomycin is not dependent on extracellular calcium. Previous studies have demonstrated that ionomycin not only allows calcium influx from the extracellular environment, but also allows calcium efflux out of the ER (200, 201). Therefore, ionomycin still increases intracellular calcium in the absence of extracellular calcium. Another small molecule that mimics this effect is thapsigargin. Thapsigargin is a SERCA inhibitor that prevents reuptake of calcium into the ER, thereby increasing cytosolic calcium concentration while also depleting calcium from the ER (221). We found that thapsigargin treatment had an inhibitory effect on AAV transduction that was similar to ionomycin treatment (data not shown). Even though AAV has yet to be identified in the ER during trafficking (71), we recently demonstrated that inhibition of ERAD by EerI increased transduction (72). Therefore, we cannot rule out the possibility that depletion of calcium in the ER is at least partially responsible for the inhibition of AAV transduction by ionomycin.

Interestingly, calcium has been shown to play a role in the interplay between the proteasome, ER stress, and autophagy (222-224). Past studies have argued that ER stress alone increases AAV transduction (70, 144, 225), although the present study may challenge the broad nature of that notion. Ionomycin and thapsigargin have both been shown to trigger ER stress (226), and both actually inhibit AAV transduction, though we cannot rule out the possibility that

the intracellular calcium increase overcomes any potential increase in transduction that would be caused by ER stress.

Additionally, we recently demonstrated that autophagy does not play a role in AAV transduction using several activators and inhibitors of autophagy (72). However, it has been shown previously that intracellular calcium concentration can alter activity of the 26S proteasome particle (222), a complex that has been identified as a major barrier to AAV infection (73, 142, 227). Yet, we did not observe any modification of proteasome activity upon treatment with either ionomycin or BAPTA-AM (Fig. 24), therefore eliminating a role for the proteasome in calcium directed modification of AAV transduction. Taken together, while ionomycin clearly decreases AAV transduction at a step prior to nuclear entry, BAPTA-AM increases at multiple steps in the infectious pathway, including binding and transcription, but not including disruption of the proteasome.

While we have demonstrated a role for intracellular calcium in the modulation of AAV transduction, an important area of inquiry is whether these results have the potential to impact rAAV-mediated gene therapies in the clinic. In this study, we demonstrate that modulation of intracellular calcium in the brain is a strategy to augment rAAV1 transduction. Calcium plays a very important role in the CNS, having a primary role in the depolarization of neurons (204, 228). Additionally, prolonged disruption of calcium homeostasis in neurons has been shown to result in neuronal cell death (229). Furthermore, several neurological conditions have been linked to perturbations in calcium homeostasis in the CNS, such as Alzheimer's disease and spinocerebellar ataxia, just to name a few (177-182). Incidentally, there are several pharmacological agents that are currently in use in the clinic for other disorders that safely alter calcium homeostasis in the CNS. Benzodiazepines and dihydropyridines represent two such

classes of drugs (230, 231). It will be important in the future that drugs such as these are evaluated for their potential use as adjuvants with rAAV-mediated gene delivery to the CNS to increase gene delivery. Nevertheless, the current study demonstrates several potential roles for calcium in AAV transduction and underscore potential approaches to take advantage of this knowledge.

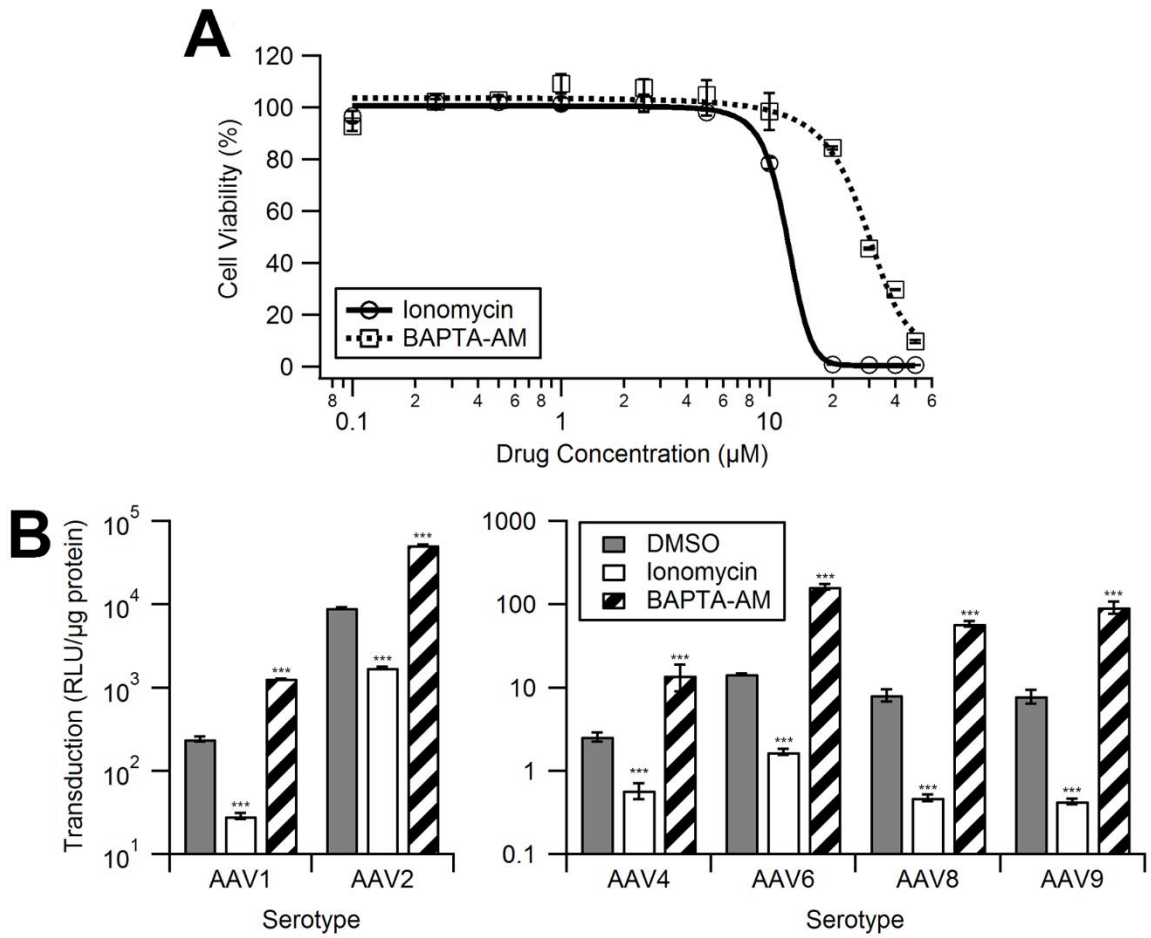

Figure 14: Intracellular calcium inversely affects AAV transduction in HeLa cells. (A) HeLa cells were treated with increasing concentrations of ionomycin (circles, solid line) or BAPTA-AM (squares, dotted line) and assayed for cell viability. (B) Luciferase reporter expression in HeLa cells pretreated with DMSO (grey bars), ionomycin (white bars), or BAPTA-AM (hashed bars) and infected with multiple serotypes of AAV-Luc. Ionomycin and BAPTA-AM were used at 10 μM and 20 μM, respectively.

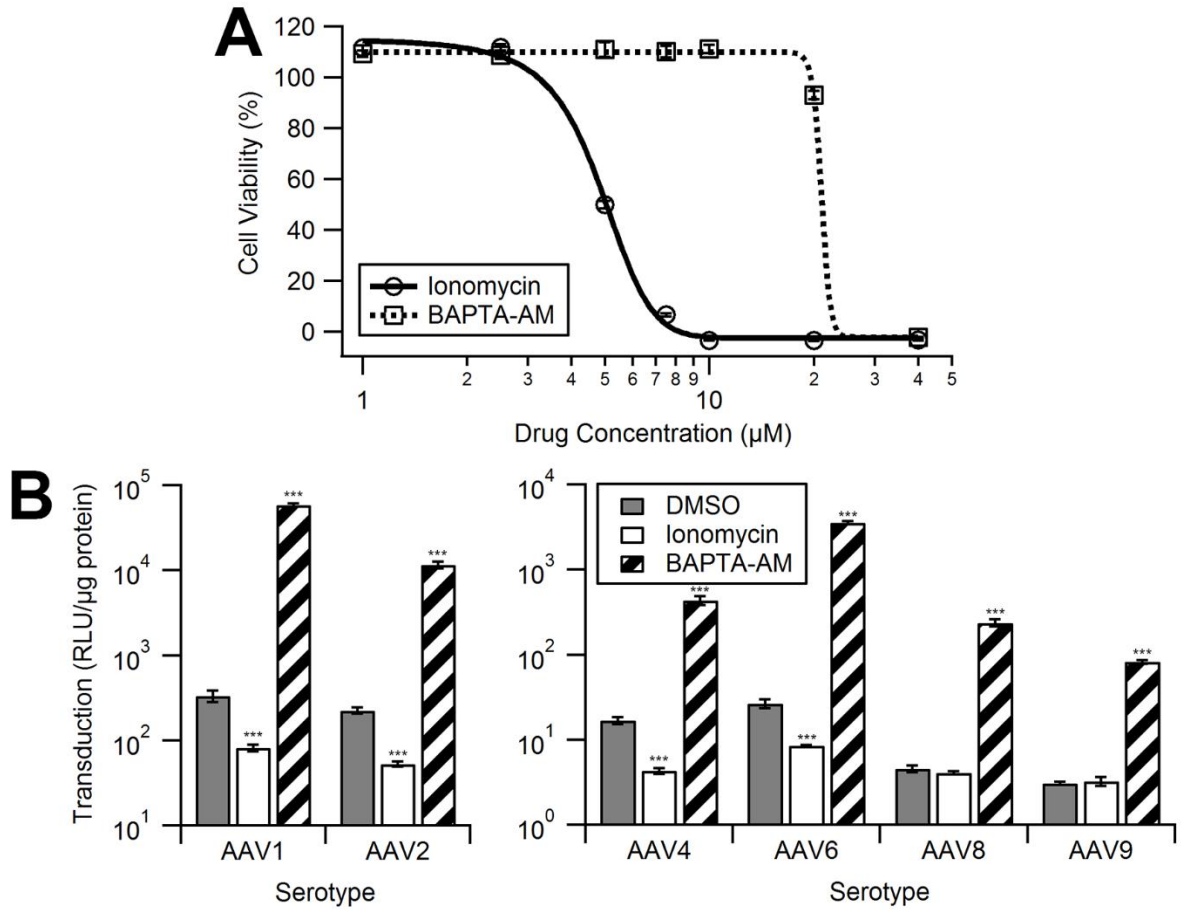

Figure 15: Intracellular calcium inversely affects AAV transduction in MB114 cells. (A) MB114 cells were treated with increasing concentrations of ionomycin (circles, solid line) or BAPTA-AM (squares, dotted line) and assayed for cell viability. (B) Luciferase reporter expression in MB114 cells pretreated with DMSO (grey bars), ionomycin (white bars), or BAPTA-AM (hashed bars) and infected with multiple serotypes of AAV-Luc. Ionomycin and BAPTA-AM were used at 2.5 μM and 20 μM, respectively.

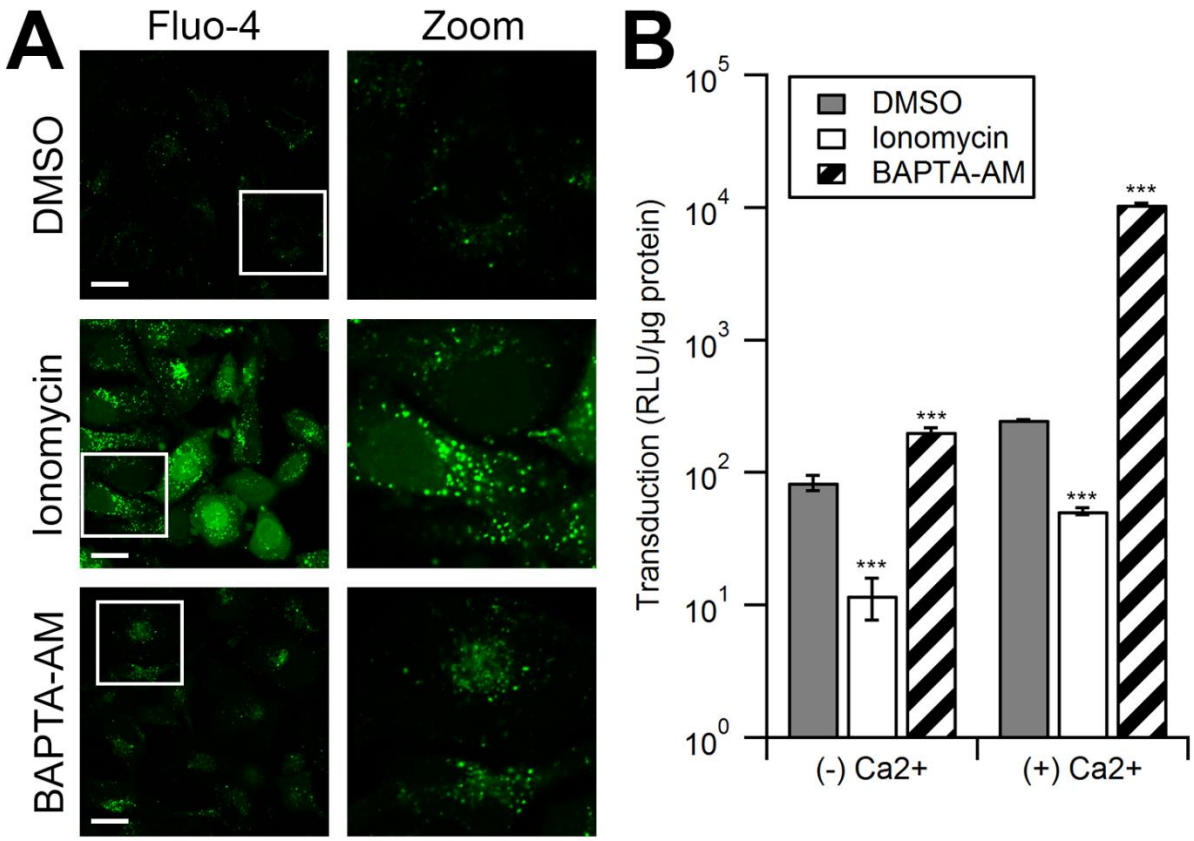

Figure 16: AAV transduction increase by BAPTA-AM is dependent on the presence of calcium in the extracellular environment. (A) HeLa cells treated with DMSO, ionomycin, or BAPTA-AM were loaded with Fluo-4-AM and imaged 8h after drug treatment. White inset boxes indicate areas imaged at higher magnification. Scale bar = 20 µm. (B) Luciferase expression in MB114 cells treated with DMSO, ionomycin, or BAPTA-AM in the presence or absence of calcium in the extracellular media.

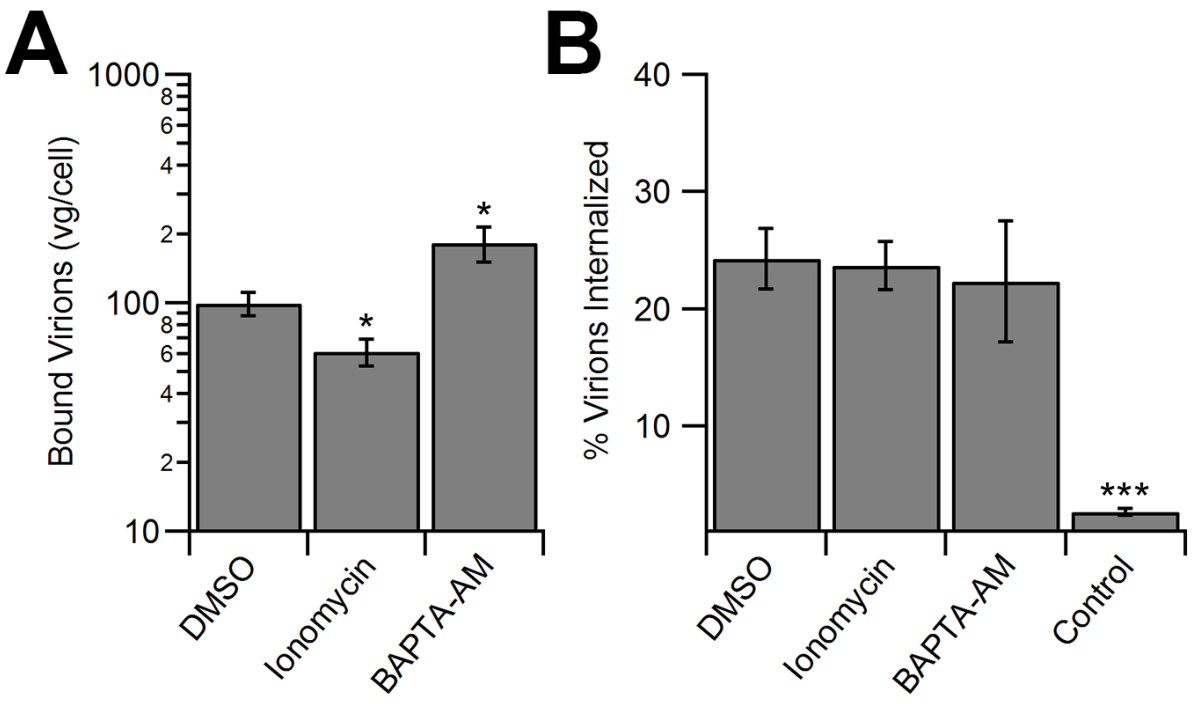

Figure 17: Intracellular calcium doesn't greatly effect AAV binding, and doesn't alter AAV internalization. (A) HeLa cells were pretreated with DMSO, ionomycin, or BAPTA-AM and AAV2-Luc was bound to the cell surface at 4°C for 1h. Cells were then washed with PBS to remove unbound virus. DNA was then extracted and subjected to qPCR. (B) HeLa cells were pretreated with DMSO, ionomycin, or BAPTA-AM drugs and AAV2-Luc was bound to the cell surface at 4°C for 1h. Cells were washed with PBS to remove unbound virions and then shifted to 37°C for 1h. Cells were then treated with trypsin to remove surface bound virions. DNA was then extracted and subjected to qPCR.

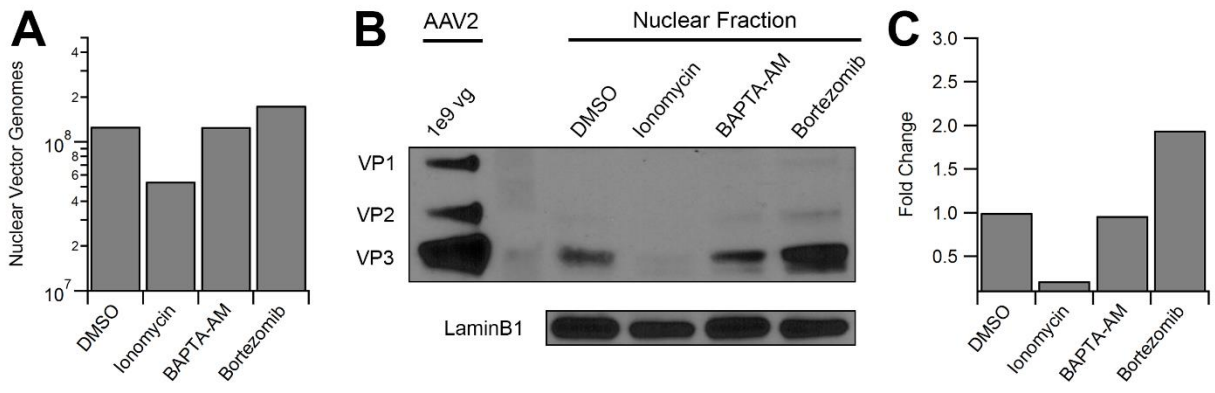

Figure 18: Intracellular calcium alters nuclear accumulation of AAV when increased by ionomycin. (A) HeLa cells were pretreated with DMSO, ionomycin, BAPTA-AM, or bortezomib (positive control) and infected with AAV2-Luc at an MOI of 10,000. Nuclear fraction was isolated 16h post-infection. DNA was extracted from the nuclear fraction and subjected to qPCR. (B) Western blot of nuclear fractions probed with B1 (anti-AAV) and anti-laminB1. (C) Densitometry analysis of the western blot.

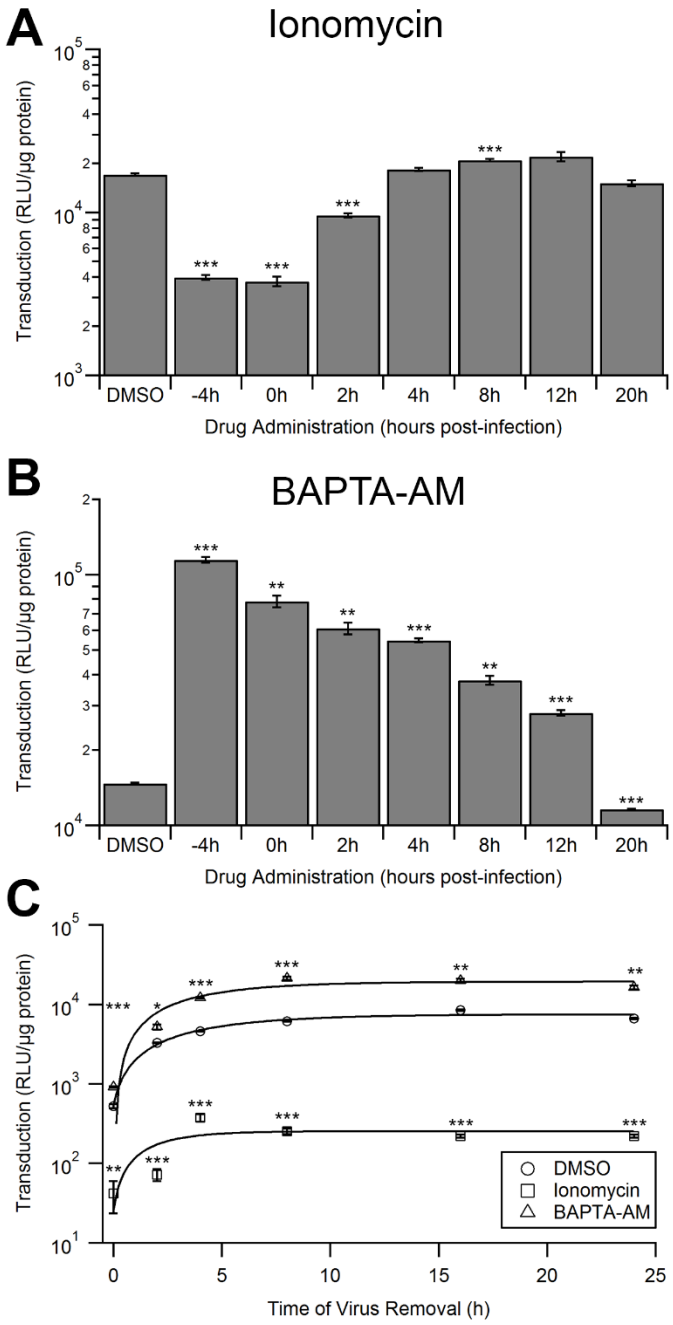

Figure 19: Time of intracellular calcium perturbation differentially affects AAV transduction. (A) Luciferase expression in HeLa cells treated with DMSO or ionomycin at various time intervals prior to transduction with AAV2-Luc vectors. (B) Luciferase expression in HeLa cells treated with DMSO or BAPTA-AM at various time intervals prior to transduction with AAV2-Luc vectors. (C) Luciferase expression in HeLa cells treated with DMSO (circles), ionomycin (squares), or BAPTA-AM (triangles) and infected with AAV2-Luc for various durations.

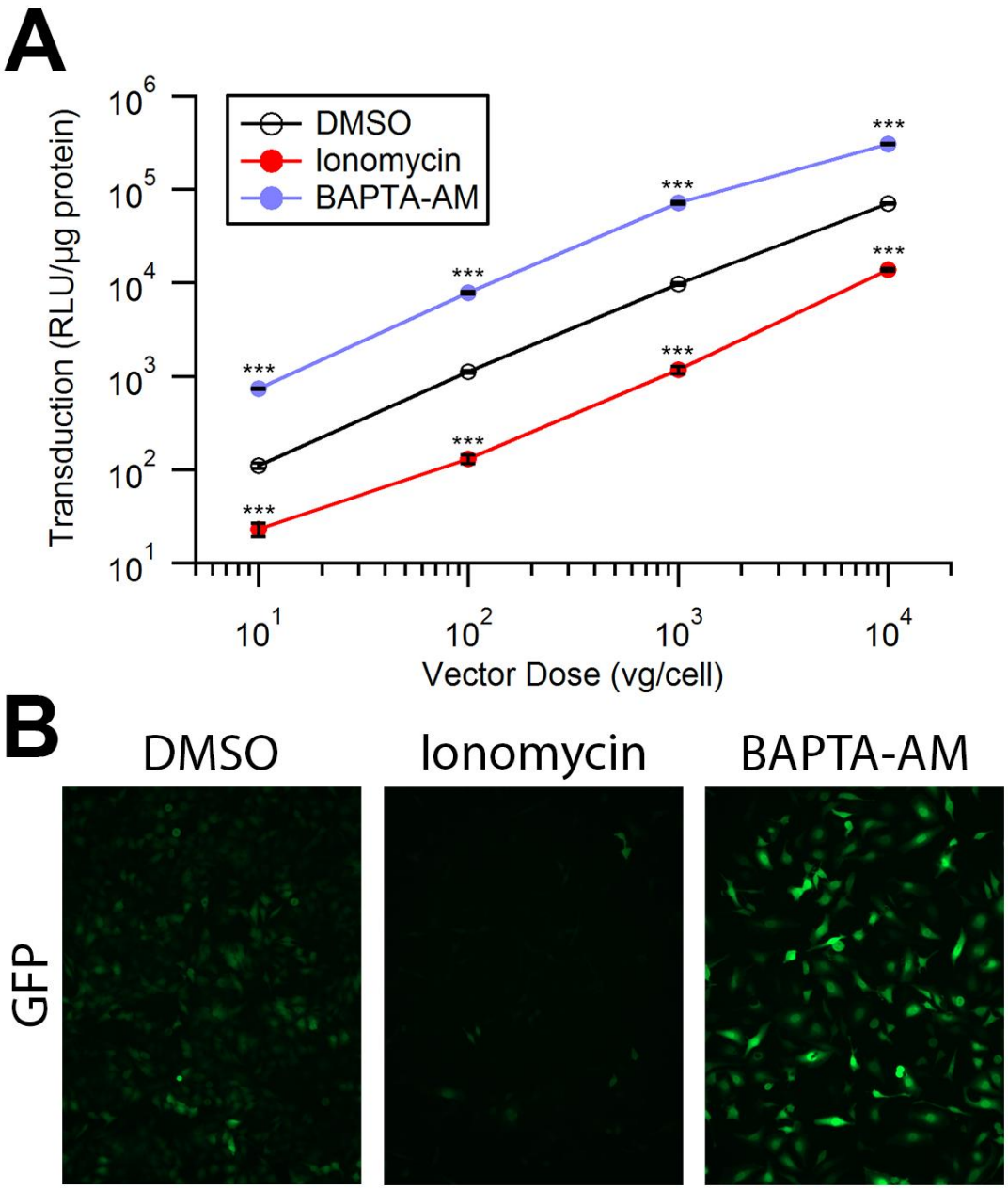

Figure 20: Intracellular calcium alters AAV transduction independent of vector genome or vector dose. (A) HeLa cells pretreated with either DMSO control (black), ionomycin (red), or BAPTA-AM (blue) and were infected with AAV2-Luc at various vector doses. (B) HeLa cells were pretreated with DMSO control or intracellular calcium modifying drugs and then infected with scAAV2-GFP. Cells were imaged 24h post-infection.

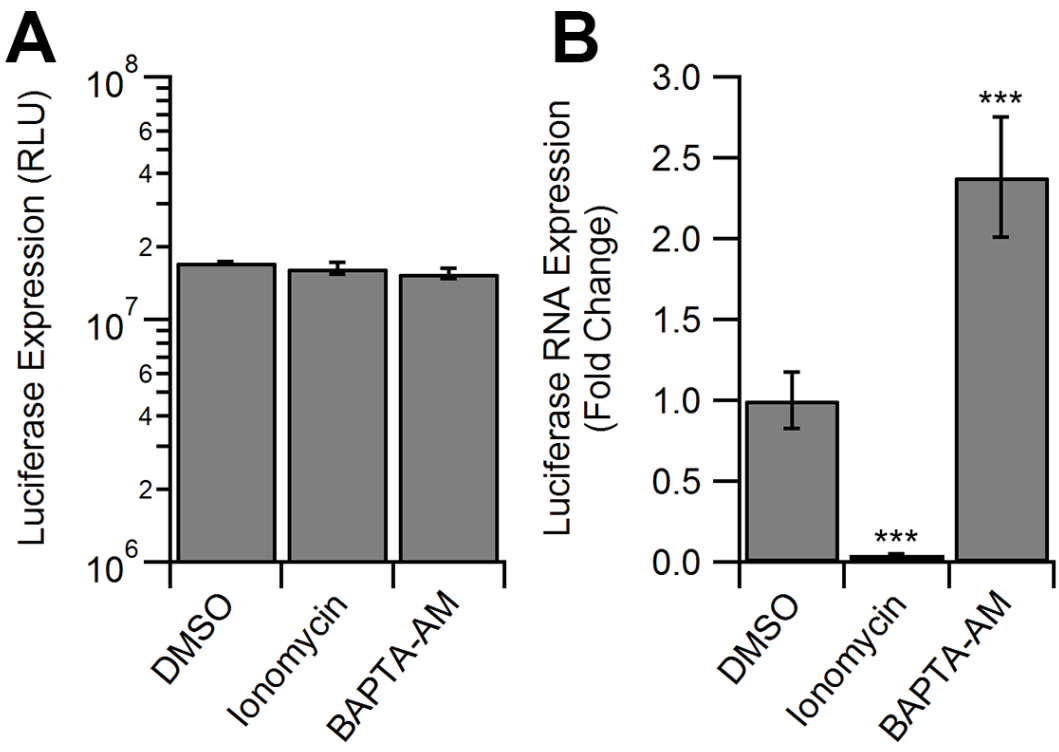

Figure 21: Intracellular calcium alters AAV transduction by altered transcript levels. (A) HeLa cells were transfected with pTR-CBA-Luc and treated with either ionomycin or BAPTA-AM 48h post-transfection. Luciferase expression was assayed 28h post-administration of drugs. (B) HeLa cells were pretreated with DMSO control or intracellular calcium modifying drugs and then infected with AAV2-Luc. RNA was isolated 24h post-infection and was subjected to qRT-PCR.

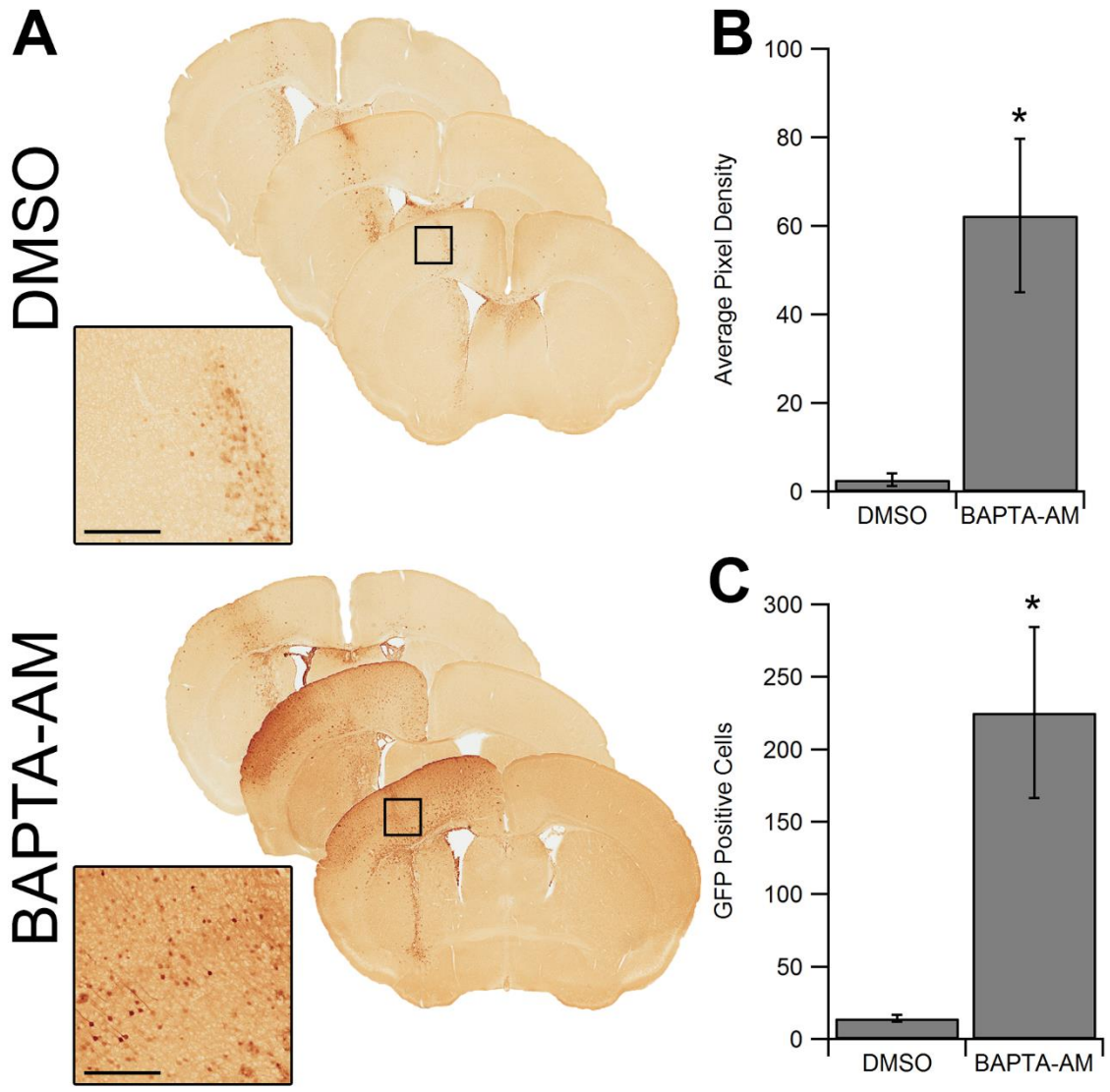

Figure 22: BAPTA-AM increases AAV1 transduction in mice injected via ICV route. P0 mice were injected ICV with 3e9 vg of scAAV1-CBh-GFP and sacrificed 2 weeks post injection. (A) Brightfield scanned micrographs of DAB stained brain sections comparing GFP expression. Black inset boxes indicate areas imaged at higher magnification. Scale bar = 300 µm. (B) Semi-quantitative analysis of DAB signal. (C) Quantification of DAB positive cells in the motor cortex.

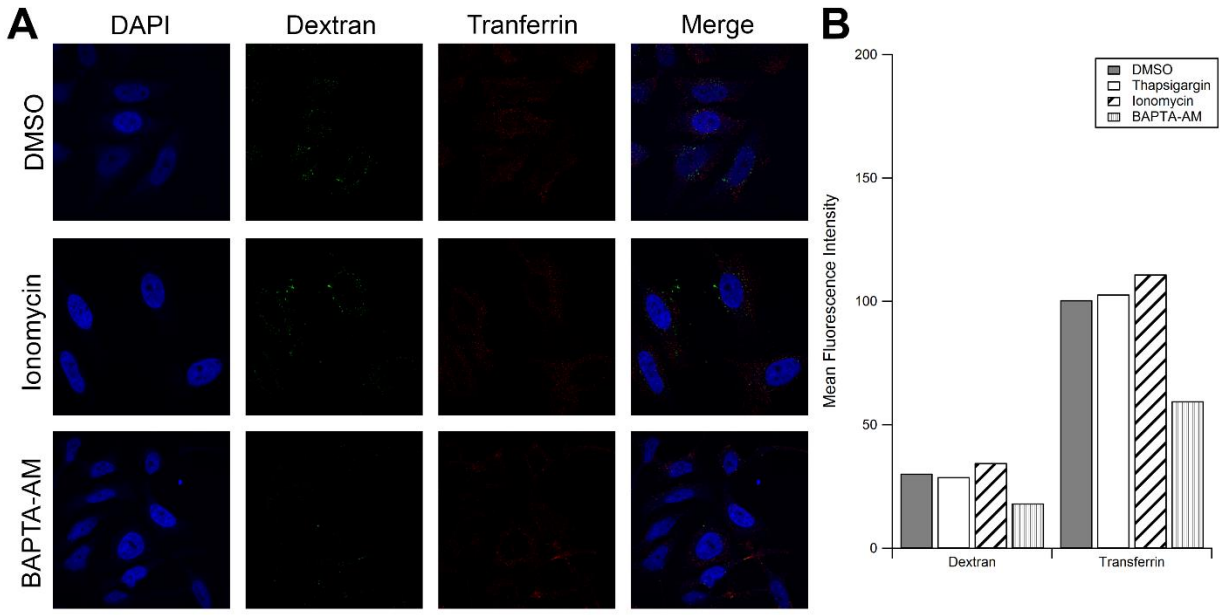

Figure 23: The effect of intracellular calcium concentration on receptor-mediated endocytosis and fluid phase uptake. (A) HeLa cells were treated with DMSO, ionomycin, or BAPTA-AM for 4 hours. Cells were then allowed to internalize Alexa Fluor 488-labeled dextran (green) for 30 minutes, followed by Alexa Fluor 597-labeled transferrin (red) for 15 minutes. Cells were then fixed with 2% PFA, counterstained with DAPI (blue), mounted, and imaged with a Zeiss 710 confocal microscope. (B) Cells were treated as above with dextran and transferrin. However, after fixation, cells were analyzed using a CyAn ADP flow cytometer.

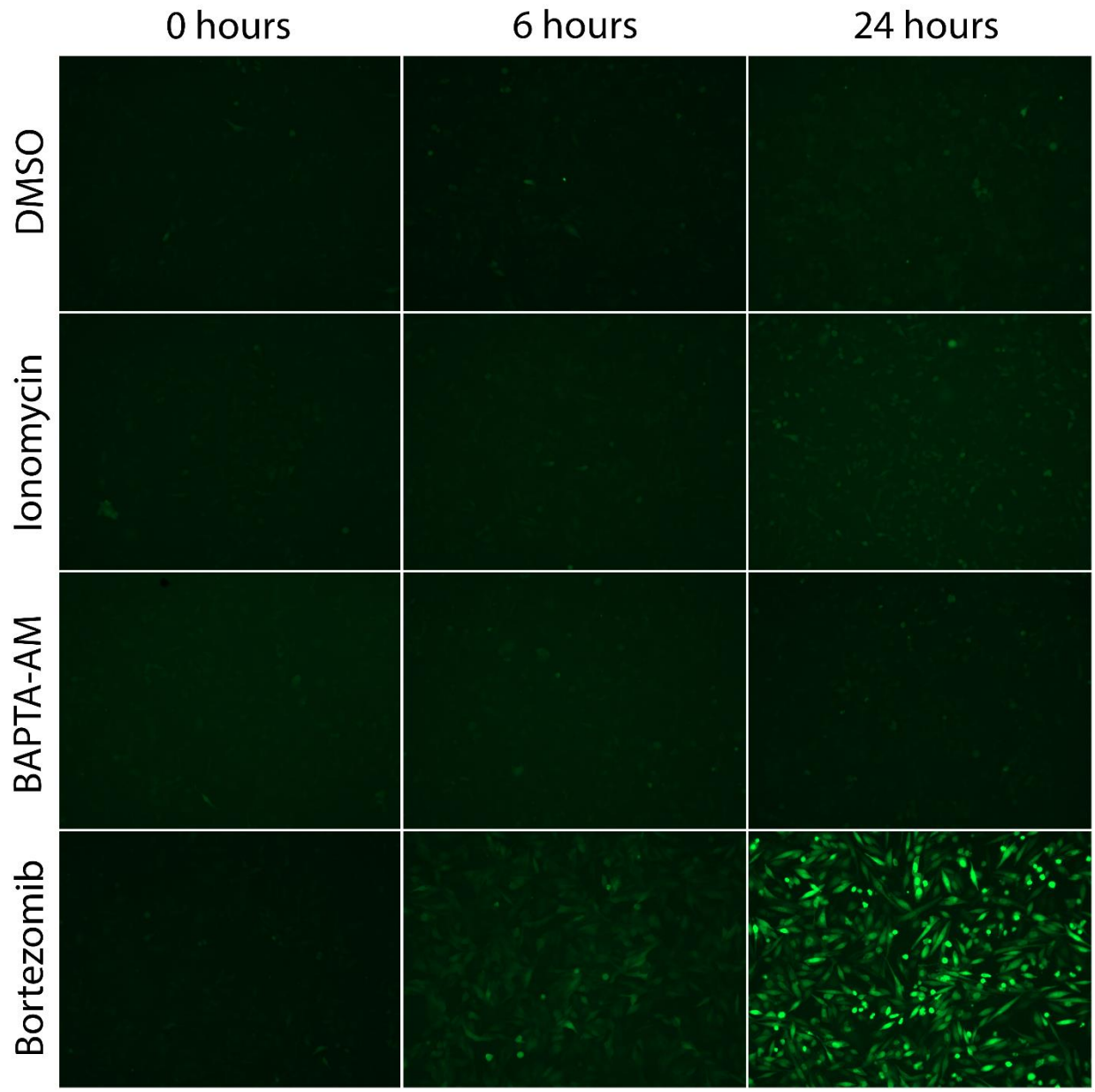

Figure 24: Intracellular calcium concentration does not affect proteasome activity. HeLa cells stably expressing ubiquitin-tagged GFP were treated with DMSO, ionomycin, BAPTA-AM, or bortezomib (positive control). Cells were imaged at various timepoints using an Evos microscope.

CHAPTER 4: Conclusions and future directions

4.1: Summary

When AAV was first identified in simian adenovirus preparations in 1965, the perception of AAV as a "defective virus particle" was largely due to the dependence of Adenovirus on AAV replication. Little did the authors realize, this one property eventually became one the biggest reasons AAV has garnered so much attention in the last 50 years. Together with the modularity and ease of design and production, AAV eventually became one of the most promising vectors for the delivery of genes to human patients in the clinic. While originally viewed as a vector poised to simply deliver functioning copies of defective or missing genes, the utility of AAV is continually being expanded into other fields that are clinically important, such as gene regulation, by delivering microRNAs or microRNA sponges, and targeted genetic engineering, using zinc-finger nucleases and the CRISPR/Cas9 system. Additionally, it is often overlooked that rAAV is also a widely used tool in cell and molecular biology that can be used to probe numerous scientific questions, both *in vitro* and *in vivo*. In fact, AAV remains an important tool in the molecular biology toolkit for neuroscience researchers that use optogenetics to study different aspects of neuronal signaling in the mammalian nervous system.

However, as AAV-mediated gene delivery continues to move closer to wide clinical use in the western world, it becomes even more imperative that the biology of the vector is as completely understood as is humanly possible. While many studies have been conducted with the goal of elucidating the specific mechanisms of AAV infection, there are still gaps in knowledge

that must be filled. In this dissertation, I continued to build upon the current foundation of knowledge regarding AAV trafficking and AAV infection with the aim to improve our current understanding of AAV biology. First, we utilized several small molecule effectors of both autophagy and the ubiquitin protease system to prove the interaction of the host cell with AAV. One particular small molecule, EerI, demonstrated the ability to increase AAV transduction and established a potential role for ERAD in the AAV infectious pathway. Additionally, we demonstrated a role for intracellular calcium in several different steps in the AAV infectious pathway using intracellular calcium modifying compounds. Further, we were able to establish modulation of intracellular calcium as a strategy to augment AAV transduction.

4.2: Modulation of AAV trafficking with Eeyarestatin I

In Chapter 2, we demonstrated that the VCP inhibitor EerI increased transduction of AAV in a serotype and cell type independent manner. We further demonstrated with confocal microscopy studies that EerI triggered a remodeling of AAV trafficking from a Golgi-directed pathway to a late endosome/lysosome directed pathway. The late endosomes/lysosomes that contained the redirected AAV particles were also enlarged as a result of EerI treatment, potentially leading to the escape of large numbers of AAV particles into the cytosol in a short period of time during endosomal escape. Interestingly, several studies have postulated that trafficking of AAV to the *trans*-Golgi network is a required step in the transduction pathway using small molecules that disrupt the Golgi apparatus. Our data seems to be in direct contradiction to this. However, it has been shown that AAV particles can utilize several different endosomal trafficking pathways, even in the same cell. However, it has been hypothesized that some of these pathways do not eventually lead to productive infection, so called “dead ends.”

One important observation is that EerI treatment completely remodeled AAV trafficking to the microtubule organizing center (MTOC) in the perinuclear region as evidenced by the lack of co-localization with the Golgi marker, Golgin-97. Intriguingly, EerI treatment also disrupted the cellular localization of syntaxin 5 (STX5). It should be noted that STX5 is a known substrate of VCP/p97 (apparent target of EerI), which in turn mediates assembly of ER and Golgi cisternae (232). In contrast to our results, recent studies observed a decrease in AAV transduction upon blocking Golgi transport by knockdown of STX5. A possible explanation for this observation is that while earlier studies sought to inhibit function or reduce STX5 levels, EerI treatment appears to mislocalize STX5 within the cytosol. These events could indirectly improve nuclear accumulation of AAV particles by promoting efficient endosomal escape and nuclear entry compared to the Golgi-directed route of entry. Such a scenario is possible due to the low pH and high protease activity within such vesicles that could more effectively prime the AAV capsid (171) by exposing the VP1 phospholipase A2 (PLA2) domain (30) and nuclear localization signals (NLS) (31). Efficient endosomal escape at a rate that surpasses proteasomal degradation is likely to then promote improved nuclear entry. This potential model of AAV trafficking is further supported by several observations, including (i) the increased recovery of vector genome copy numbers from cells at time intervals as late as 16-24 hours following EerI treatment; (ii) increased nuclear accumulation of AAV capsids similar to that observed with the proteasomal inhibitor, MG132 and (iii) the additive effect of EerI and MG132 on AAV transduction. Taken together, the latter observations suggest that ERAD and proteasomal degradation might function in a mutually exclusive fashion to enhance post-entry AAV trafficking.

It is tempting to speculate that VCP/p97 or more broadly, ERAD might play a role in AAV trafficking. However, it is noteworthy that the interrogation of such virus-host interactions

has been particularly challenging due to overt toxicity displayed during RNAi-mediated knockdown of VCP as well as over-expression of WT/DN forms of VCP. Another important consideration is the pleotropic effect of chemical inhibitors such as EerI. For instance, EerI has been previously shown to augment cellular processes separate from ERAD (168-170, 173). Moreover, DBeQ, ML240, and NMS-873, additional small molecule inhibitors of VCP/p97, and Kif, another ERAD inhibitor, only displayed modest-to-negligible effects on AAV transduction.

4.3: Modulation of AAV transduction with intracellular calcium modulators

In Chapter 3, we demonstrated that modulation of intracellular calcium altered transduction of AAV. Interestingly, AAV transduction inversely correlated with intracellular calcium levels in HeLa and MB114 cells. Ionomycin, an ionophore that allows the flow of calcium ions across biological membranes and increases intracellular calcium, decreased transduction by approximately 5 to 10-fold. Conversely, reduction of intracellular calcium by BAPTA-AM, a cell permeable highly specific calcium chelator, increased transduction by approximately 10-fold in HeLa cells, and almost 100-fold in MB114 cells. Much like eeyarestatin I, the transduction changes seen was independent of serotype. Interestingly, the transduction effects seen with ionomycin and BAPTA-AM appeared to be distinct from each other. The only similarity seen was a minor effect in binding that was limited to approximately 2-fold in the case of both compounds. Ionomycin affected an early step in transduction, most likely a step prior to nuclear entry. Although, we cannot rule out the possibility that ionomycin blocks nuclear entry. BAPTA-AM, however, appeared to augment RNA transcription, but only from the recombinant AAV vector, as expression from a plasmid vector introduced via transfection did not change as a result of treatment with BAPTA-AM. This increase in RNA seen

did not correspond with an increase in nuclear capsid or vector DNA accumulation. However, while it is not known for sure if the 2.5-fold RNA increase is solely responsible for the approximately 10-fold increase in transduction, another role for transduction increase by BAPTA-AM cannot be ruled out.

Previously, BAPTA-AM has been shown to alter the intracellular trafficking of various cellular cargoes at certain steps, while not affecting other steps in the same pathway. Interestingly, BAPTA-AM was shown to block the retrograde transport of Shiga toxin B to the Golgi apparatus. Intriguingly, EerI was also shown to inhibit this very same step in the trafficking pathway of STB. Furthermore, both BAPTA-AM and EerI were shown to have no effect on the endocytosis of cargo. Therefore, it is interesting to speculate that the augmenting action of both BAPTA-AM and EerI are both related to the redirection of AAV from the *trans*-Golgi network. However, due to the pleiotropic effects of BATPA-AM, affecting both binding and RNA transcription to differing degrees, the degree by which this potential effect may have on transduction is difficult to determine. However, it will be important in the future to address the specific mechanisms of calcium modulation on AAV transduction at each step in the transduction pathway.

4.4: Clinical Implications

Several key questions regarding the work contained within this dissertation regard the potential for translational impact in the clinic. In the case of VCP, several chemicals are being assessed for their potential as chemotherapeutics. Much like proteasome inhibitors, several distinct cancer types have shown vulnerability of VCP inhibitors. However, it is important to determine the effective dose and toxicity of these molecules in animal models before they can be

explored for use as adjuvants for AAV-mediated gene delivery. Similar to VCP inhibitors, ERAD inhibitors may also be a promising approach to augmenting AAV transduction in the clinic. Much like proteasome inhibition, ERAD inhibition also triggers ER stress. Therefore, use of this class of molecules would potentially provide yet another avenue for increasing AAV transduction, thereby allowing decreased vector doses.

Fortuitously, in the case of intracellular calcium, there are several classes of drugs that are currently approved for use in the clinic that modulate calcium levels within the cell. Many of these compounds act specifically on neural tissue, making them good candidates for combination therapies involving AAV-mediated gene delivery to the CNS. One such class of drugs are the benzodiazepines, such as midazolam and alprazolam. These GABA agonists trigger calcium uptake in neurons by activating the GABA receptor. Conversely, the dihydropyridines act as calcium channel blockers, thereby restricting the flow of calcium into cells. Another major class of promising drugs is the NMDA receptor antagonists, such as ketamine and amantadine. In addition to exploring the use of these reagents as adjuvants, their potential role for blocking AAV transduction is another important area of study, as treating patients that are on drug regiments involving such pharmacologics could severely hinder the efficacy of gene delivery.

Additionally, these findings address an important area of inquiry for studies aiming towards gene therapy for CNS diseases, as dysregulation of cellular calcium homeostasis is a phenotype for several CNS disorders, such as Alzheimer's and multiple subtypes of spinocerebellar ataxias. Therefore, it is possible that AAV transduction in these diseases can be altered by the specific intracellular calcium phenotypes associated with each disease. With this knowledge, it could be expected that specific diseases are refractory to AAV-mediated gene delivery, where other diseases are particularly susceptible.

4.5: Final Remarks

All viruses must utilize countless host cellular pathways to successfully infect cells, while at the same time avoiding countless other host cellular pathways that have evolved to thwart the virus at any cost. For any virus, an intricate understanding of all host cellular pathways involved is important. In the case of viruses such as CPV and FPV, knowledge allows for the continuing heath of our pets. In the case of human parvovirus B19, knowledge will allow for the prevention of numerous miscarriages that are caused by prenatal infection.

Generally speaking, the human population seeks to undermine the virus, sometimes taking full advantage of the knowledge available to eradicate the virus entirely, as is the case with smallpox, and likely poliovirus in the coming years. However, in the case of AAV, the focus is the exact opposite; how can we undermine the cells in order to provide the highest possible transduction levels in the safest possible manner? These questions can only be answered with complete or near complete knowledge of the infectious pathways utilized by the virus, as well as the cellular defense mechanisms that are evolved to undermine the goal of AAV-vectored gene therapy; delivery and expression of foreign genetic material.

In this dissertation, we have utilized a number of small molecules to elucidate several steps in the AAV trafficking and transduction pathway. Further, we were able to add to the current body of knowledge in the field of AAV-mediated gene delivery. Armed with this knowledge, further gene delivery approaches can be investigated and optimized. Any knowledge relating to the AAV infectious pathway has the potential to impact AAV-mediated gene therapy approaches in the clinic, therefore allowing for safer and more efficacious therapies for decades to come.

APPENDIX: Analysis of the VP1 unique region of various natural AAV serotypes

A.1: Overview

Parvoviruses, specifically *Parvovirinae*, are a family of small, non-enveloped viruses that infect a range of vertebrate hosts. One property shared by all parvoviruses is the existence of a phospholipase A2 (PLA2) domain within the capsid, a domain required for infectivity. In the case of the parvovirus Adeno-associated virus (AAV), the PLA2 domain lies within a region on the capsid termed the VP1 unique region, or VP1u. There are many natural serotypes of AAV that have been isolated, each with unique tropism and transduction properties. However, due to the unique nature of these different serotypes, the specific efficiencies of the VP1u region of each serotype remain unknown. In this study, we investigated the properties of the VP1u regions of AAV2, AAV3b, AAV5, and AAV9 by grafting them onto the AAV1 capsid backbone, generating the P series of capsids. While AAV1p2 demonstrated similar transduction to the parental AAV1, AAV1p3, AAV1p5, and AAV1p9 demonstrated reduced transduction. In addition to the P mutants, we generated a synthetic truncated VP1u based on homology with the VP1u region of human bocavirus 1 (HBoV) on the AAV1 capsid, called AAV1-miniPLA. However, this mutant was severely transduction compromised. Aside from transduction changes, all mutants generated were able to assemble into full capsids, package DNA, and incorporate VP1 subunits into the capsid structures. Taken together, these results demonstrate the ability to transfer the VP1u region of one AAV serotype onto another to achieve different transduction properties, thereby providing a new avenue for the construction of new AAV-based gene therapy vectors.

A.2: Introduction

Adeno-associated virus (AAV) is a helper-dependent member of the parvoviridae family that has garnered much attention due to a range of properties that make it a promising vector for use in the clinic for gene therapy applications. These properties include low immunogenicity, ability to infect both dividing and quiescent cells, lack of pathogenicity, and lack of random integration into the genome of host cells (233). There are numerous natural AAV serotypes that have been isolated that each demonstrate a unique tissue tropism. However, many recent efforts have focused on generating new vectors that have unique properties that can be fine-tuned to meet specific gene delivery goals. Two such approaches can be broadly categorized as capsid shuffling followed by directed evolution and rational capsid engineering (105-107, 113). One recent example of the former is the generation of AAV-LK03, a novel capsid that largely resembles AAV3b, but transduces human hepatocytes with a 6.5-fold greater efficiency (234). Interestingly, AAV3b and AAV-LK03 are nearly identical, with the exception of the VP1u region.

The VP1u region of AAV has multiple features that are necessary for transduction, specifically for endosomal escape and nuclear entry. AAV has been shown to have 3 basic regions (BRs) within the VP1/2 shared region that act as nuclear localization signals, one of which is solely in the VP1u region (31, 76). Mutation of any or all of these BRs severely disrupts translocation of AAV into the nucleus and subsequent transduction. In addition to the BRs, the AAV VP1u region has a phospholipase A2 (PLA2) domain that is required for infectivity (79). The PLA2 domain has been shown to be needed for escape of AAV from the endomembrane system into the cytosol (30, 78). However, the impact of different serotype-specific VP1u regions on transduction has yet to be explored. Unfortunately, different AAV serotypes have

been shown to utilize different receptors, different entry pathways, and even different intracellular trafficking pathways, thereby making investigation of any VP1u differences difficult (199).

To overcome these challenges, we grafted the VP1u regions of several natural AAV serotypes onto AAV1. This approach allowed the standardization of several upstream infection steps, such as receptor binding and viral entry, thus allowing the study of the specific effects of the different VP1u regions on transduction. We generated five new AAV1 mutants; AAV1p2, AAV1p3, AAV1p5, AAV1p9, and the synthetic AAV1-miniPLA. The mutants generated have different transduction properties both in vitro and in vivo, demonstrating a fundamental difference in the VP1u regions of different AAV serotypes. Thus, we have demonstrated a novel method to study the specific effects of VP1u differences on AAV transduction that could be applied to a range of AAV serotypes. The resulting capsids have the potential to play an important role in the clinic for delivery of genetic material using AAV vectors.

A.3: Materials and Methods

Plasmids and production of mutants. Sequence alignments were performed using Vector NTI software from Invitrogen (Carlsbad, CA). The plasmid pXR1, which contains the capsid gene from AAV1, was utilized as a backbone to make the VP1u mutants AAV1p2, AAV1p3, AAV1p4, AAV1p5, and AAV1p9. PCR was used to amplify the VP1u segments from AAV2, AAV3b, AAV4, and AAV9 from pXR2, pXR3b, pXR4, and pXR9, respectively, using the following primers: Vp1u_F 5'- TGG TCA ATG TGG ATT TGG ATG ACT G - 3'and Vp1u_R 5'- TTC TTG GCC TGG AAG ACT GC - 3'. To amplify the VP1u region of AAV5 from pXR5, the primer Vp1u_R was used with the following modified forward primer: pXR5-Vp1u5_F 5'-

TTA AAT CAG GTA TGG CTT TTG TTG ATC ACC CTC C - 3'. The purified VP1u PCR products were then used as a megaprimer with pXR1 in a new PCR to produce the mutants. The resulting PCR reaction was digested with DpnI prior to transformation to remove parental pXR1 plasmid. To generate pXR1-miniPLA, a gBlock was ordered from IDT Technologies (Coralville, IA) that contained the synthetic VP1u sequence. pXR1 backbone was then PCR amplified using the following primers: F 5'- CAA TTT CGG TCA GAC TGG CGA CAC - 3' and R 5'- GAG CCA ATC TGG AAG ATA ACC ATC GG - 3'. The gBlock was then inserted into the amplified backbone by Gibson assembly as previously described (235).

Cell culture. HeLa cells were maintained in Dulbecco's Modified Eagle's Medium with 10% FBS, 100 U/ml of penicillin, 100 µg/ml of streptomycin. MB114 cells were maintained in Dulbecco's Modified Eagle's Medium with 5% FBS, 100 U/ml of penicillin, and 100 µg/ml of streptomycin. All cells were maintained at 37°C and 5% CO2.

Recombinant AAV Production. Recombinant AAV packaging chicken beta actin (CBA) promoter driven firefly luciferase (fLuc) was produced in HEK293 cells using the triple plasmid transfection protocol, purified and titers determined as described earlier (72, 163).

Western blotting. $1x10^9$ vg were incubated at 85°C with LDS loading buffer and 50 mM DTT for 10 minutes to denature the capsid. The mix was then run on a precast 10% Bis-Tris gel (Invitrogen). The protein was then transferred to 0.45 um nitrocellulose membrane and blotted with anti-capsid protein antibody B1 (161).

Transduction assays. Cells were plated at a density of 5x104 cells/well in 24-well plates and allowed to adhere overnight. Cells were transduced with AAV1 or AAV1 mutants packaging CBA-fLuc at 1,000 vg/cell. Cells were lysed 24 hours after using the luciferase assay system from Promega (Madison, WI) according to manufacturer instructions and read on a Wallac® 1420 Victor3 automated plate reader. Transduction is expressed at relative light units (RLU).

Animal studies. Animal experiments were carried out with BALB/c mice bred and maintained in accordance to NIH guidelines and as approved by the UNC Institutional Animal Care and Use Committee (IACUC). At 8-10 weeks of age, intramuscular (IM) injections were performed by injecting mice in the gastrocnemius muscle with $5x10^9$ vector genome-containing particles in a total volume of 25 μl in each leg with either AAV1-CBA-Luc or the P series mutants. Luciferase expression in animals was imaged at 4 weeks post-injection using a Xenogen IVIS Lumina imaging system from Caliper Life Sciences (Hopkinton, MA) following intraperitoneal injection of 120 mg/kg of RediJect D-luciferin bioluminescent substrate (770504) from Perkin Elmer (Waltham, MA). Total flux was quantified using Living Image software and is expressed as photons/second (p/s).

Statistical analysis. All data is expressed as mean with error bars representing standard error of the mean (SEM). A two-tailed unpaired student t-test was used for all statistical analysis. P values less than 0.05 were considered significant. Asterisks are used to indicate P values as follows: *P < 0.05; **P < 0.01; ***P < 0.005.

A.4: Results and Discussion

Unique VP1u sequences in diverse natural AAV serotypes. In order to determine which serotypes would be used to study their various VP1u domains, we aligned the amino acid sequence of the VP1u regions from AAV1-9 (Fig. 25). This analysis revealed a high degree of conservation among all the natural serotypes. However, the VP1u region of AAV6, AAV7, and AAV8 demonstrated the highest degree of conservation. Therefore, we did not include these serotypes in these studies. The AAV9 VP1u was also fairly well conserved with the AAV1 VP1u. However, AAV9 is of particular interest due to the prevalence of clinical trials utilizing AAV9-based therapies. Further, the VP1u regions from AAV2, AAV3b, AAV4, and AAV5 demonstrate varying degrees of divergence from AAV1, with AAV5 being the least conserved. Taken together, this data prompted us to produce AAV1 capsid mutants containing the VP1u region from AAV2, AAV3b, AAV4, AAV5, and AAV9.

To construct the P mutant series, the VP1u region of AAV2, AAV3b, AAV4, AAV5, and AAV9, were amplified by PCR. The resulting amplicon was purified and subsequently used as a megaprimer to prime replication on the pXR1 plasmid backbone. This process yielded mutants for all VP1u regions. The resulting mutants were dubbed the P mutants (where "p" stands for PLA2, a feature contained within each VP1u region), such as AAV1p2, AAV1p3, and so on.

Structural analysis of AAV1 P mutants. After generation of the pXR1 P mutants, virus was produced packaging the TR-CBA-Luc transgene cassette. The virus was then titered using qPCR. As seen in Fig. 26A, all mutants packaged DNA with similar efficiency to the parental AAV1, with the exception of AAV1p4. While it is tempting to speculate that AAV1p4 is defective, one caveat of the method used to generate the P mutants is possibility of PCR-introduced mutations

in the AAV rep gene. Possible mutations in the rep gene in pXR1p4 could result in both packaging and assembly defects. Furthermore, there exists a splice acceptor site located early within the VP1u DNA sequence that is important for generating the other cap genes, VP2, VP3, and AAP (236). Mutation of this splice acceptor site would alter the mRNA pool and subsequent production of the necessary cap genes, leading to disruption of capsid assembly. Therefore, further analysis of the pXR1p4 plasmid is necessary to rule out any possible artefactual causes.

Next, to confirm proper assembly of the AAV1 P mutants and incorporation of the mutant VP1, we performed a western blot of iodixanol-purified capsids (Fig. 26B). Additionally, this approach has the added benefit of allowing the indirect assessment of differences in packaging efficiencies, as we loaded equal vector genome amounts of each virus. Interestingly, while all P mutants assembled and incorporated VP1 subunits, AAV1p5 incorporated less VP1 protein than the other P mutants. Moreover, there were no observable differences in the amount of capsid protein loaded, indicating no observable differences in the ratio of empty to full particles in any of the mutants. Taken together, this data demonstrates that the AAV1 P mutants, with the exception of AAV1p4, efficiently assemble and package DNA.

Transduction analysis of AAV1 P mutants. We next sought to further characterize the P mutants by assessing transduction in cell culture. We infected HeLa cells with the P mutants packaging a luciferase transgene and assayed for transduction 24 hours later. As seen in Fig 27A, AAV1p2 is similar in transduction profile to AAV1. However, both AAV1p3 and AAV1p5 are both significantly transduction impaired. Additionally, while AAV1p9 displayed reduced transduction when compared to the parental AAV1, the reduction is less than 2-fold.Next, we assessed transduction in MB114 cells. MB114 cells are a mouse brain microvascular endothelial

cell line that is more permissive to AAV1 infection than other natural AAV serotypes. Transduction of MB114 cells by the P mutants largely reflected the transduction seen in HeLa cells (Fig. 27B). One interesting observation is that AAV1p5 demonstrates only ~2-fold reduction in transduction over AAV1, in stark contrast to HeLa cells. Moreover, since AAV1p5 was shown to have reduced incorporation of VP1 protein (Fig. 26B), this data might indicate a delicate relationship between the amounts of VP1 protein incorporated into the capsid, infected cell type, and transduction efficiency. However, further studies utilizing engineered capsids containing varying levels of VP1 protein will be required to test this.

Finally, we sought to determine the transduction characteristics of the P mutants in vivo. Previously, AAV1 has been shown to be effective at transducing skeletal muscle (237). Therefore, we performed intramuscular injections of AAV1 and the P mutants in BALB/c mice and assayed for luciferase expression by live animal imaging 4 weeks post-injection (Fig. 28). As expected, transduction of mouse muscle with AAV1p2 was similar to AAV1, AAV1p3 exhibited the most reduced transduction, with AAV1p5 also demonstrating reduced transduction. Interestingly, contrary to the in vitro data, AAV1p9 showed a more severe decrease in transduction in mice, performing similarly to AAV1p5.

Collectively, this data demonstrated striking differences in the P mutants that are due solely to the different VP1u regions. The transduction differences observed could be the result of varying efficiencies of the PLA2 enzymes contained within each VP1u region. Nonetheless, further studies are required to assess the phospholipase activity of each VP1u PLA2 enzyme to determine if this is the cause of the transduction differences.

Design and transduction of AAV1-miniPLA. In an effort to further understand the VP1u-based determinants of AAV transduction, we designed a synthetic AAV construct based on the AAV1 backbone with a small VP1u region. We termed this construct AAV1-miniPLA, to reflect the presence of the PLA domain within the mini VP1u region. As seen in Fig. 29A, this region was designed based on the sequence homology of AAV1 with the related parvovirus, human bocavirus 1 (HBoV). We retained the first 11 amino acids of AAV1 to avoid disrupting the aforementioned splice acceptor site. Furthermore, it is worth noting that we also removed the cryptic start codon that typically results in translation of the AAV1 VP2 protein. However, it has been previously shown that AAV capsids that lack VP2 remain infectious (238). To generate this mutant, we synthesized the synthetic portion of AAV1-miniPLA and used Gibson assembly to clone the synthetic DNA into the AAV1 backbone (235).

In order to characterize AAV1-miniPLA, we performed transduction assays on MB114 cells. It is important to note that AAV1-miniPLA is not defective in assembly or packaging. However, AAV1-miniPLA transduction is completely indistinguishable from background levels, indicating that AAV1-miniPLA is a completely defective virus particle (Fig. 29B). While this data demonstrates that the VP1u domain of our AAV1-miniPLA is nonfunctional, further optimization is needed to identify the regions of the AAV VP1u that are necessary and sufficient to allow for successful transduction. While studies have identified the BRs as necessary, they are not sufficient. Indeed, studies have shown that the PLA2 activity of the VP1u region is necessary for transduction (79). Further, some studies have begun to identify particular residues within the VP1u region that are required for viral PLA2 activity (239, 240). However, all of the residues of the VP1u region that are sufficient for function of the PLA2 enzyme remain to be fully elucidated. When designing AAV1-miniPLA, we utilized the sequence of HBoV, which has a

functional PLA2, to attempt to preserve the PLA2 activity of the AAV1 VP1u. Yet, as AAV1-miniPLA is transduction defective, further investigation of the PLA2 activity of AAV1-miniPLA is needed to determine if disruption of the PLA2 enzyme is the cause of the effect seen.

One property of AAV that reduces the clinical utility of AAV-based vectors is the limited packaging capacity. Indeed, it has been postulated that the internalized VP1u domain is responsible for limiting the packaging capacity of AAV to ~5kb due to steric hindrance. Intriguingly, other parvoviruses have similar capsid sizes while exhibiting a considerably larger packaging capacity. One such example is HBoV, which can package a genome of ~5.6kb. Therefore, a decrease in the size of the VP1u domain of AAV could potentially increase the packaging capacity. However, this has yet to be investigated in the case of AAV1-miniPLA.

In summary, we have taken the first steps toward elucidation of the functional differences between the VP1u regions of several natural AAV serotypes. Transferring the VP1u region from one AAV serotype onto another serotype is a viable strategy that could potentially yield novel AAV capsids with unique properties. However, further studies will need to be performed with the various VP1u/capsid combinations to identify promising vector candidates. In addition, we have utilized a homology-driven approach to generate a synthetic small AAV VP1u. While AAV1-miniPLA is transduction deficient, it will inform future studies that aim to determine the necessary and sufficient domains within the VP1u region to generate more unique vectors. Nevertheless, the capsids described in this study as well as other capsids generated using this system will likely prove valuable in future clinical gene therapy applications.

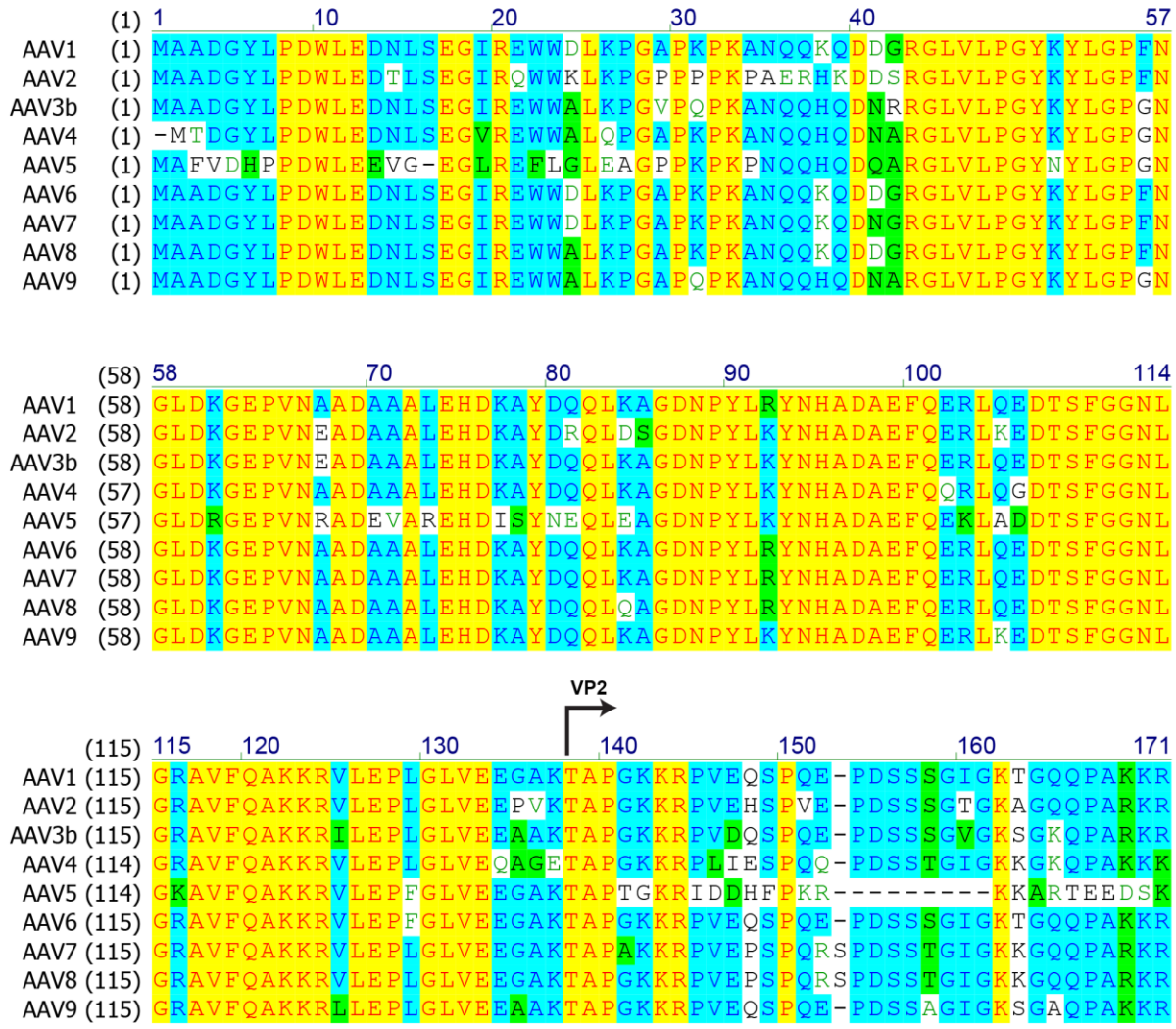

Figure 25: Alignment of the VP1 region of AAV serotypes 1-9. Using Vector NTI, the amino acid sequence of AAV serotypes 1-9 were aligned. Only amino acids 1-171 are presented. The black arrow indicates the start codon for the VP2 capsid protein.

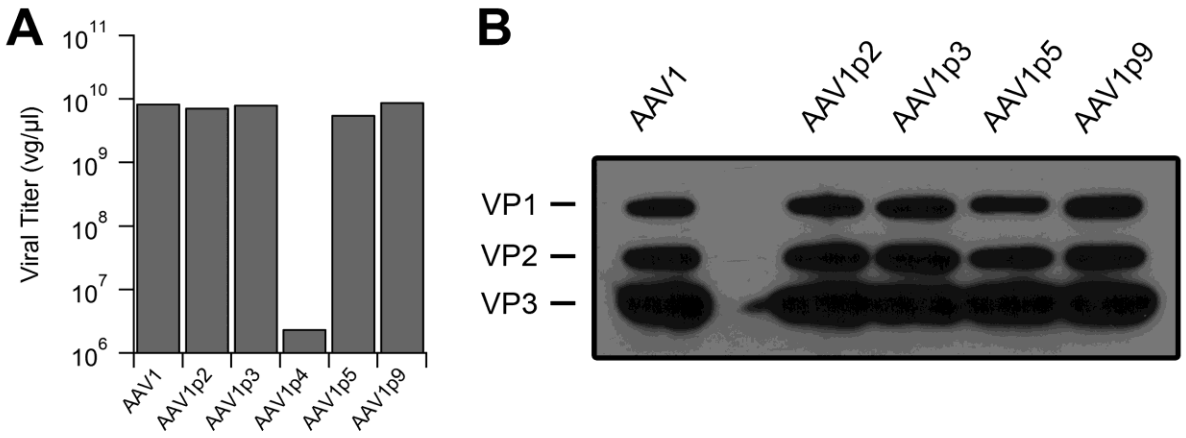

Figure 26: Structural characterization of the AAV1 P mutants. (A) Purified AAV1 and AAV1 P mutants were subjected to qPCR to determine viral titer. (B) 1e9 vg of purified AAV1 and AAV1 P mutants, with the exception of AAV1p4, were denatured and run on an SDS-PAGE gel and transferred to a nitrocellulose membrane. The membrane was then subjected to western blot with antibody B1 to blot for AAV capsid protein to determine incorporation rates of VP1.

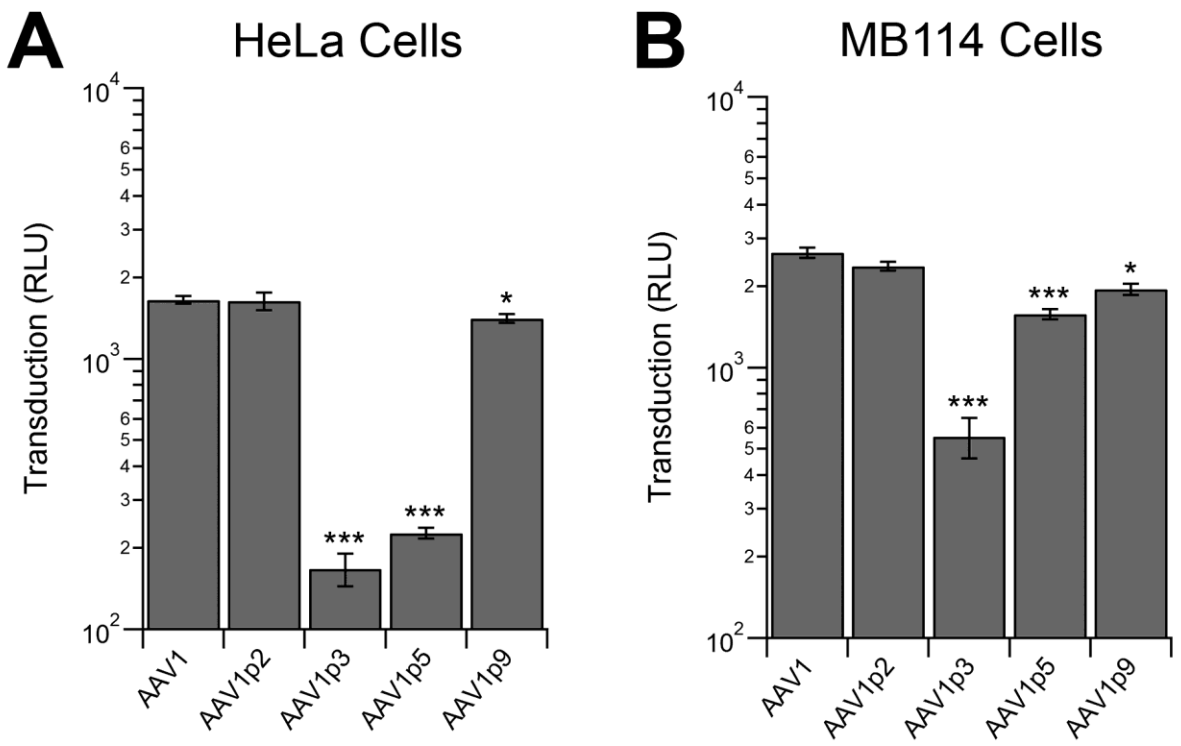

Figure 27: Grafting of other VP1u regions onto AAV1 alters transduction of both HeLa cells and MB114 cells. (A) Luciferase reporter expression of HeLa cells infected with 1,000 vg/cell of either AAV1 or the AAV1 P mutants. (B) Luciferase reporter expression of MB114 cells infected with 1,000 vg/cell of either AAV1 or the AAV1 P mutants. Cells were assayed 24 hours post-infection.

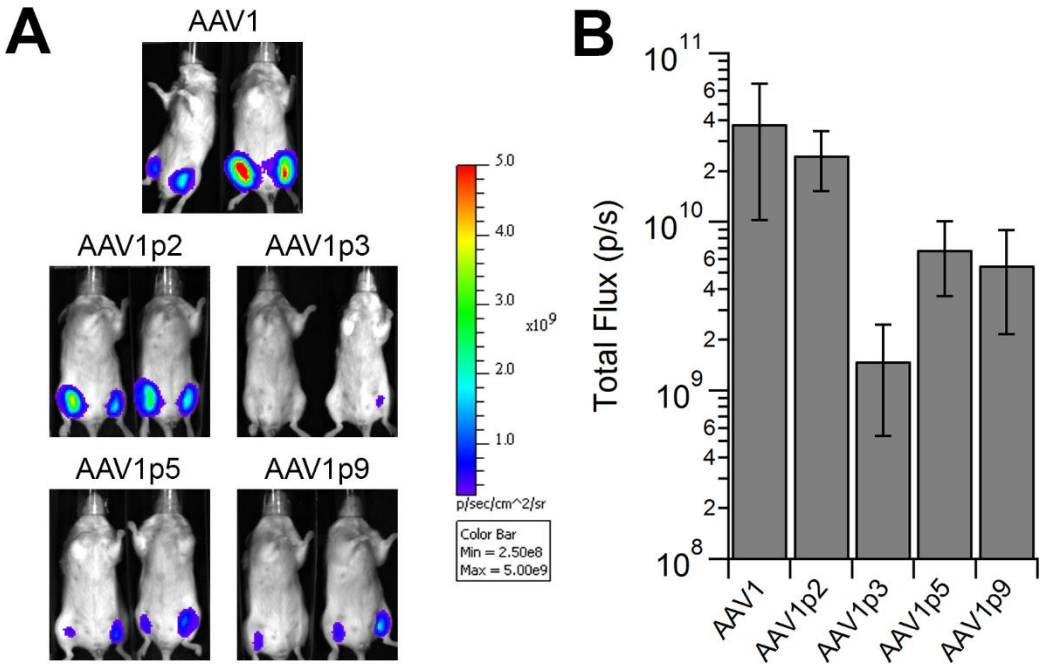

Figure 28: AAV1 P mutants differentially transduce mouse muscle tissue. BALB/c mice were injected with 5e9 vg of either AAV1 or the AAV1 P mutants intramuscularly into both left and right gastrocnemius muscles. Live animal imaging was performed 4 weeks post injection. (A) Luciferase expression of the IM injected mice. (B) Quantification of the luciferase signal resulting from the live animal imaging. Total flux, or photons/second, is shown.

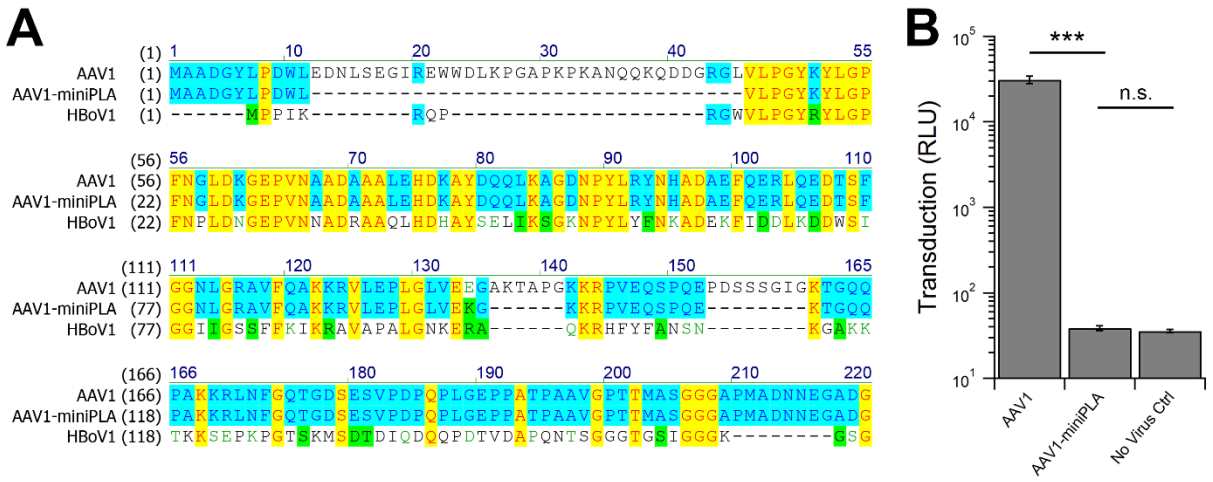

Figure 29: AAV1-miniPLA is transduction defective. (A) Vector NTI was used to align the amino acid capsid sequence for AAV1, HBov, and AAV1-miniPLA. Only amino acids 1-220 are presented. (B) Luciferase reporter expression of MB114 cells infected with 10,000 vg/cell of either AAV1 or AAV1-miniPLA. Cells were assayed 24 hours post-infection.

REFERENCES

1. **Berns K, Parrish CR**. 2007. Parvoviridae, p. 2437-2477. *In* Knipe DM, Howley PM (eds.), Fields Virology, 5th ed, vol II. Lippincott Williams & Wilkins, Philadelphia, PA.

2. **International Committee on Taxonomy of Viruses, F. A. Murphy, and International Union of Microbiological Societies. Virology Division.** 1995. Virus taxonomy: classification and nomenclature of viruses : sixth report of the International Committee on Taxonomy of Viruses. Springer-Verlag, Wien ; New York.

3. **Cotmore SF, Agbandje-McKenna M, Chiorini JA, Mukha DV, Pintel DJ, Qiu J, Soderlund-Venermo M, Tattersall P, Tijssen P, Gatherer D, Davison AJ**. 2014. The family Parvoviridae. Arch. Virol. **159:**1239-1247.

4. **Chinea B, Ramirez Ronda CH**. 1996. Infections caused by parvovirus B19. Bol. Asoc. Med. P. R. **88:**20-26.

5. **Podsakoff G, Wong KK,Jr, Chatterjee S**. 1994. Efficient gene transfer into nondividing cells by adeno-associated virus-based vectors. J. Virol. **68:**5656-5666.

6. **Mueller C, Flotte TR**. 2008. Clinical gene therapy using recombinant adeno-associated virus vectors. Gene Ther. **15:**858-863.

7. **Xiao X, Li J, Samulski RJ**. 1996. Efficient long-term gene transfer into muscle tissue of immunocompetent mice by adeno-associated virus vector. J. Virol. **70:**8098-8108.

8. **Nault JC, Datta S, Imbeaud S, Franconi A, Mallet M, Couchy G, Letouze E, Pilati C, Verret B, Blanc JF, Balabaud C, Calderaro J, Laurent A, Letexier M, Bioulac-Sage P, Calvo F, Zucman-Rossi J**. 2015. Recurrent AAV2-related insertional mutagenesis in human hepatocellular carcinomas. Nat. Genet. **47:**1187-1193.

9. **Xiao X, Xiao W, Li J, Samulski RJ**. 1997. A novel 165-base-pair terminal repeat sequence is the sole cis requirement for the adeno-associated virus life cycle. J. Virol. **71:**941-948.

10. **Leone P, Shera D, McPhee SW, Francis JS, Kolodny EH, Bilaniuk LT, Wang DJ, Assadi M, Goldfarb O, Goldman HW, Freese A, Young D, During MJ, Samulski RJ, Janson CG**. 2012. Long-term follow-up after gene therapy for canavan disease. Sci. Transl. Med. **4:**165ra163.

11. **Marks WJ,Jr, Baumann TL, Bartus RT**. 2016. Long-Term Safety of Patients with Parkinson's Disease Receiving rAAV2-Neurturin (CERE-120) Gene Transfer. Hum. Gene Ther.

12. **George LA, Fogarty PF**. 2016. Gene therapy for hemophilia: past, present and future. Semin. Hematol. **53:**46-54.

13. **Testa F, Maguire AM, Rossi S, Pierce EA, Melillo P, Marshall K, Banfi S, Surace EM, Sun J, Acerra C, Wright JF, Wellman J, High KA, Auricchio A, Bennett J, Simonelli F**. 2013. Three-year follow-up after unilateral subretinal delivery of adeno-associated virus in patients with Leber congenital Amaurosis type 2. Ophthalmology. **120:**1283-1291.

14. **Weleber RG, Pennesi ME, Wilson DJ, Kaushal S, Erker LR, Jensen L, McBride MT, Flotte TR, Humphries M, Calcedo R, Hauswirth WW, Chulay JD, Stout JT**. 2016. Results at 2 Years after Gene Therapy for RPE65-Deficient Leber Congenital Amaurosis and Severe Early-Childhood-Onset Retinal Dystrophy. Ophthalmology. .

15. **Gaudet D, Methot J, Kastelein J**. 2012. Gene therapy for lipoprotein lipase deficiency. Curr. Opin. Lipidol. **23:**310-320.

16. **ATCHISON RW, CASTO BC, HAMMON WM**. 1965. Adenovirus-Associated Defective Virus Particles. Science. **149:**754-756.

17. **Georg-Fries B, Biederlack S, Wolf J, zur Hausen H**. 1984. Analysis of proteins, helper dependence, and seroepidemiology of a new human parvovirus. Virology. **134:**64-71.

18. **Walz C, Deprez A, Dupressoir T, Durst M, Rabreau M, Schlehofer JR**. 1997. Interaction of human papillomavirus type 16 and adeno-associated virus type 2 co-infecting human cervical epithelium. J. Gen. Virol. **78 (Pt 6):**1441-1452.

19. **Schlehofer JR, Ehrbar M, zur Hausen H**. 1986. Vaccinia virus, herpes simplex virus, and carcinogens induce DNA amplification in a human cell line and support replication of a helpervirus dependent parvovirus. Virology. **152:**110-117.

20. **Masat E, Pavani G, Mingozzi F**. 2013. Humoral immunity to AAV vectors in gene therapy: challenges and potential solutions. Discov. Med. **15:**379-389.

21. **Kyostio SR, Owens RA, Weitzman MD, Antoni BA, Chejanovsky N, Carter BJ**. 1994. Analysis of adeno-associated virus (AAV) wild-type and mutant Rep proteins for their abilities to negatively regulate AAV p5 and p19 mRNA levels. J. Virol. **68:**2947-2957.

22. **Brister JR, Muzyczka N**. 1999. Rep-mediated nicking of the adeno-associated virus origin requires two biochemical activities, DNA helicase activity and transesterification. J. Virol. **73:**9325-9336.

23. **Im DS, Muzyczka N**. 1990. The AAV origin binding protein Rep68 is an ATP-dependent site-specific endonuclease with DNA helicase activity. Cell. **61:**447-457.

24. **Ni TH, Zhou X, McCarty DM, Zolotukhin I, Muzyczka N**. 1994. In vitro replication of adeno-associated virus DNA. J. Virol. **68:**1128-1138.

25. **Kotin RM, Siniscalco M, Samulski RJ, Zhu XD, Hunter L, Laughlin CA, McLaughlin S, Muzyczka N, Rocchi M, Berns KI**. 1990. Site-specific integration by adeno-associated virus. Proc. Natl. Acad. Sci. U. S. A. **87:**2211-2215.

26. **King JA, Dubielzig R, Grimm D, Kleinschmidt JA**. 2001. DNA helicase-mediated packaging of adeno-associated virus type 2 genomes into preformed capsids. Embo j. **20:**3282-3291.

27. **Sonntag F, Schmidt K, Kleinschmidt JA**. 2010. A viral assembly factor promotes AAV2 capsid formation in the nucleolus. Proc. Natl. Acad. Sci. U. S. A. **107:**10220-10225.

28. **Naumer M, Sonntag F, Schmidt K, Nieto K, Panke C, Davey NE, Popa-Wagner R, Kleinschmidt JA**. 2012. Properties of the adeno-associated virus assembly-activating protein. J. Virol. **86:**13038-13048.

29. **Kronenberg S, Kleinschmidt JA, Bottcher B**. 2001. Electron cryo-microscopy and image reconstruction of adeno-associated virus type 2 empty capsids. EMBO Rep. **2:**997-1002.

30. **Girod A, Wobus CE, Zadori Z, Ried M, Leike K, Tijssen P, Kleinschmidt JA, Hallek M**. 2002. The VP1 capsid protein of adeno-associated virus type 2 is carrying a phospholipase A2 domain required for virus infectivity. J. Gen. Virol. **83:**973-978.

31. **Grieger JC, Snowdy S, Samulski RJ**. 2006. Separate basic region motifs within the adeno-associated virus capsid proteins are essential for infectivity and assembly. J. Virol. **80:**5199-5210.

32. **Johnson JS, Li C, DiPrimio N, Weinberg MS, McCown TJ, Samulski RJ**. 2010. Mutagenesis of adeno-associated virus type 2 capsid protein VP1 uncovers new roles for basic amino acids in trafficking and cell-specific transduction. J. Virol. **84:**8888-8902.

33. **Sonntag F, Kother K, Schmidt K, Weghofer M, Raupp C, Nieto K, Kuck A, Gerlach B, Bottcher B, Muller OJ, Lux K, Horer M, Kleinschmidt JA**. 2011. The assembly-activating protein promotes capsid assembly of different adeno-associated virus serotypes. J. Virol. **85:**12686-12697.

34. **Earley LF, Kawano Y, Adachi K, Sun XX, Dai MS, Nakai H**. 2015. Identification and characterization of nuclear and nucleolar localization signals in the adeno-associated virus serotype 2 assembly-activating protein. J. Virol. **89:**3038-3048.

35. **Srivastava A, Lusby EW, Berns KI**. 1983. Nucleotide sequence and organization of the adeno-associated virus 2 genome. J. Virol. **45:**555-564.

36. **Hermonat PL, Santin AD, De Greve J, De Rijcke M, Bishop BM, Han L, Mane M, Kokorina N**. 1999. Chromosomal latency and expression at map unit 96 of a wild-type plus adeno-associated virus (AAV)/Neo vector and identification of p81, a new AAV transcriptional promoter. J. Hum. Virol. **2:**359-368.

37. **Cao M, You H, Hermonat PL**. 2014. The X gene of adeno-associated virus 2 (AAV2) is involved in viral DNA replication. PLoS One. **9:**e104596.

38. **Stutika C, Gogol-Doring A, Botschen L, Mietzsch M, Weger S, Feldkamp M, Chen W, Heilbronn R**. 2015. A Comprehensive RNA Sequencing Analysis of the Adeno-Associated Virus (AAV) Type 2 Transcriptome Reveals Novel AAV Transcripts, Splice Variants, and Derived Proteins. J. Virol. **90:**1278-1289.

39. **Summerford C, Samulski RJ**. 1998. Membrane-associated heparan sulfate proteoglycan is a receptor for adeno-associated virus type 2 virions. J. Virol. **72:**1438-1445.

40. **Handa A, Muramatsu S, Qiu J, Mizukami H, Brown KE**. 2000. Adeno-associated virus (AAV)-3-based vectors transduce haematopoietic cells not susceptible to transduction with AAV-2-based vectors. J. Gen. Virol. **81:**2077-2084.

41. **Kaludov N, Brown KE, Walters RW, Zabner J, Chiorini JA**. 2001. Adeno-associated virus serotype 4 (AAV4) and AAV5 both require sialic acid binding for hemagglutination and efficient transduction but differ in sialic acid linkage specificity. J. Virol. **75:**6884-6893.

42. **Walters RW, Yi SM, Keshavjee S, Brown KE, Welsh MJ, Chiorini JA, Zabner J**. 2001. Binding of adeno-associated virus type 5 to 2,3-linked sialic acid is required for gene transfer. J. Biol. Chem. **276:**20610-20616.

43. **Wu Z, Miller E, Agbandje-McKenna M, Samulski RJ**. 2006. Alpha2,3 and alpha2,6 N-linked sialic acids facilitate efficient binding and transduction by adeno-associated virus types 1 and 6. J. Virol. **80:**9093-9103.

44. **Wu Z, Asokan A, Grieger JC, Govindasamy L, Agbandje-McKenna M, Samulski RJ**. 2006. Single amino acid changes can influence titer, heparin binding, and tissue tropism in different adeno-associated virus serotypes. J. Virol. **80:**11393-11397.

45. **Shen S, Bryant KD, Brown SM, Randell SH, Asokan A**. 2011. Terminal N-linked galactose is the primary receptor for adeno-associated virus 9. J. Biol. Chem. **286:**13532-13540.

46. **Qing K, Mah C, Hansen J, Zhou S, Dwarki V, Srivastava A**. 1999. Human fibroblast growth factor receptor 1 is a co-receptor for infection by adeno-associated virus 2. Nat. Med. **5:**71-77.

47. **Ling C, Lu Y, Kalsi JK, Jayandharan GR, Li B, Ma W, Cheng B, Gee SW, McGoogan KE, Govindasamy L, Zhong L, Agbandje-McKenna M, Srivastava A**. 2010. Human hepatocyte growth factor receptor is a cellular coreceptor for adeno-associated virus serotype 3. Hum. Gene Ther. **21:**1741-1747.

48. **Di Pasquale G, Davidson BL, Stein CS, Martins I, Scudiero D, Monks A, Chiorini JA**. 2003. Identification of PDGFR as a receptor for AAV-5 transduction. Nat. Med. **9:**1306-1312.

49. **Summerford C, Bartlett JS, Samulski RJ**. 1999. AlphaVbeta5 integrin: a co-receptor for adeno-associated virus type 2 infection. Nat. Med. **5:**78-82.

50. **Asokan A, Hamra JB, Govindasamy L, Agbandje-McKenna M, Samulski RJ**. 2006. Adeno-associated virus type 2 contains an integrin alpha5beta1 binding domain essential for viral cell entry. J. Virol. **80:**8961-8969.

51. **Kaminsky PM, Keiser NW, Yan Z, Lei-Butters DC, Engelhardt JF**. 2012. Directing integrin-linked endocytosis of recombinant AAV enhances productive FAK-dependent transduction. Mol. Ther. **20:**972-983.

52. **Shen S, Berry GE, Castellanos Rivera RM, Cheung RY, Troupes AN, Brown SM, Kafri T, Asokan A**. 2015. Functional analysis of the putative integrin recognition motif on adeno-associated virus 9. J. Biol. Chem. **290:**1496-1504.

53. **Pillay S, Meyer NL, Puschnik AS, Davulcu O, Diep J, Ishikawa Y, Jae LT, Wosen JE, Nagamine CM, Chapman MS, Carette JE**. 2016. An essential receptor for adeno-associated virus infection. Nature. **530:**108-112.

54. **Shen S, Bryant KD, Sun J, Brown SM, Troupes A, Pulicherla N, Asokan A**. 2012. Glycan binding avidity determines the systemic fate of adeno-associated virus type 9. J. Virol. **86:**10408-10417.

55. **Murlidharan G, Corriher T, Ghashghaei HT, Asokan A**. 2015. Unique glycan signatures regulate adeno-associated virus tropism in the developing brain. J. Virol. **89:**3976-3987.

56. **Duan D, Li Q, Kao AW, Yue Y, Pessin JE, Engelhardt JF**. 1999. Dynamin is required for recombinant adeno-associated virus type 2 infection. J. Virol. **73:**10371-10376.

57. **Bartlett JS, Wilcher R, Samulski RJ**. 2000. Infectious entry pathway of adeno-associated virus and adeno-associated virus vectors. J. Virol. **74:**2777-2785.

58. **Nonnenmacher M, Weber T**. 2011. Adeno-associated virus 2 infection requires endocytosis through the CLIC/GEEC pathway. Cell. Host Microbe. **10:**563-576.

59. **Sanlioglu S, Benson PK, Yang J, Atkinson EM, Reynolds T, Engelhardt JF**. 2000. Endocytosis and nuclear trafficking of adeno-associated virus type 2 are controlled by rac1 and phosphatidylinositol-3 kinase activation. J. Virol. **74:**9184-9196.

60. **Weinberg MS, Nicolson S, Bhatt AP, McLendon M, Li C, Samulski RJ**. 2014. Recombinant adeno-associated virus utilizes cell-specific infectious entry mechanisms. J. Virol. **88:**12472-12484.

61. **Di Pasquale G, Chiorini JA**. 2006. AAV transcytosis through barrier epithelia and endothelium. Mol. Ther. **13:**506-516.

62. **Rothberg KG, Heuser JE, Donzell WC, Ying YS, Glenney JR, Anderson RG**. 1992. Caveolin, a protein component of caveolae membrane coats. Cell. **68:**673-682.

63. **Kotchey NM, Adachi K, Zahid M, Inagaki K, Charan R, Parker RS, Nakai H**. 2011. A potential role of distinctively delayed blood clearance of recombinant adeno-associated virus serotype 9 in robust cardiac transduction. Mol. Ther. **19:**1079-1089.

64. **Preta G, Cronin JG, Sheldon IM**. 2015. Dynasore - not just a dynamin inhibitor. Cell. Commun. Signal. **13:**24-015-0102-1.

65. **Koivusalo M, Welch C, Hayashi H, Scott CC, Kim M, Alexander T, Touret N, Hahn KM, Grinstein S**. 2010. Amiloride inhibits macropinocytosis by lowering submembranous pH and preventing Rac1 and Cdc42 signaling. J. Cell Biol. **188:**547-563.

66. **Gekle M, Drumm K, Mildenberger S, Freudinger R, Gassner B, Silbernagl S**. 1999. Inhibition of Na+-H+ exchange impairs receptor-mediated albumin endocytosis in renal proximal tubule-derived epithelial cells from opossum. J. Physiol. **520 Pt 3:**709-721.

67. **Harbison CE, Lyi SM, Weichert WS, Parrish CR**. 2009. Early steps in cell infection by parvoviruses: host-specific differences in cell receptor binding but similar endosomal trafficking. J. Virol. **83:**10504-10514.

68. **Ding W, Zhang LN, Yeaman C, Engelhardt JF**. 2006. rAAV2 traffics through both the late and the recycling endosomes in a dose-dependent fashion. Mol. Ther. **13:**671-682.

69. **Bantel-Schaal U, Hub B, Kartenbeck J**. 2002. Endocytosis of adeno-associated virus type 5 leads to accumulation of virus particles in the Golgi compartment. J. Virol. **76:**2340-2349.

70. **Johnson JS, Gentzsch M, Zhang L, Ribeiro CM, Kantor B, Kafri T, Pickles RJ, Samulski RJ**. 2011. AAV exploits subcellular stress associated with inflammation, endoplasmic reticulum expansion, and misfolded proteins in models of cystic fibrosis. PLoS Pathog. **7:**e1002053.

71. **Nonnenmacher ME, Cintrat JC, Gillet D, Weber T**. 2015. Syntaxin 5-dependent retrograde transport to the trans-Golgi network is required for adeno-associated virus transduction. J. Virol. **89:**1673-1687.

72. **Berry GE, Asokan A**. 2016. Chemical Modulation of Endocytic Sorting Augments Adeno-associated Viral Transduction. J. Biol. Chem. **291:**939-947.

73. **Douar AM, Poulard K, Stockholm D, Danos O**. 2001. Intracellular trafficking of adeno-associated virus vectors: routing to the late endosomal compartment and proteasome degradation. J. Virol. **75:**1824-1833.

74. **Nam HJ, Gurda BL, McKenna R, Potter M, Byrne B, Salganik M, Muzyczka N, Agbandje-McKenna M**. 2011. Structural studies of adeno-associated virus serotype 8 capsid transitions associated with endosomal trafficking. J. Virol. **85:**11791-11799.

75. **Kronenberg S, Bottcher B, von der Lieth CW, Bleker S, Kleinschmidt JA**. 2005. A conformational change in the adeno-associated virus type 2 capsid leads to the exposure of hidden VP1 N termini. J. Virol. **79:**5296-5303.

76. **Sonntag F, Bleker S, Leuchs B, Fischer R, Kleinschmidt JA**. 2006. Adeno-associated virus type 2 capsids with externalized VP1/VP2 trafficking domains are generated prior to passage through the cytoplasm and are maintained until uncoating occurs in the nucleus. J. Virol. **80:**11040-11054.

77. **Salganik M, Venkatakrishnan B, Bennett A, Lins B, Yarbrough J, Muzyczka N, Agbandje-McKenna M, McKenna R**. 2012. Evidence for pH-dependent protease activity in the adeno-associated virus capsid. J. Virol. **86:**11877-11885.

78. **Stahnke S, Lux K, Uhrig S, Kreppel F, Hosel M, Coutelle O, Ogris M, Hallek M, Buning H**. 2011. Intrinsic phospholipase A2 activity of adeno-associated virus is involved in endosomal escape of incoming particles. Virology. **409:**77-83.

79. **Grieger JC, Johnson JS, Gurda-Whitaker B, Agbandje-McKenna M, Samulski RJ**. 2007. Surface-exposed adeno-associated virus Vp1-NLS capsid fusion protein rescues infectivity of noninfectious wild-type Vp2/Vp3 and Vp3-only capsids but not that of fivefold pore mutant virions. J. Virol. **81:**7833-7843.

80. **Castle MJ, Perlson E, Holzbaur EL, Wolfe JH**. 2014. Long-distance axonal transport of AAV9 is driven by dynein and kinesin-2 and is trafficked in a highly motile Rab7-positive compartment. Mol. Ther. **22:**554-566.

81. **Nicolson SC, Samulski RJ**. 2014. Recombinant adeno-associated virus utilizes host cell nuclear import machinery to enter the nucleus. J. Virol. **88:**4132-4144.

82. **Kelich JM, Ma J, Dong B, Wang Q, Chin M, Magura CM, Xiao W, Yang W**. 2015. Super-resolution imaging of nuclear import of adeno-associated virus in live cells. Mol. Ther. Methods Clin. Dev. **2:**15047.

83. **Qiu J, Brown KE**. 1999. A 110-kDa nuclear shuttle protein, nucleolin, specifically binds to adeno-associated virus type 2 (AAV-2) capsid. Virology. **257:**373-382.

84. **Bevington JM, Needham PG, Verrill KC, Collaco RF, Basrur V, Trempe JP**. 2007. Adeno-associated virus interactions with B23/Nucleophosmin: identification of sub-nucleolar virion regions. Virology. **357:**102-113.

85. **Johnson JS, Samulski RJ**. 2009. Enhancement of adeno-associated virus infection by mobilizing capsids into and out of the nucleolus. J. Virol. **83:**2632-2644.

86. **Horowitz ED, Rahman KS, Bower BD, Dismuke DJ, Falvo MR, Griffith JD, Harvey SC, Asokan A**. 2013. Biophysical and ultrastructural characterization of adeno-associated virus capsid uncoating and genome release. J. Virol. **87:**2994-3002.

87. **Ferrari FK, Samulski T, Shenk T, Samulski RJ**. 1996. Second-strand synthesis is a rate-limiting step for efficient transduction by recombinant adeno-associated virus vectors. J. Virol. **70:**3227-3234.

88. **Qing K, Wang XS, Kube DM, Ponnazhagan S, Bajpai A, Srivastava A**. 1997. Role of tyrosine phosphorylation of a cellular protein in adeno-associated virus 2-mediated transgene expression. Proc. Natl. Acad. Sci. U. S. A. **94:**10879-10884.

89. **Qing K, Khuntirat B, Mah C, Kube DM, Wang XS, Ponnazhagan S, Zhou S, Dwarki VJ, Yoder MC, Srivastava A**. 1998. Adeno-associated virus type 2-mediated gene transfer: correlation of tyrosine phosphorylation of the cellular single-stranded D sequence-binding protein with transgene expression in human cells in vitro and murine tissues in vivo. J. Virol. **72:**1593-1599.

90. **Choi VW, McCarty DM, Samulski RJ**. 2006. Host cell DNA repair pathways in adeno-associated viral genome processing. J. Virol. **80:**10346-10356.

91. **Schwartz RA, Palacios JA, Cassell GD, Adam S, Giacca M, Weitzman MD**. 2007. The Mre11/Rad50/Nbs1 complex limits adeno-associated virus transduction and replication. J. Virol. **81:**12936-12945.

92. **Lentz TB, Samulski RJ**. 2015. Insight into the mechanism of inhibition of adeno-associated virus by the Mre11/Rad50/Nbs1 complex. J. Virol. **89:**181-194.

93. **Zentilin L, Marcello A, Giacca M**. 2001. Involvement of cellular double-stranded DNA break binding proteins in processing of the recombinant adeno-associated virus genome. J. Virol. **75:**12279-12287.

94. **Choi VW, Samulski RJ, McCarty DM**. 2005. Effects of adeno-associated virus DNA hairpin structure on recombination. J. Virol. **79:**6801-6807.

95. **Surosky RT, Urabe M, Godwin SG, McQuiston SA, Kurtzman GJ, Ozawa K, Natsoulis G**. 1997. Adeno-associated virus Rep proteins target DNA sequences to a unique locus in the human genome. J. Virol. **71:**7951-7959.

96. **Salganik M, Aydemir F, Nam HJ, McKenna R, Agbandje-McKenna M, Muzyczka N**. 2014. Adeno-associated virus capsid proteins may play a role in transcription and second-strand synthesis of recombinant genomes. J. Virol. **88:**1071-1079.

97. **Schreiber CA, Sakuma T, Izumiya Y, Holditch SJ, Hickey RD, Bressin RK, Basu U, Koide K, Asokan A, Ikeda Y**. 2015. An siRNA Screen Identifies the U2 snRNP Spliceosome as a Host Restriction Factor for Recombinant Adeno-associated Viruses. PLoS Pathog. **11:**e1005082.

98. **Xiao X, Li J, Samulski RJ**. 1998. Production of high-titer recombinant adeno-associated virus vectors in the absence of helper adenovirus. J. Virol. **72:**2224-2232.

99. **Li J, Samulski RJ, Xiao X**. 1997. Role for highly regulated rep gene expression in adeno-associated virus vector production. J. Virol. **71:**5236-5243.

100. **Grimm D, Kern A, Rittner K, Kleinschmidt JA**. 1998. Novel tools for production and purification of recombinant adenoassociated virus vectors. Hum. Gene Ther. **9:**2745-2760.

101. **Rabinowitz JE, Rolling F, Li C, Conrath H, Xiao W, Xiao X, Samulski RJ**. 2002. Cross-packaging of a single adeno-associated virus (AAV) type 2 vector genome into multiple AAV serotypes enables transduction with broad specificity. J. Virol. **76:**791-801.

102. **Bowles DE, McPhee SW, Li C, Gray SJ, Samulski JJ, Camp AS, Li J, Wang B, Monahan PE, Rabinowitz JE, Grieger JC, Govindasamy L, Agbandje-McKenna M, Xiao X, Samulski RJ**. 2012. Phase 1 gene therapy for Duchenne muscular dystrophy using a translational optimized AAV vector. Mol. Ther. **20:**443-455.

103. **Gao GP, Alvira MR, Wang L, Calcedo R, Johnston J, Wilson JM**. 2002. Novel adeno-associated viruses from rhesus monkeys as vectors for human gene therapy. Proc. Natl. Acad. Sci. U. S. A. **99:**11854-11859.

104. **Vercauteren K, Hoffman BE, Zolotukhin I, Keeler GD, Xiao JW, Basner-Tschakarjan E, High KA, Ertl HC, Rice CM, Srivastava A, de Jong YP, Herzog RW**. 2016. Superior In vivo Transduction of Human Hepatocytes Using Engineered AAV3 Capsid. Mol. Ther. .

105. **Asokan A, Conway JC, Phillips JL, Li C, Hegge J, Sinnott R, Yadav S, DiPrimio N, Nam HJ, Agbandje-McKenna M, McPhee S, Wolff J, Samulski RJ**. 2010. Reengineering a receptor footprint of adeno-associated virus enables selective and systemic gene transfer to muscle. Nat. Biotechnol. **28:**79-82.

106. **Crameri A, Raillard SA, Bermudez E, Stemmer WP**. 1998. DNA shuffling of a family of genes from diverse species accelerates directed evolution. Nature. **391:**288-291.

107. **Maheshri N, Koerber JT, Kaspar BK, Schaffer DV**. 2006. Directed evolution of adeno-associated virus yields enhanced gene delivery vectors. Nat. Biotechnol. **24:**198-204.

108. **Koerber JT, Jang JH, Schaffer DV**. 2008. DNA shuffling of adeno-associated virus yields functionally diverse viral progeny. Mol. Ther. **16:**1703-1709.

109. **Li W, Asokan A, Wu Z, Van Dyke T, DiPrimio N, Johnson JS, Govindaswamy L, Agbandje-McKenna M, Leichtle S, Redmond DE,Jr, McCown TJ, Petermann KB, Sharpless NE, Samulski RJ**. 2008. Engineering and selection of shuffled AAV genomes: a new strategy for producing targeted biological nanoparticles. Mol. Ther. **16:**1252-1260.

110. **Gray SJ, Blake BL, Criswell HE, Nicolson SC, Samulski RJ, McCown TJ, Li W**. 2010. Directed evolution of a novel adeno-associated virus (AAV) vector that crosses the seizure-compromised blood-brain barrier (BBB). Mol. Ther. **18:**570-578.

111. **Pulicherla N, Shen S, Yadav S, Debbink K, Govindasamy L, Agbandje-McKenna M, Asokan A**. 2011. Engineering liver-detargeted AAV9 vectors for cardiac and musculoskeletal gene transfer. Mol. Ther. **19:**1070-1078.

112. **Bell CL, Gurda BL, Van Vliet K, Agbandje-McKenna M, Wilson JM**. 2012. Identification of the galactose binding domain of the adeno-associated virus serotype 9 capsid. J. Virol. **86:**7326-7333.

113. **Shen S, Horowitz ED, Troupes AN, Brown SM, Pulicherla N, Samulski RJ, Agbandje-McKenna M, Asokan A**. 2013. Engraftment of a galactose receptor footprint onto adeno-associated viral capsids improves transduction efficiency. J. Biol. Chem. **288:**28814-28823.

114. **Carrillo-Carrasco N, Chandler RJ, Chandrasekaran S, Venditti CP**. 2010. Liver-directed recombinant adeno-associated viral gene delivery rescues a lethal mouse model of methylmalonic acidemia and provides long-term phenotypic correction. Hum. Gene Ther. **21:**1147-1154.

115. **Cotugno G, Annunziata P, Tessitore A, O'Malley T, Capalbo A, Faella A, Bartolomeo R, O'Donnell P, Wang P, Russo F, Sleeper MM, Knox VW, Fernandez S, Levanduski L, Hopwood J, De Leonibus E, Haskins M, Auricchio A**. 2011. Long-term amelioration of feline Mucopolysaccharidosis VI after AAV-mediated liver gene transfer. Mol. Ther. **19:**461-469.

116. **Bell P, Gao G, Haskins ME, Wang L, Sleeper M, Wang H, Calcedo R, Vandenberghe LH, Chen SJ, Weisse C, Withnall E, Wilson JM**. 2011. Evaluation of adeno-associated viral vectors for liver-directed gene transfer in dogs. Hum. Gene Ther. **22:**985-997.

117. **Kugler S, Lingor P, Scholl U, Zolotukhin S, Bahr M**. 2003. Differential transgene expression in brain cells in vivo and in vitro from AAV-2 vectors with small transcriptional control units. Virology. **311:**89-95.

118. **Nathanson JL, Yanagawa Y, Obata K, Callaway EM**. 2009. Preferential labeling of inhibitory and excitatory cortical neurons by endogenous tropism of adeno-associated virus and lentivirus vectors. Neuroscience. **161:**441-450.

119. **Diester I, Kaufman MT, Mogri M, Pashaie R, Goo W, Yizhar O, Ramakrishnan C, Deisseroth K, Shenoy KV**. 2011. An optogenetic toolbox designed for primates. Nat. Neurosci. **14:**387-397.

120. **Lawlor PA, Bland RJ, Mouravlev A, Young D, During MJ**. 2009. Efficient gene delivery and selective transduction of glial cells in the mammalian brain by AAV serotypes isolated from nonhuman primates. Mol. Ther. **17:**1692-1702.

121. **von Jonquieres G, Mersmann N, Klugmann CB, Harasta AE, Lutz B, Teahan O, Housley GD, Frohlich D, Kramer-Albers EM, Klugmann M**. 2013. Glial promoter selectivity following AAV-delivery to the immature brain. PLoS One. **8:**e65646.

122. **Portales-Casamar E, Swanson DJ, Liu L, de Leeuw CN, Banks KG, Ho Sui SJ, Fulton DL, Ali J, Amirabbasi M, Arenillas DJ, Babyak N, Black SF, Bonaguro RJ, Brauer E, Candido TR, Castellarin M, Chen J, Chen Y, Cheng JC, Chopra V, Docking TR, Dreolini L, D'Souza CA, Flynn EK, Glenn R, Hatakka K, Hearty TG, Imanian B, Jiang S, Khorasan-zadeh S, Komljenovic I, Laprise S, Liao NY, Lim JS, Lithwick S, Liu F, Liu J, Lu M, McConechy M, McLeod AJ, Milisavljevic M, Mis J, O'Connor K, Palma B, Palmquist DL, Schmouth JF, Swanson MI, Tam B, Ticoll A, Turner JL, Varhol R, Vermeulen J, Watkins RF, Wilson G, Wong BK, Wong SH, Wong TY, Yang GS, Ypsilanti AR, Jones SJ, Holt RA, Goldowitz D, Wasserman WW, Simpson EM**. 2010. A regulatory toolbox of MiniPromoters to drive selective expression in the brain. Proc. Natl. Acad. Sci. U. S. A. **107:**16589-16594.

123. **de Leeuw CN, Dyka FM, Boye SL, Laprise S, Zhou M, Chou AY, Borretta L, McInerny SC, Banks KG, Portales-Casamar E, Swanson MI, D'Souza CA, Boye SE, Jones SJ, Holt RA, Goldowitz D, Hauswirth WW, Wasserman WW, Simpson EM**. 2014. Targeted CNS Delivery Using Human MiniPromoters and Demonstrated Compatibility with Adeno-Associated Viral Vectors. Mol. Ther. Methods Clin. Dev. **1:**5.

124. **de Leeuw CN, Korecki AJ, Berry GE, Hickmott JW, Lam SL, Lengyell TC, Bonaguro RJ, Borretta LJ, Chopra V, Chou AY, D'Souza CA, Kaspieva O, Laprise S, McInerny SC, Portales-Casamar E, Swanson-Newman MI, Wong K, Yang GS, Zhou M, Jones SJ, Holt RA, Asokan A, Goldowitz D, Wasserman WW, Simpson EM**. 2016. rAAV-compatible MiniPromoters for restricted expression in the brain and eye. Mol. Brain. **9:**52-016-0232-4.

125. **Gray SJ, Foti SB, Schwartz JW, Bachaboina L, Taylor-Blake B, Coleman J, Ehlers MD, Zylka MJ, McCown TJ, Samulski RJ**. 2011. Optimizing promoters for recombinant adeno-associated virus-mediated gene expression in the peripheral and central nervous system using self-complementary vectors. Hum. Gene Ther. **22:**1143-1153.

126. **Karali M, Manfredi A, Puppo A, Marrocco E, Gargiulo A, Allocca M, Corte MD, Rossi S, Giunti M, Bacci ML, Simonelli F, Surace EM, Banfi S, Auricchio A**. 2011. MicroRNA-restricted transgene expression in the retina. PLoS One. **6:**e22166.

127. **Ahmed SS, Li H, Cao C, Sikoglu EM, Denninger AR, Su Q, Eaton S, Liso Navarro AA, Xie J, Szucs S, Zhang H, Moore C, Kirschner DA, Seyfried TN, Flotte TR, Matalon R, Gao G**. 2013. A single intravenous rAAV injection as late as P20 achieves efficacious and sustained CNS Gene therapy in Canavan mice. Mol. Ther. **21:**2136-2147.

128. **Qiao C, Yuan Z, Li J, He B, Zheng H, Mayer C, Li J, Xiao X**. 2011. Liver-specific microRNA-122 target sequences incorporated in AAV vectors efficiently inhibits transgene expression in the liver. Gene Ther. **18:**403-410.

129. **McCarty DM, Monahan PE, Samulski RJ**. 2001. Self-complementary recombinant adeno-associated virus (scAAV) vectors promote efficient transduction independently of DNA synthesis. Gene Ther. **8:**1248-1254.

130. **Loeb JE, Cordier WS, Harris ME, Weitzman MD, Hope TJ**. 1999. Enhanced expression of transgenes from adeno-associated virus vectors with the woodchuck hepatitis virus posttranscriptional regulatory element: implications for gene therapy. Hum. Gene Ther. **10:**2295-2305.

131. **Virella-Lowell I, Zusman B, Foust K, Loiler S, Conlon T, Song S, Chesnut KA, Ferkol T, Flotte TR**. 2005. Enhancing rAAV vector expression in the lung. J. Gene Med. **7:**842-850.

132. **Donello JE, Loeb JE, Hope TJ**. 1998. Woodchuck hepatitis virus contains a tripartite posttranscriptional regulatory element. J. Virol. **72:**5085-5092.

133. **Aslanidi, G. V., L. Govindasamy, C. Ling, S. Zolotukhin, M. Agbandje-McKenna, and A. Srivastava.** 2011. Abstr. Site-Directed Mutagenesis of a Surface-Exposed Serine Residue Leads to High-Efficiency Transduction by Recombinant Adeno-Associated Virus 2 Vectors. Mol. Ther. **19:**S128.

134. **Aslanidi GV, Rivers AE, Ortiz L, Song L, Ling C, Govindasamy L, Van Vliet K, Tan M, Agbandje-McKenna M, Srivastava A**. 2013. Optimization of the capsid of recombinant adeno-associated virus 2 (AAV2) vectors: the final threshold? PLoS One. **8:**e59142.

135. **Russell DW, Miller AD, Alexander IE**. 1994. Adeno-associated virus vectors preferentially transduce cells in S phase. Proc. Natl. Acad. Sci. U. S. A. **91:**8915-8919.

136. **Alexander IE, Russell DW, Miller AD**. 1994. DNA-damaging agents greatly increase the transduction of nondividing cells by adeno-associated virus vectors. J. Virol. **68:**8282-8287.

137. **Russell DW, Alexander IE, Miller AD**. 1995. DNA synthesis and topoisomerase inhibitors increase transduction by adeno-associated virus vectors. Proc. Natl. Acad. Sci. U. S. A. **92:**5719-5723.

138. **Zhao W, Zhong L, Wu J, Chen L, Qing K, Weigel-Kelley KA, Larsen SH, Shou W, Warrington KH,Jr, Srivastava A**. 2006. Role of cellular FKBP52 protein in intracellular trafficking of recombinant adeno-associated virus 2 vectors. Virology. **353:**283-293.

139. **Yan Z, Zak R, Luxton GW, Ritchie TC, Bantel-Schaal U, Engelhardt JF**. 2002. Ubiquitination of both adeno-associated virus type 2 and 5 capsid proteins affects the transduction efficiency of recombinant vectors. J. Virol. **76:**2043-2053.

140. **Yan Z, Zak R, Zhang Y, Ding W, Godwin S, Munson K, Peluso R, Engelhardt JF**. 2004. Distinct classes of proteasome-modulating agents cooperatively augment recombinant adeno-associated virus type 2 and type 5-mediated transduction from the apical surfaces of human airway epithelia. J. Virol. **78:**2863-2874.

141. **Nathwani AC, Cochrane M, McIntosh J, Ng CY, Zhou J, Gray JT, Davidoff AM**. 2009. Enhancing transduction of the liver by adeno-associated viral vectors. Gene Ther. **16:**60-69.

142. **Mitchell AM, Samulski RJ**. 2013. Mechanistic insights into the enhancement of adeno-associated virus transduction by proteasome inhibitors. J. Virol. **87:**13035-13041.

143. **Arastu-Kapur S, Anderl JL, Kraus M, Parlati F, Shenk KD, Lee SJ, Muchamuel T, Bennett MK, Driessen C, Ball AJ, Kirk CJ**. 2011. Nonproteasomal targets of the proteasome inhibitors bortezomib and carfilzomib: a link to clinical adverse events. Clin. Cancer Res. **17:**2734-2743.

144. **Zhong L, Qing K, Si Y, Chen L, Tan M, Srivastava A**. 2004. Heat-shock treatment-mediated increase in transduction by recombinant adeno-associated virus 2 vectors is independent of the cellular heat-shock protein 90. J. Biol. Chem. **279:**12714-12723.

145. **Mitchell AM, Li C, Samulski RJ**. 2013. Arsenic trioxide stabilizes accumulations of adeno-associated virus virions at the perinuclear region, increasing transduction in vitro and in vivo. J. Virol. **87:**4571-4583.

146. **Wang Q, Mora-Jensen H, Weniger MA, Perez-Galan P, Wolford C, Hai T, Ron D, Chen W, Trenkle W, Wiestner A, Ye Y**. 2009. ERAD inhibitors integrate ER stress with an epigenetic mechanism to activate BH3-only protein NOXA in cancer cells. Proc. Natl. Acad. Sci. U. S. A. **106:**2200-2205.

147. **Brem GJ, Mylonas I, Bruning A**. 2013. Eeyarestatin causes cervical cancer cell sensitization to bortezomib treatment by augmenting ER stress and CHOP expression. Gynecol. Oncol. **128:**383-390.

148. **Christianson JC, Ye Y**. 2014. Cleaning up in the endoplasmic reticulum: ubiquitin in charge. Nat. Struct. Mol. Biol. **21:**325-335.

149. **Byun H, Gou Y, Zook A, Lozano MM, Dudley JP**. 2014. ERAD and how viruses exploit it. Front. Microbiol. **5:**330.

150. **Noack J, Bernasconi R, Molinari M**. 2014. How viruses hijack the ERAD tuning machinery. J. Virol. **88:**10272-10275.

151. **Bennett SM, Jiang M, Imperiale MJ**. 2013. Role of cell-type-specific endoplasmic reticulum-associated degradation in polyomavirus trafficking. J. Virol. **87:**8843-8852.

152. **Boya P, Reggiori F, Codogno P**. 2013. Emerging regulation and functions of autophagy. Nat. Cell Biol. **15:**713-720.

153. **Kirkegaard K**. 2009. Subversion of the cellular autophagy pathway by viruses. Curr. Top. Microbiol. Immunol. **335:**323-333.

154. **Jackson WT**. 2015. Viruses and the autophagy pathway. Virology. **479-480C:**450-456.

155. **Lennemann NJ, Coyne CB**. 2015. Catch me if you can: the link between autophagy and viruses. PLoS Pathog. **11:**e1004685.

156. **Bar S, Rommelaere J, Nuesch JP**. 2013. Vesicular transport of progeny parvovirus particles through ER and Golgi regulates maturation and cytolysis. PLoS Pathog. **9:**e1003605.

157. **Bowles DE, Rabinowitz JE, Samulski RJ**. 2006. The genus *Dependovirus*, p. 15-24. *In* Kerr JR, Cotmore SF, Bloom ME, Linden RM, Parrish CR (eds.), Parvoviruses. Edward Arnold Ltd., New York.

158. **Huang LY, Halder S, Agbandje-McKenna M**. 2014. Parvovirus glycan interactions. Curr. Opin. Virol. **7C:**108-118.

159. **Xiao PJ, Samulski RJ**. 2012. Cytoplasmic trafficking, endosomal escape, and perinuclear accumulation of adeno-associated virus type 2 particles are facilitated by microtubule network. J. Virol. **86:**10462-10473.

160. **Duan D, Yue Y, Yan Z, Yang J, Engelhardt JF**. 2000. Endosomal processing limits gene transfer to polarized airway epithelia by adeno-associated virus. J. Clin. Invest. **105:**1573-1587.

161. **Wobus CE, Hugle-Dorr B, Girod A, Petersen G, Hallek M, Kleinschmidt JA**. 2000. Monoclonal antibodies against the adeno-associated virus type 2 (AAV-2) capsid: epitope mapping and identification of capsid domains involved in AAV-2-cell interaction and neutralization of AAV-2 infection. J. Virol. **74:**9281-9293.

162. **Wistuba A, Weger S, Kern A, Kleinschmidt JA**. 1995. Intermediates of adeno-associated virus type 2 assembly: identification of soluble complexes containing Rep and Cap proteins. J. Virol. **69:**5311-5319.

163. **Shen S, Troupes AN, Pulicherla N, Asokan A**. 2013. Multiple roles for sialylated glycans in determining the cardiopulmonary tropism of adeno-associated virus 4. J. Virol. **87:**13206-13213.

164. **Mateo R, Nagamine CM, Spagnolo J, Mendez E, Rahe M, Gale M,Jr, Yuan J, Kirkegaard K**. 2013. Inhibition of cellular autophagy deranges dengue virion maturation. J. Virol. **87:**1312-1321.

165. **Raaben M, Posthuma CC, Verheije MH, te Lintelo EG, Kikkert M, Drijfhout JW, Snijder EJ, Rottier PJ, de Haan CA**. 2010. The ubiquitin-proteasome system plays an important role during various stages of the coronavirus infection cycle. J. Virol. **84:**7869-7879.

166. **Wang Q, Shinkre BA, Lee JG, Weniger MA, Liu Y, Chen W, Wiestner A, Trenkle WC, Ye Y**. 2010. The ERAD inhibitor Eeyarestatin I is a bifunctional compound with a membrane-binding domain and a p97/VCP inhibitory group. PLoS One. **5:**e15479.

167. **McKibbin C, Mares A, Piacenti M, Williams H, Roboti P, Puumalainen M, Callan AC, Lesiak-Mieczkowska K, Linder S, Harant H, High S, Flitsch SL, Whitehead RC, Swanton E**. 2012. Inhibition of protein translocation at the endoplasmic reticulum promotes activation of the unfolded protein response. Biochem. J. **442:**639-648.

168. **Cross BC, McKibbin C, Callan AC, Roboti P, Piacenti M, Rabu C, Wilson CM, Whitehead R, Flitsch SL, Pool MR, High S, Swanton E**. 2009. Eeyarestatin I inhibits Sec61-mediated protein translocation at the endoplasmic reticulum. J. Cell. Sci. **122:**4393-4400.

169. **Aletrari MO, McKibbin C, Williams H, Pawar V, Pietroni P, Lord JM, Flitsch SL, Whitehead R, Swanton E, High S, Spooner RA**. 2011. Eeyarestatin 1 interferes with both retrograde and anterograde intracellular trafficking pathways. PLoS One. **6:**e22713.

170. **Ramanathan HN, Ye Y**. 2012. The p97 ATPase associates with EEA1 to regulate the size of early endosomes. Cell Res. **22:**346-359.

171. **Venkatakrishnan B, Yarbrough J, Domsic J, Bennett A, Bothner B, Kozyreva OG, Samulski RJ, Muzyczka N, McKenna R, Agbandje-McKenna M**. 2013. Structure and dynamics of adeno-associated virus serotype 1 VP1-unique N-terminal domain and its role in capsid trafficking. J. Virol. **87:**4974-4984.

172. **Hanson PI, Whiteheart SW**. 2005. AAA+ proteins: have engine, will work. Nat. Rev. Mol. Cell Biol. **6:**519-529.

173. **Ramadan K, Bruderer R, Spiga FM, Popp O, Baur T, Gotta M, Meyer HH**. 2007. Cdc48/p97 promotes reformation of the nucleus by extracting the kinase Aurora B from chromatin. Nature. **450:**1258-1262.

174. **Magnaghi P, D'Alessio R, Valsasina B, Avanzi N, Rizzi S, Asa D, Gasparri F, Cozzi L, Cucchi U, Orrenius C, Polucci P, Ballinari D, Perrera C, Leone A, Cervi G, Casale E, Xiao Y, Wong C, Anderson DJ, Galvani A, Donati D, O'Brien T, Jackson PK, Isacchi A**. 2013. Covalent and allosteric inhibitors of the ATPase VCP/p97 induce cancer cell death. Nat. Chem. Biol. **9:**548-556.

175. **Yi P, Higa A, Taouji S, Bexiga MG, Marza E, Arma D, Castain C, Le Bail B, Simpson JC, Rosenbaum J, Balabaud C, Bioulac-Sage P, Blanc JF, Chevet E**. 2012. Sorafenib-mediated targeting of the AAA(+) ATPase p97/VCP leads to disruption of the secretory pathway, endoplasmic reticulum stress, and hepatocellular cancer cell death. Mol. Cancer. Ther. **11:**2610-2620.

176. **Brini M, Cali T, Ottolini D, Carafoli E**. 2013. Intracellular calcium homeostasis and signaling. Met. Ions Life. Sci. **12:**119-168.

177. **Lazzari C, Kipanyula MJ, Agostini M, Pozzan T, Fasolato C**. 2015. Abeta42 oligomers selectively disrupt neuronal calcium release. Neurobiol. Aging. **36:**877-885.

178. **McBrayer M, Nixon RA**. 2013. Lysosome and calcium dysregulation in Alzheimer's disease: partners in crime. Biochem. Soc. Trans. **41:**1495-1502.

179. **Chen X, Tang TS, Tu H, Nelson O, Pook M, Hammer R, Nukina N, Bezprozvanny I**. 2008. Deranged calcium signaling and neurodegeneration in spinocerebellar ataxia type 3. J. Neurosci. **28:**12713-12724.

180. **Liu J, Tang TS, Tu H, Nelson O, Herndon E, Huynh DP, Pulst SM, Bezprozvanny I**. 2009. Deranged calcium signaling and neurodegeneration in spinocerebellar ataxia type 2. J. Neurosci. **29:**9148-9162.

181. **Bezprozvanny I**. 2011. Role of inositol 1,4,5-trisphosphate receptors in pathogenesis of Huntington's disease and spinocerebellar ataxias. Neurochem. Res. **36:**1186-1197.

182. **Kasumu A, Bezprozvanny I**. 2012. Deranged calcium signaling in Purkinje cells and pathogenesis in spinocerebellar ataxia 2 (SCA2) and other ataxias. Cerebellum. **11:**630-639.

183. **Hu K, Carroll J, Fedorovich S, Rickman C, Sukhodub A, Davletov B**. 2002. Vesicular restriction of synaptobrevin suggests a role for calcium in membrane fusion. Nature. **415:**646-650.

184. **Benarroch EE**. 2013. Synaptic vesicle exocytosis: molecular mechanisms and clinical implications. Neurology. **80:**1981-1988.

185. **Leitz J, Kavalali ET**. 2015. Ca2+ Dependence of Synaptic Vesicle Endocytosis. Neuroscientist. .

186. **Chen JL, Ahluwalia JP, Stamnes M**. 2002. Selective effects of calcium chelators on anterograde and retrograde protein transport in the cell. J. Biol. Chem. **277:**35682-35687.

187. **Fujioka Y, Tsuda M, Nanbo A, Hattori T, Sasaki J, Sasaki T, Miyazaki T, Ohba Y**. 2013. A Ca(2+)-dependent signalling circuit regulates influenza A virus internalization and infection. Nat. Commun. **4:**2763.

188. **Hyser JM, Collinson-Pautz MR, Utama B, Estes MK**. 2010. Rotavirus disrupts calcium homeostasis by NSP4 viroporin activity. Mbio. **1:**10.1128/mBio.00265-10.

189. **Crawford SE, Hyser JM, Utama B, Estes MK**. 2012. Autophagy hijacked through viroporin-activated calcium/calmodulin-dependent kinase kinase-beta signaling is required for rotavirus replication. Proc. Natl. Acad. Sci. U. S. A. **109:**E3405-13.

190. **Han Z, Harty RN**. 2007. Influence of calcium/calmodulin on budding of Ebola VLPs: implications for the involvement of the Ras/Raf/MEK/ERK pathway. Virus Genes. **35:**511-520.

191. **Sakurai Y, Kolokoltsov AA, Chen CC, Tidwell MW, Bauta WE, Klugbauer N, Grimm C, Wahl-Schott C, Biel M, Davey RA**. 2015. Ebola virus. Two-pore channels control Ebola virus host cell entry and are drug targets for disease treatment. Science. **347:**995-998.

192. **Canaan S, Zadori Z, Ghomashchi F, Bollinger J, Sadilek M, Moreau ME, Tijssen P, Gelb MH**. 2004. Interfacial enzymology of parvovirus phospholipases A2. J. Biol. Chem. **279:**14502-14508.

193. **Zadori Z, Szelei J, Lacoste MC, Li Y, Gariepy S, Raymond P, Allaire M, Nabi IR, Tijssen P**. 2001. A viral phospholipase A2 is required for parvovirus infectivity. Dev. Cell. **1:**291-302.

194. **Lupescu A, Bock CT, Lang PA, Aberle S, Kaiser H, Kandolf R, Lang F**. 2006. Phospholipase A2 activity-dependent stimulation of Ca2+ entry by human parvovirus B19 capsid protein VP1. J. Virol. **80:**11370-11380.

195. **Jain MK, Yu BZ, Rogers J, Gelb MH, Tsai MD, Hendrickson EK, Hendrickson HS**. 1992. Interfacial catalysis by phospholipase A2: the rate-limiting step for enzymatic turnover. Biochemistry. **31:**7841-7847.

196. **Cotmore SF, Hafenstein S, Tattersall P**. 2010. Depletion of virion-associated divalent cations induces parvovirus minute virus of mice to eject its genome in a 3'-to-5' direction from an otherwise intact viral particle. J. Virol. **84:**1945-1956.

197. **Simpson AA, Chandrasekar V, Hebert B, Sullivan GM, Rossmann MG, Parrish CR**. 2000. Host range and variability of calcium binding by surface loops in the capsids of canine and feline parvoviruses. J. Mol. Biol. **300:**597-610.

198. **Grieger JC, Samulski RJ**. 2012. Adeno-associated virus vectorology, manufacturing, and clinical applications. Methods Enzymol. **507:**229-254.

199. **Nonnenmacher M, Weber T**. 2012. Intracellular transport of recombinant adeno-associated virus vectors. Gene Ther. **19:**649-658.

200. **Liu C, Hermann TE**. 1978. Characterization of ionomycin as a calcium ionophore. J. Biol. Chem. **253:**5892-5894.

201. **Beeler TJ, Jona I, Martonosi A**. 1979. The effect of ionomycin on calcium fluxes in sarcoplasmic reticulum vesicles and liposomes. J. Biol. Chem. **254:**6229-6231.

202. **Gee KR, Brown KA, Chen WN, Bishop-Stewart J, Gray D, Johnson I**. 2000. Chemical and physiological characterization of fluo-4 Ca(2+)-indicator dyes. Cell Calcium. **27:**97-106.

203. **Maravall M, Mainen ZF, Sabatini BL, Svoboda K**. 2000. Estimating intracellular calcium concentrations and buffering without wavelength ratioing. Biophys. J. **78:**2655-2667.

204. **Brini M, Cali T, Ottolini D, Carafoli E**. 2014. Neuronal calcium signaling: function and dysfunction. Cell Mol. Life Sci. **71:**2787-2814.

205. **Zhou Y, Xue S, Yang JJ**. 2013. Calciomics: integrative studies of Ca2+-binding proteins and their interactomes in biological systems. Metallomics. **5:**29-42.

206. **Forstner G, Zhang Y, McCool D, Forstner J**. 1993. Mucin secretion by T84 cells: stimulation by PKC, Ca2+, and a protein kinase activated by Ca2+ ionophore. Am. J. Physiol. **264:**G1096-102.

207. **Kim JK, Choi JW, Lim S, Kwon O, Seo JK, Ryu SH, Suh PG**. 2011. Phospholipase C-eta1 is activated by intracellular Ca(2+) mobilization and enhances GPCRs/PLC/Ca(2+) signaling. Cell. Signal. **23:**1022-1029.

208. **Conus NM, Hemmings BA, Pearson RB**. 1998. Differential regulation by calcium reveals distinct signaling requirements for the activation of Akt and p70S6k. J. Biol. Chem. **273:**4776-4782.

209. **Danciu TE, Adam RM, Naruse K, Freeman MR, Hauschka PV**. 2003. Calcium regulates the PI3K-Akt pathway in stretched osteoblasts. FEBS Lett. **536:**193-197.

210. **Zhou Y, Frey TK, Yang JJ**. 2009. Viral calciomics: interplays between Ca2+ and virus. Cell Calcium. **46:**1-17.

211. **Tisdale EJ, Shisheva A, Artalejo CR**. 2014. Overexpression of atypical protein kinase C in HeLa cells facilitates macropinocytosis via Src activation. Cell. Signal. **26:**1235-1242.

212. **Yoshida S, Gaeta I, Pacitto R, Krienke L, Alge O, Gregorka B, Swanson JA**. 2015. Differential signaling during macropinocytosis in response to M-CSF and PMA in macrophages. Front. Physiol. **6:**8.

213. **Chatila T, Silverman L, Miller R, Geha R**. 1989. Mechanisms of T cell activation by the calcium ionophore ionomycin. J. Immunol. **143:**1283-1289.

214. **Dieter P, Fitzke E, Duyster J**. 1993. BAPTA induces a decrease of intracellular free calcium and a translocation and inactivation of protein kinase C in macrophages. Biol. Chem. Hoppe Seyler. **374:**171-174.

215. **Mercer J, Helenius A**. 2009. Virus entry by macropinocytosis. Nat. Cell Biol. **11:**510-520.

216. **van de Graaf SF, Rescher U, Hoenderop JG, Verkaart S, Bindels RJ, Gerke V**. 2008. TRPV5 is internalized via clathrin-dependent endocytosis to enter a Ca2+-controlled recycling pathway. J. Biol. Chem. **283:**4077-4086.

217. **Marshall IC, Gant TM, Wilson KL**. 1997. Ionophore-releasable lumenal Ca2+ stores are not required for nuclear envelope assembly or nuclear protein import in Xenopus egg extracts. Cell Calcium. **21:**151-161.

218. **Strubing C, Clapham DE**. 1999. Active nuclear import and export is independent of lumenal Ca2+ stores in intact mammalian cells. J. Gen. Physiol. **113:**239-248.

219. **Okada M, Ishimoto T, Naito Y, Hirata H, Yagisawa H**. 2005. Phospholipase Cdelta1 associates with importin beta1 and translocates into the nucleus in a Ca2+-dependent manner. FEBS Lett. **579:**4949-4954.

220. **Ryan AJ, Larson-Casey JL, He C, Murthy S, Carter AB**. 2014. Asbestos-induced disruption of calcium homeostasis induces endoplasmic reticulum stress in macrophages. J. Biol. Chem. **289:**33391-33403.

221. **Lytton J, Westlin M, Hanley MR**. 1991. Thapsigargin inhibits the sarcoplasmic or endoplasmic reticulum Ca-ATPase family of calcium pumps. J. Biol. Chem. **266:**17067-17071.

222. **Kawahara H, Yokosawa H**. 1994. Intracellular calcium mobilization regulates the activity of 26 S proteasome during the metaphase-anaphase transition in the ascidian meiotic cell cycle. Dev. Biol. **166:**623-633.

223. **Djakovic SN, Schwarz LA, Barylko B, DeMartino GN, Patrick GN**. 2009. Regulation of the proteasome by neuronal activity and calcium/calmodulin-dependent protein kinase II. J. Biol. Chem. **284:**26655-26665.

224. **Williams JA, Hou Y, Ni HM, Ding WX**. 2013. Role of intracellular calcium in proteasome inhibitor-induced endoplasmic reticulum stress, autophagy, and cell death. Pharm. Res. **30:**2279-2289.

225. **Sanlioglu S, Engelhardt JF**. 1999. Cellular redox state alters recombinant adeno-associated virus transduction through tyrosine phosphatase pathways. Gene Ther. **6:**1427-1437.

226. **Booth C, Koch GL**. 1989. Perturbation of cellular calcium induces secretion of luminal ER proteins. Cell. **59:**729-737.

227. **Zhong L, Li B, Mah CS, Govindasamy L, Agbandje-McKenna M, Cooper M, Herzog RW, Zolotukhin I, Warrington KH,Jr, Weigel-Van Aken KA, Hobbs JA, Zolotukhin S, Muzyczka N, Srivastava A**. 2008. Next generation of adeno-associated virus 2 vectors: point mutations in tyrosines lead to high-efficiency transduction at lower doses. Proc. Natl. Acad. Sci. U. S. A. **105:**7827-7832.

228. **Simons TJ**. 1988. Calcium and neuronal function. Neurosurg. Rev. **11:**119-129.

229. **Zundorf G, Reiser G**. 2011. Calcium dysregulation and homeostasis of neural calcium in the molecular mechanisms of neurodegenerative diseases provide multiple targets for neuroprotection. Antioxid. Redox Signal. **14:**1275-1288.

230. **Braunwald E**. 1982. Mechanism of action of calcium-channel-blocking agents. N. Engl. J. Med. **307:**1618-1627.

231. **Skolnick P, Paul SM**. 1981. The mechanism(s) of action of the benzodiazepines. Med. Res. Rev. **1:**3-22.

232. **Rabouille C, Kondo H, Newman R, Hui N, Freemont P, Warren G**. 1998. Syntaxin 5 is a common component of the NSF- and p97-mediated reassembly pathways of Golgi cisternae from mitotic Golgi fragments in vitro. Cell. **92:**603-610.

233. **Mitchell AM, Nicolson SC, Warischalk JK, Samulski RJ**. 2010. AAV's anatomy: roadmap for optimizing vectors for translational success. Curr. Gene Ther. **10:**319-340.

234. **Lisowski L, Dane AP, Chu K, Zhang Y, Cunningham SC, Wilson EM, Nygaard S, Grompe M, Alexander IE, Kay MA**. 2014. Selection and evaluation of clinically relevant AAV variants in a xenograft liver model. Nature. **506:**382-386.

235. **Gibson DG**. 2011. Enzymatic assembly of overlapping DNA fragments. Methods Enzymol. **498:**349-361.

236. **Trempe JP, Carter BJ**. 1988. Alternate mRNA splicing is required for synthesis of adeno-associated virus VP1 capsid protein. J. Virol. **62:**3356-3363.

237. **Chao H, Liu Y, Rabinowitz J, Li C, Samulski RJ, Walsh CE**. 2000. Several log increase in therapeutic transgene delivery by distinct adeno-associated viral serotype vectors. Mol. Ther. **2:**619-623.

238. **Warrington KH,Jr, Gorbatyuk OS, Harrison JK, Opie SR, Zolotukhin S, Muzyczka N**. 2004. Adeno-associated virus type 2 VP2 capsid protein is nonessential and can tolerate large peptide insertions at its N terminus. J. Virol. **78:**6595-6609.

239. **Stahnke S, Lux K, Uhrig S, Kreppel F, Hosel M, Coutelle O, Ogris M, Hallek M, Buning H**. 2011. Intrinsic phospholipase A2 activity of adeno-associated virus is involved in endosomal escape of incoming particles. Virology. **409:**77-83.

240. **Popa-Wagner R, Porwal M, Kann M, Reuss M, Weimer M, Florin L, Kleinschmidt JA**. 2012. Impact of VP1-specific protein sequence motifs on adeno-associated virus type 2 intracellular trafficking and nuclear entry. J. Virol. **86:**9163-9174.